Study on ‘Pfeiffer effect’ of Eu(III)$(FOD)_3$ in (*S*)-/(*R*)-α-pinene as non-coordinating solvents by circularly polarized luminescence (CPL) and ^{19}F-NMR spectroscopies

円偏光発光分光法と ^{19}F-NMR 分光法による、非配位性(*S*)-/(*R*)-α-ピネンを溶媒にした Eu(III)$(FOD)_3$ の Pfeiffer 効果に関する研究

JALILAH BINTI ABD JALIL

Graduate School of Materials Science

Nara Institute of Science and Technology (NAIST)

Abstract

This work highlighted the 'Pfeiffer effect' of Eu(III)$(FOD)_3$ in neat α-pinene (***Eu_S/R-α-Pinene***), β-pinene and *trans*-pinane. The solvents are purely chiral hydrocarbons and contravene the conventional hard-soft-acid-base theory. Circular dichroism (CD) and CPL spectra showed that the optical activity of ***Eu_S/R-α-Pinene*** is almost absent at the ground state but remarkably induced at the photoexcited state. The absence of undetectable CPL signals in non-fluorinated Eu(III)$(DPM)_3$ in neat α-pinene suggests weak C-*F*/*H*-C interactions is crucial as multiple attractive Coulombic forces between $(FOD)_3$-ligands and α-pinene. An equimolar ratio of Eu(III)$(FOD)_3$ and chiral BINAP (***Eu_S/R*-BINAP)** confirmed the absence of detectable CD signals but exhibited clear CPL signals. Contrarily, an equimolar ratio of Eu(III)$(FOD)_3$ and chiral BINAPO (***Eu_S/R* -BINAPO)** and Eu(III)$(FOD)_3$ in neat chiral α-phenylethylamine (PEA) (***Eu_S/R-α*-PEA)** exhibited mirror-images of CD and CPL spectra. These two different behaviours were further studied by ^{19}F-NMR and ^{31}P-NMR spectroscopies.

^{19}F-NMR profiles displayed that Eu(III)$(FOD)_3$ in the chiral environments (except for BINAP) showed preference towards one enantiomer. The peak integral ratios due to the three $(FOD)_3$-ligands in $CDCl_3$ suggested that C_3-symmetric *facial* is dominant for Eu(III)$(FOD)_3$, ***Eu_S/R*-X (X** = *α*-pinene and BINAP) but *pseudo* C_3-symmetry or possibly C_1-symmetry for ***Eu_S/R*-X (X** = BINAPO and *α*–PEA**)**. The difference in these two classes of chiral environments was also observed in the

difference of chemical shift direction in which the former shifted upfield and the latter shifted downfield. ^{31}P-NMR spectroscopy confirmed a significant upfield shift (≈ 100 ppm) of P element of BINAPO upon complexation with Eu(III)$(FOD)_3$ indicating direct coordination at the inner sphere. Thus, we are convinced that the upfield shift from ^{19}F-NMR is attributable to a collective effect of weak coordinations that take place at the outer sphere.

The Mulliken charge distributions by Møller-Plesset second-order perturbation (MP2) calculations further support that weak C-*F*/*H*-C interactions between $(FOD)_3$-ligands and α-pinene and C-*H*/*P*, C-*F*/*P*, and/or C-*F*/*H*-C between $(FOD)_3$-ligands and BINAP are the possible interactions that cause the equilibrium shift of the *Δ*- and *Λ*-species. Contrarily, BINAPO shows tendency of O=P towards the Sc(III) metal ion which is in accordance to the ^{31}P-NMR analysis that suggests direct coordination. Negatively charged N-atom of PEA also displays tendency of direct coordination towards the positively charged Sc(III) metal ion. This explains the highest g_{em} values obtained by CPL.

The extension of 'Pfeiffer effect' study by the highly solubile Eu(III)$(FOD)_3$ and the environmentally green α-pinene would promote CD-*silent*/CPL-*active* ***Eu_S/R-α*-pinene** to be a potential candidate in security materials and chiral sensing system. Moreover, one can determine a suitable chiral environment for a Pfeiffer-perturbed system in a racemic fluorinated lanthanide (III) complex by ^{19}F-NMR analysis. This study may serve as a basis for designing chiral photoluminescence polymer(s) by their intermolecular weak interactions in the future.

Dedicated to

my husband, Muhammad Izham

and my late father, Abd Jalil

Acknowledgements

Alhamdulillah, praise to Allah the Almighty for the strength and His blessings after all the challenges and difficulties in completing this thesis.

First and foremost, I wish to extend my sincere gratitude to my supervisor, Prof. Fujiki Michiya for giving me the opportunity to join his laboratory. His continuous support, guidance and extensive knowledge have shaped the research and sharpened its outcome. My gratitude also goes to Prof. Daimon Hiroshi, Prof. Nakashima Takuya and Prof. Kamikubo Hironari for their insightful comments and fruitful discussions in constructing this project.

I am indebted to Mr. Asanoma for his assistance in NMR measurements. He has always been cooperative in obtaining good data. His cooperation and availability are highly appreciated.

I would also like to acknowledge the *Majlis Amanah Rakyat* (*MARA*) *Education Foundation* and *Universiti Malaysia Perlis* (*UNIMAP*) for the financial support throughout this study period.

Special thanks dedicated to all my fellow laboratory members, Sibo Guo, Wang Lai Bing, Duong Thi Sang, Yokokura Ai, Kamite Hiroki, Katsurada Yota, Toshiki Nagai, Yoshimoto Shisei, Yoshida Keisuke, Okubo Asuka, Nanami Ogata, Okazaki Shun, Nozomu Suzuki and not to forget our secretary Mrs. Tanimoto Sanae for their helps, cooperation and cheerful moments in the laboratory throughout the years. In particular, I would like to thank Yamazaki Kazuki who has been a good companion

when conducting research in the laboratory.

I also appreciate that I have been blessed with supportive friends, Farrah Shameen Ashray, Haiza Haroon and Nor Azura Abdul Rahim for the sustenance of emotional strength.

My deepest appreciation goes to my beloved husband and children for their prayers, encouragement, sacrifices and endless supports. Not forgetting all the family members in Malaysia especially my parents and sister in-laws, my brothers and their families for their supports starting from the beginning of the journey till the end. Without all of them mentioned above, this thesis would not have been completed.

Last but not least, I would like to express my love and special thoughts to my late father for his helps, supports, patience and prayers till his very last moments. May *Allah* grant him with the highest level in *Jannah*.

Table of Contents

Chapter 1

Introduction

1.1. Terpene-induced chirality transfer

Mirror symmetry breaking by solvent chirality transfer is an attractive approach in designing chiral materials in a sophisticated way. This simple, economical and convenient approach has widely spread into the areas of organic and inorganic chemistry as well as supramolecular, polymer and materials science. Chiroptical properties in the ground and photoexcited states of optically-inactive molecules, supramolecules and polymers are significantly affected by the surrounding solvent molecules through non-covalent bonding interactions[1]. Among the solvents including alcohols, amines, and hydrocarbons, non-toxic inexpensive chiral terpenes are alternative and attractive solvents for environmental friendly production of optically-active materials. Previously, Holder *et al*. reported on the generation of circular dichroism (CD)-active poly(dialkylsilane)s by (*S*)-2-methylbutoxy derivatives (a solvent without specific functional groups)[2]. Inspired by his work, Fujiki *et al*. demonstrated induced-CD- and/or –circularly polarized luminescence (CPL) in optically-inactive π-conjugate polymers by chiral α-pinene and limonene[3a-e]. The optical activity is a consequence of weak intermolecular interactions such as hydrogen bonding and π-π interaction. Later, Kwak and colleagues successfully produced CD-active poly(diphenylacetylene)s carrying a *p*-trimethylsilylphenyl and an unsubstituted phenyl in α-pinene with the help of achiral Rh catalyst[4]. The

intermolecular interactions of van der Waals, π - π and CH- π between the side phenyl ring and limonene led to the induced-CD signals.

Terpene chirality transfer may be applicable and is advantage in generating CD- and CPL-active materials if exploited in 'Pfeiffer effect'[5a-c]. This effect is a perturbation of equilibrium phenomena in a racemic mixture of metal complex upon addition of an optically active compound. Many luminescence lanthanide complexes have exemplified the 'Pfeiffer effect'[6a-e]. In most cases, the effect takes place at the outer sphere between the racemic lanthanide complex and the chiral environment substances[6d,e] due to weak intermolecular interactions. A suitable combination of a racemic lanthanide complex and a terpene solvent could lead to perturbation of the equilibrium through weak interactions.

1.2. Perucca and Pfeiffer observed phenomena

In 1919, Perucca[7] reported optical rotatory dispersion (ORD) signals in the region of 500-600 nm from a racemic mixture of triarylmethane textile dye (extra China blue) dispersed into polycrystalline $NaClO_3$ that is one of the representatives' chiral inorganic crystals involving α-quartz and HgS (cinnabar). In the early 1930s, Pfeiffer and coworkers observed an apparent increase and decrease of optical rotation of optically active chiral compounds in solutions in the presence of a racemic enantiomeric transition metal (Zn(II), Cd(II), Ni(II)) complexes[5a-c], the so-called Pfeiffer effect[8]. Two decades later, Gyarfas and Dwyer proposed (i) that a dynamic equilibrium between two optically labile metal complexes (*dextro* and *levo)* exist in solution and (ii) that the

optical activity of one enantiomer is different from that of the opposite one in the presence of an optically active 'environment' due to configurational optical activity[9]. Later, Kirschner and colleagues confirmed that the source of the increased optical activity is due to an equilibrium perturbation of the metal complex equilibria[10].

1.3. Detection of 'Pfeiffer effect' by CPL spectroscopy

In recent years, elucidating "Pfeiffer effect" using CPL spectroscopy with a good signal-to-noise (SN) ratio is one of the attractive topics in relation to efficient, selective recognition and sensing technique in the realm of molecular chirality and biopolymer chirality and/or helicity. A comprehensive review by Riehl and Muller emphasizes that CPL spectroscopic technique facilitates to detect structural information of chiral species and to study photoexcited state chirality of lanthanide complexes[11].

Brittain, Muller, and Riehl observed CPL spectra arising from the dissymmetrical perturbation between *Δ*- and *Λ*-species of D_3-symmetrical Tb(III) tris(2,6-pyridinedicarboxylate) complex (2,6-pyridinedicarboxylate: DPA) by solely adding chiral biomolecular substances (e.g. amino acids[6c,12a] and derivatives of tartrate[6d] and sugar)[12b]. It is understood that the outer-sphere interactions by these additives are responsible for the equilibrium shift revealed by the CPL spectra.[6d-f,12a]. Further investigation by Muller and coworkers reported that the chiral-induced equilibrium shift of D_3-symmetrical Tb(III) complexes with chelidamic acid $[Tb(CDA)_3]^{6-}$ by *L*-amino acids was largely influenced by the hydrogen-bonding networks between the ligand interface of racemic [Tb(III) $(CDA)_3$] and the added chiral agents[12a]. The study

suggested that the hydrogen bonding networks could serve as the basis for further non-covalent discriminatory interactions in the particular solvent-chelate system.

Nonetheless, the above-mentioned studies exemplified a chiral perturbation of racemic lanthanide complex by hard bases. More recently, Imai, Fujiki, and coworkers[13] reported on induced-CD and induced-CPL spectra by solely mixing Eu(III)$(hfa)_3$ (hfa = hexafluoroacetylacetonate) in the presence of C_2-symmetrical BINAP in an equimolar ratio. Eu(III)$(hfa)_3$ may occur in solution as a racemic mixture of chiral metal complex, and exists as CD- and CPL-silent states. The work inferred a certain perturbation affecting the left-right equilibrium at the inner-sphere by an ultraweak chiral interaction between the soft-base P(III) to the hard-acid Eu(III). This scenario may contradict the conventional hard-soft-acid-base (HSAB) theory[14], which predicts that lanthanide ions prefer to bind to hard bases such as oxygen and nitrogen elements[10]. According to the HSAB theory, a lanthanide (III), which is regarded as a representative Lewis acid, would prefer to bind to hard bases.

1.4. This work

Those findings associated with the recent works prompted us to revisit induced-CPL/PL spectra of Eu(III) tris(6,6,7,7,8,8,8-heptafluoro-2,2-dimethyl-3,5-octanedionate) (6,6,7,7,8,8,8-heptafluoro-2,2-dimethyl-3,5-octanedionate: FOD) because Eu(III)$(FOD)_3$ is readily soluble in common organic solvents, such as chloroform, acetone, and aromatic solvents. Moreover, a total of 21 fluorine elements of the fluoroalkyl ligand acts as a good probe of ^{19}F-NMR spectroscopy and facilitates us

to detect any subtle changes in dynamic behaviour of the molecular symmetry. Herein, we chose non-charged chiral terpenes without the presence of oxygen and nitrogen elements to afford ultraweak dissymmetrical perturbation to Eu(III)$(FOD)_3$ in solution, including (*S*)-/(*R*) –limonene, (*S*)-/(*R*)-α-pinene, (*S*)-β-pinene and (*S*)-/(*R*)-*trans*-pinane. Optical activity of Eu(III)$(FOD)_3$ was undetectable by (*S*)-/(*R*)-limonene but inducible by (*S*)-/(*R*)-α-pinene , (*S*)-β-pinene and (*S*)-/(*R*)-*trans*-pinane. However, the CPL magnitudes by (*S*)-β-pinene and (*S*)-/(*R*)-*trans*-pinane were not as obvious as α-pinenes. Similar to emerging CPL spectra from Eu(III)$(HFA)_3$ induced by equimolar amount of *(S)-/(R)*-2,2-bis(diphenylphosphino)-1,1-binaphthalene (BINAP) and (*S*)-/(*R*)-2,2-bis-(diphenylphosphinyl)-1,1-binaphthalene (BINAPO) in chloroform, we also observed clear CPL spectra from Eu(III)$(FOD)_3$ in the presence of equimolar amount of (*S*)-/(*R*)-BINAP and (*S*)-/(*R*)-BINAPO in chloroform. In addition, we obtained a clear mirror-image CPL spectra from Eu(III)$(FOD)_3$ in neat α–phenylethylamine and also in equimolar mixture of Eu(III)$(FOD)_3$ and α–phenylethylamine. As a comparison to Eu(III)$(FOD)_3$, we tested D_3-symmetric Eu(III)$(DPM)_3$ (DPM = 2,2,6,6-tetramethyl-heptane-3,5-dione) but did not detect any CPL signals. The molecular structures of the Eu(III) complexes, chiral solvents and chiral additives used in this study are given in Scheme 1.1.

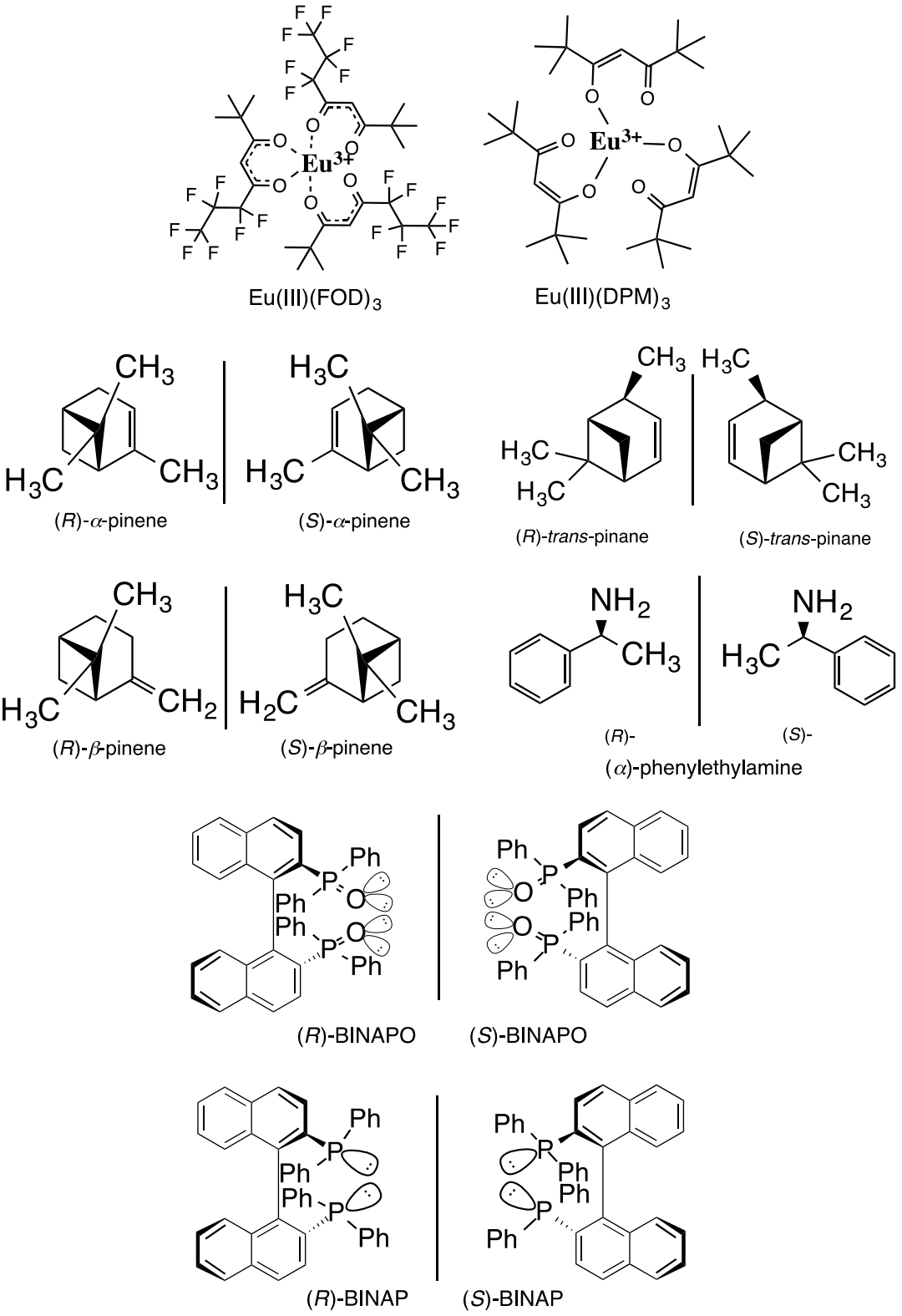

Scheme 1.1. Molecular structures of Eu(III) complexes, chiral solvents and additives used in this study

The complex Eu(III)(FOD)$_3$ is assumed to have two different stereochemical structures; polar C_3-symmetric *facial* and less-polar C_1-symmetric *meridional* forms in

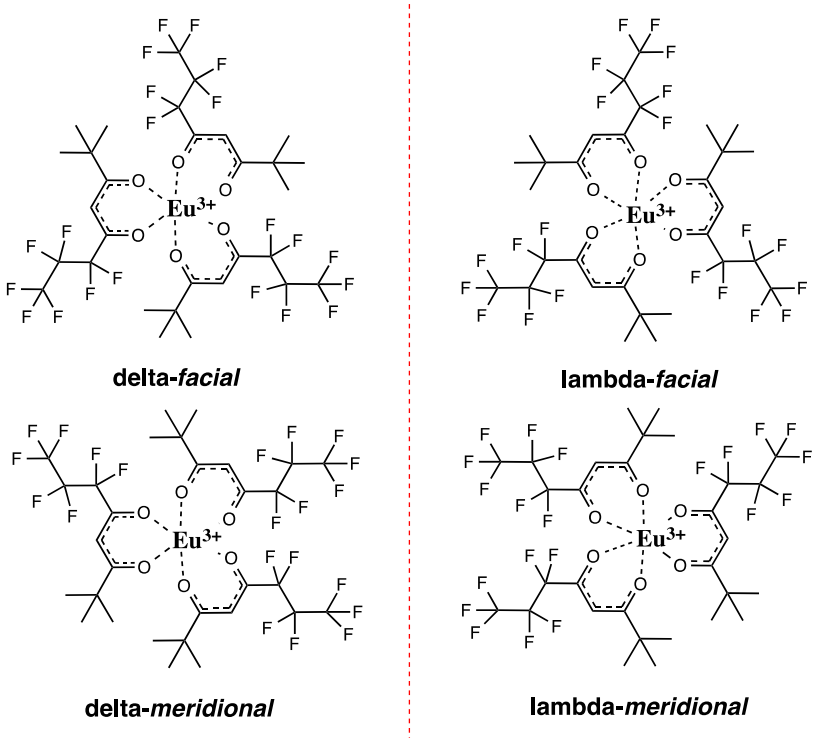

Scheme 1.2. Four possible stereochemical structures of labile Eu(III)(FOD)$_3$ existing in solution

solution (Scheme 1.2). Single crystal analysis of Eu(III)(FOD)$_3$ provides a detail geometrical information in the solid, but possibly this molecular information is not applied in fluidic solution at ambient temperature. In principle, Eu(III)(FOD)$_3$ may adopt two enantiopairs of *Δ*- and *Λ*-species. These four species are interchangeable in response to chiral chemical influences, solvent polarity, and temperature in the ground and photoexcited states. The chiral substances added in solution should perturb the enantiomeric and diastreomeric equilibria resulting in a non-covalent diastereoisomeric species in an unequal ratio between *Δ*- and *Λ*-species in the photoexcited and ground

states chirality. This imbalance is detectable by CPL spectrum in the photoexcited state and CD spectrum in the ground state.

The present work is the first clear observation of 'Pfeiffer effect' in Eu(III)$(FOD)_3$ with α-pinene as a solvent consisting of only soft-base elements, that should break the conventional HSAB theory. ^{19}F-NMR spectral analysis reveals the existence of one dominated species and suggests that Eu(III)$(FOD)_3$ adopts the *facial*-C_3-symmetry geometrical structure in chloroform. The structure is seen to remain as *facial*-C_3-symmetry in pure (*S*)/(*R*)-α-pinene. The weak interactions of C*H*/π, C*H*/*C*H and/or C*F*/*H*C as well as chiral London dispersion forces, occur at the outer-sphere in the ground chiral state, and are responsible for the induced CPL spectra in the photoexcited state chirality. Contrarily, the ^{19}F-NMR profiles of Eu(III)$(FOD)_3$ with equimolar BINAPO in $CDCl_3$ displays clearly triplet signals that greatly shifted to opposite direction with Eu(III)$(FOD)_3$ in (*S*)/(*R*)-α-pinene and the profiles suggest *pseudo*-C_3-symmetry or C_1-symmetrical Eu(III)$(FOD)_3$ due to close coordination to Eu(III) ion by O=P of BINAPO. This assumption was further confirmed by ^{31}P-NMR analysis.

Not all combination of metal-ion ligand complexes and solvents should exhibit 'Pfeiffer effect'[15]. Hence, it is anticipated that the choice of highly soluble Eu(III)$(FOD)_3$ with a non-toxic solvent would offer a simple, convenient method in obtaining CPL-functional Eu(III) complexes and should help to understand the dynamic behaviours of complicated lanthanide complexes in fluidic solutions.

1.5. Objectives

In this work, we aimed to prove that optical activity in racemic mixture of C_3-symmetry fluorinated Eu(III)$(FOD)_3$ complex could be induced by a purely hydrocarbon terpene solvent and produce CPL-active luminophores. The second objective is to investigate the equilibrium displacement mechanism that caused the emergence of optical activity and the absolute configurations of dissymmetric Eu(III)$(FOD)_3$. Our final goal is to determine whether or not the chirality transfer from α-pinene to Eu(III)$(FOD)_3$ complex can be regarded as 'Pfeiffer effect'.

1.6. Scope of study

Chapter 1 covers the background in details, objectives and focus of this study. Chapter 2 presents the CPL spectra from Eu(III)$(FOD)_3$ dissolved in terpenes of (*S*)-/(*R*)–limonene, (*S*)-/(*R*)-α-pinene, (*S*)-β-pinene and (*S*)-/(*R*)-*trans*-pinane. This chapter then focuses on chirality at the ground state and optical properties of CPL-active Eu(III)$(FOD)_3$ in (*S*)-/(*R*)-α-pinene, (***Eu_S/R-α*-pinene**). In chapter 3, the chiroptical properties (CD and CPL) of Eu(III)$(FOD)_3$ complexed with solvents that possess P, O and N elements, ***Eu_S/R*-X** *(*X = BINAP, BINAPO, α-phenylethylamine (neat and diluted)) are presented for comparison with that of ***Eu_S/R-α*-pinene**. This chapter also shows CPL from non-fluorinated Eu(III) complex in ***Eu_S/R-α*-pinene.** Chapter 4 reveals the geometrical structures adopted by ***Eu_S/R-α*-pinene** as well as in BINAP, BINAPO, neat α-phenylethylamine and diluted α-phenylethylamine. From this chapter, we can conclude on the interactions involved and where it occurred. The 'Pfeiffer effect'

is mainly discussed in this chapter as well. Supporting evidences by theoretical MP2 calculations are presented in Chapter 5 and Chapter 6 summarizes the whole findings.

1.7. References

[1] M. Fujiki, *Symmetry,* 2014, **6**, 677-703.

[2] P. Dellaportas, R.G. Jones, and S.J. Holder, *Macromol. Rapid Commun., 2002, **23**, 99-103.*

[3] (a) Y. Kawagoe, M. Fujiki, and Y. Nakano, *New J. Chem*, 2010, **34**, 637-647. (b) Y. Nakano, Y. Liu, and M. Fujiki, *Polym. Chem.*, 2010, **1**, 460-469. (c) W. Zhang, K. Yoshida, M. Fujiki, and X. Zhu, *Macromolecules*, 2011, **44**, 5105-5111. (d) M. Fujiki, A. J. Jalilah, N. Suzuki, M. Taguchi, W. Zhang, M. M. Abdellatif, and K. Nomura, *RSC Adv.*, 2012, **2**, 6663-6671. (e) M. Fujiki, Y. Kawagoe, Y. Nakano, and Y. Nakao, *Molecules*, 2013, **18**, 7035-7057.

[4] D. Lee, Y.-J. Jin, N. Suzuki, M. Fujiki, T. Sakaguchi, S. Kim, W.-E. Lee, and G. Kwak, *Macromolecules*, 2012, **45**, 5379-5386.

[5] (a) P. Peiffer and K. Quehl, *Ber. Dtsch. Chem. Ges*., 1931, **64**, 2667. (b) P. Peiffer and K. Quehl, *Ber. Dtch. Chem. Ges*., 1932, **65**, 560. (c) P. Peiffer and Y. Nakatsuka, *Ber. Dutsch. Chem. Ges*., 1933, **66**, 415.

[6] (a) J. S. Madaras and H. G. Brittain, *Inorg. Chem.*, 1980, **19**, 3841. (b) J. S. Madaras and H. G. Brittain, *Inorg. Chim. Acta*, 1980, **42**, 109. (c) H. G. Brittain, *Inorg. Chem.*, 1981, **20**, 3007. (d) F. Yan, R. A. Copeland, and H. G. Brittain, *Inorg. Chem.*, 1982, **21**, 1180. (e) F. Yan and H. G. Brittain, *Polyhedron*, 1982, **1**, 195.

[7] E. Perucca, *Nuovo Cimento*, 1919, **18**, 112.

[8] F. Basolo and R. Pearson, *Mechanism of Inorganic Reactions,* J.Wiley and Sons, Inc., N.Y., 1958, 286.

[9] E. C. Gyarfas and F. P. Dwyer, *Revs. Pure and Appl. Chem.,* 1954, **4**, 73.

[10] S. Kirschner and I. Bakkar, *Coordination Chemistry Reviews, 1982,* **43,** 325-335.

[11] J. P. Riehl and G. Muller, *Circularly Polarized Luminescence Spectroscopy from Lanthanide Systems. In*: K. A. Gschneidner, Jr., J.-C. G. Bünzli, and V. K. Pecharsky, eds. *Handbook on the Physics and Chemistry of Rare Earths*. 34. North Holland Publishing Co.; Amsterdam: 2005, pp. 289-357 and references therein.

[12] (a) A. Moussa, C. Pham, S. Bommireddy, and G. Muller, *Chirality*, 2009, **21**, 497-506. (b) D. Italiano and H. G. Brittain, *Lanthanide, Actinide Res.*, 1985, **1**, 21.

[13] Y. Kono, K. Nakabayashi, S. Kitamura, M. Shizuma, M. Fujiki, and Y. Imai, *RSC Adv*., 2016, **6**, 40219.

[14] R. G. Pearson, *J. Am. Chem. Soc.*, 1963, ***85***, 3533–3539.

[15] S. Kirschner, N. Ahmad, and K. Magnell, *Coord. Chem. Rev.,* 1968*,* ***3,*** 201-206.

Chapter 2

Chiroptical and optical properties

2.1. Introduction

CPL measurement were carried out for Eu(III)$(FOD)_3$ in terpenes as chiral solvents. The terpenes were the monocyclic limonene, bicyclic α-pinene, β-pinene and *trans*-pinane (refer scheme 1.1 for molecular structures). Induced-CPL was observed for Eu(III)$(FOD)_3$ dissolved in neat α-pinene and β-pinene. Significant photo-excited state optical activity at $^5D_0 \rightarrow {}^7F_1$ Eu^{3+} ion transition was seen for ***Eu_S/R-α-pinene***. Thus, we proceeded with the investigation of CPLE, CD and PL of ***Eu_S/R -α-pinene***.

2.2. Measurements

2.2.1. CD/UV-visible Measurement

The CD/UV-visible spectra solution in a square quartz (SQ)-grade cuvette was recorded simultaneously at room temperature by JASCO (Hachioji-Tokyo, Japan) J-820 spectropolarimeter equipped with Peltier controlled equipment. Scanning speed of 50 nm/min with 4 sec response time of photomultiplier tube (PMT), 5 nm bandwidth, and 10 nm bandwidth for excitation were applied. The spectra were smoothed by 2 time accumulations without numerical smoothing. *Ethanol* (*EtOH*)-free dehydrated chloroform (Wako) was used for spectroscopic measurement to avoid unfavorable coordination of oxygen sources (EtOH and water molecules)

2.2.2. CPL/PL Measurement and CPL Excitation (CPLE)/PLE) Measurements

The CPL/PL spectra were obtained using JASCO (Hachioji, Japan) CPL-200 spectrofluoropolarimeter using an SQ-grade cuvette at room temperature. A scattering angle of 0°C was used for the excitation of nano-polarised monochromatic incident light with bandwidth of 10 nm. Scanning speed of 50 nm/min with 8sec response time was applied. The spectra were smoothed by 4 time accumulations without numerical smoothing. The excitation wavelengths applied were varied according to samples. *EtOH*-free dehydrated chloroform (Wako) was used for spectroscopic measurement.

CPL/PL spectra were obtained corresponding to their CPL signals by adjusting the detection wavelength using a bandwidth of 10 nm, a scanning rate of 50 nm/min with 8 sec response time.

2.2.3. PL Measurement

The PL spectra were obtained using JASCO FP-6500 spectrofluorometer at room temperature. The measurement was carried out using 1 cm path length synthetic quartz (SQ)-grade cuvette at 100 nm/min scanning speed and 1 sec PMT response time with 5-20 nm excitation bandwidth and 1 nm emission bandwidth. The excitation wavelengths applied were varied according to samples. *EtOH*-free dehydrated chloroform (Wako) was used for spectroscopic measurement.

2.3. Preparation of Eu(III)(FOD)$_3$ in chiral terpenes (*Eu_S/R*-X ; X= limonene, *α*-pinene, β-pinene, *trans*-pinane)

Eu(III)(FOD)$_3$ was purchased from Sigma-Aldrich (Japan). Chloroform was purchased from (Wako). The chloroform used was *EtOH*-free and contained amylene as stabilizer. (*1S*-(+)-/(*1R*)-(-)-limonene, (*1S*)-(+)-/(1*R*)-(-)-α-pinene, and (*1S*)-(-)-β-pinene were purchased from TCI (Japan). (*1S*)-(+)-/ *(1R*)-(-)-*trans*-pinane was purchased from Fluka (Japan). ***Eu_S/R-***X (X = limonene, α-pinene, β-pinene, and *trans*-pinane) were prepared by dissolving Eu(III)(FOD)$_3$ in neat terpene solvent. The solutions were heated at mild temperature of 50-60°C for about 5 min and left to cool to room temperature prior spectroscopic measurements.

2.4. Chiroptical properties

2.4.1. Circularly polarized luminescence (CPL)

2.4.1.1. The absence of CPL signals in Eu(III)(FOD)$_3$ in chloroform, Eu_S/R-limonene and Eu_S/R-trans-pinane

CPL was not satisfactorily detected for Eu(III)(FOD)$_3$ in chloroform, neat chiral limonene (Fig. 2.1) and also in neat chiral *trans*-pinane. (Fig. 2.2) This suggests that the *Δ*- and *Λ*-species of Eu(III)(FOD)$_3$ exists equally in non-coordinating solvent, chloroform and the equilibrium is not much perturbed by limonene, a floppy monocyclic terpene, and by *trans*-pinane, a rigid bicyclic terpene without C-C double-bond (refer Scheme 1.1 for molecular structures) due to inefficient interactions between the complex and the chiral terpene solvents.

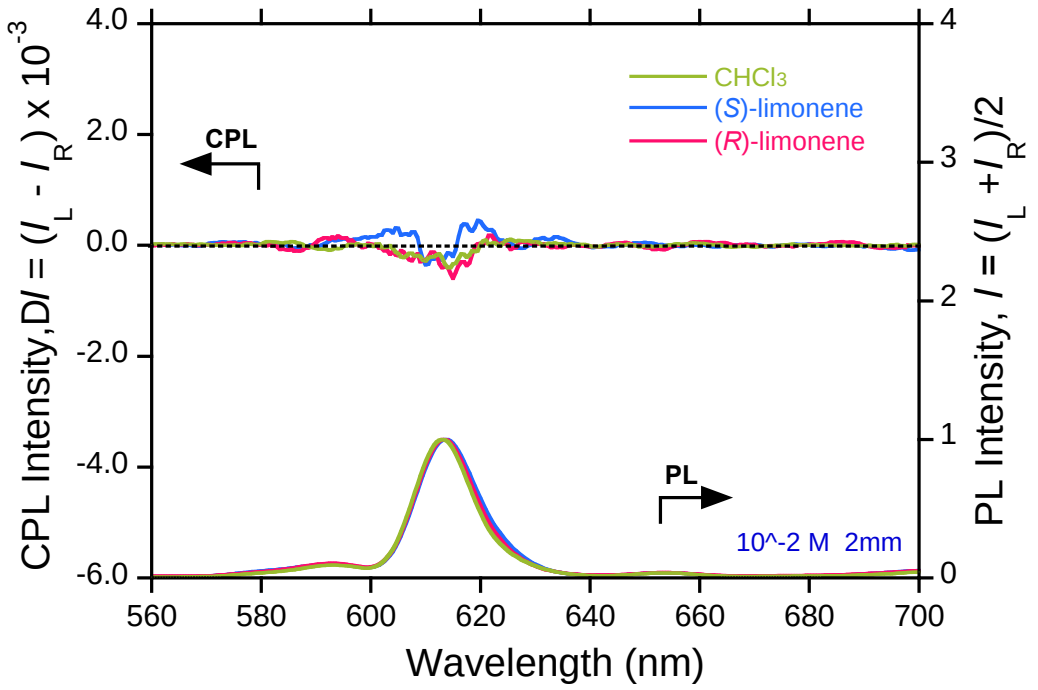

Fig. 2.1 CPL/PL spectra of Eu(III)(FOD)$_3$ in $CHCl_3$ and ***Eu_S/R*-limonene** at $^5D_0 \rightarrow {}^7F_1$ and $^5D \rightarrow {}^7F_2$ transitions (Ex 335nm)

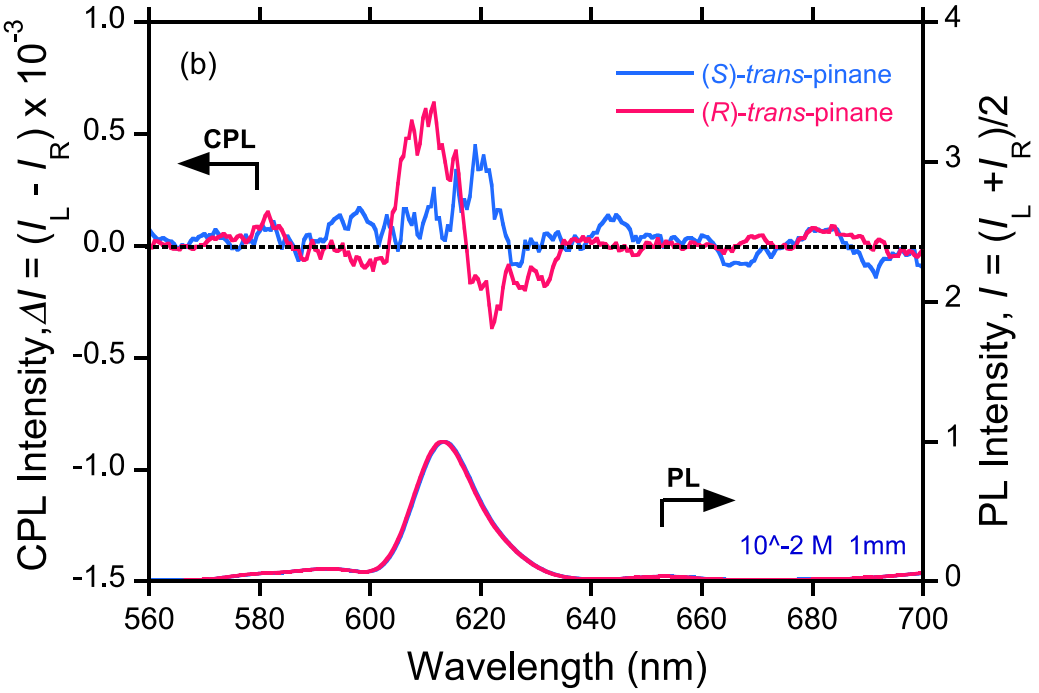

Fig. 2.2 CPL/PL spectra of ***Eu-S/R-trans*-pinane** at $^5D_0 \rightarrow {}^7F_1$ and $^5D \rightarrow {}^7F_2$ transitions (Ex 330nm)

2.4.1.2. Induced-CPL in Eu_S/R-X (X= α-pinene, β-pinene)

***Eu-S*-α-pinene** and ***Eu-R*-α-pinene** at 1.0 × 10^{-2} M exhibited nearly mirror-image CPL signals at 592 nm corresponding to $^5D_0 \rightarrow {}^7F_1$ transition and bands in the region of 612-613 nm corresponding to $^5D \rightarrow {}^7F_2$ transition of the Eu(III) ion, respectively (Fig. 2.3). The PL maxima appeared at $^5D_0 \rightarrow {}^7F_J$ transitions (J=1-6) at 592, 613, 653, 702, 751 and 809 nm wavelengths. We could also observe the CPL signals at

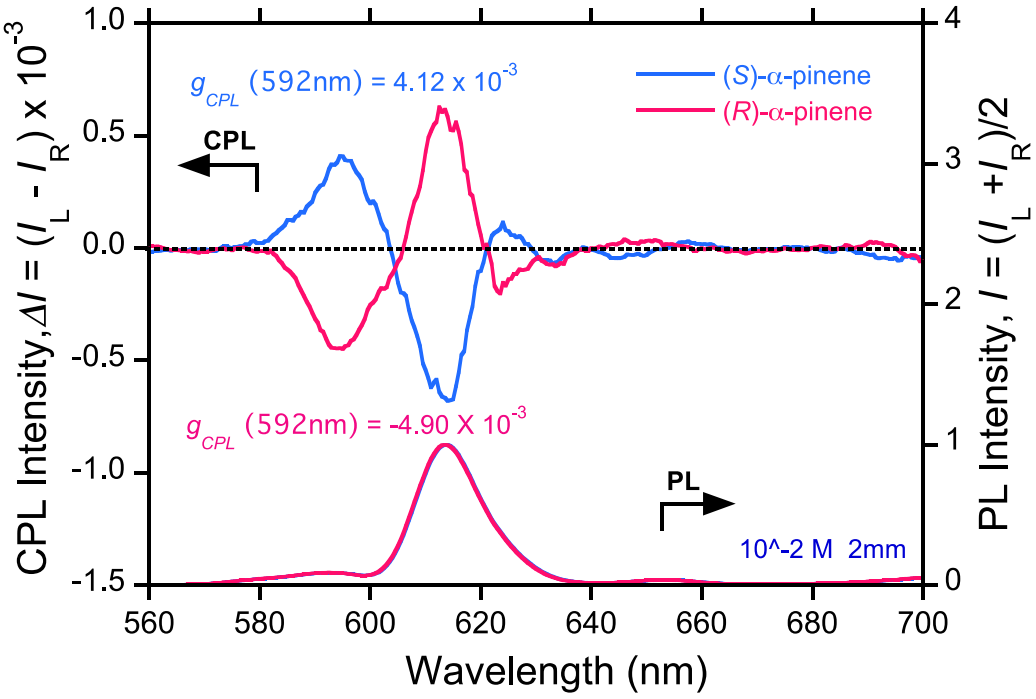

Fig. 2.3 CPL/PL spectra of ***Eu_S/R*-α-pinene** at $^5D_0 \rightarrow {}^7F_1$ and $^5D \rightarrow {}^7F_2$ transitions (Ex 345nm)

$^5D_0 \rightarrow {}^7F_J$ transitions (J= 3), but the signals were not obvious to discuss. The emergence of the CPL spectra indicates that perturbation of the equilibrium in Eu(III)$(FOD)_3$ is induced by the α-pinene chirality. The CPL of the $^5D_0 \rightarrow {}^7F_1$ magnetic-dipole allowed transition at 592 nm gave the largest value g_{em} values of +4.12 × 10^{-3} and -4.90 × 10^{-3} for ***Eu_S*-α-pinene** and ***Eu_R*-α-pinene,** respectively. The degree of CPL in terms of

the luminescence dissymmetry factor g_{em} is defined as in equation (1):

$$g_{em} = \frac{DI}{I} = \frac{I_L - I_R}{1/2(I_L + I_R)} \quad (1)$$

where I_L and I_R refer respectively to the intensity of left and right circularly polarized emitted light[1a,b].

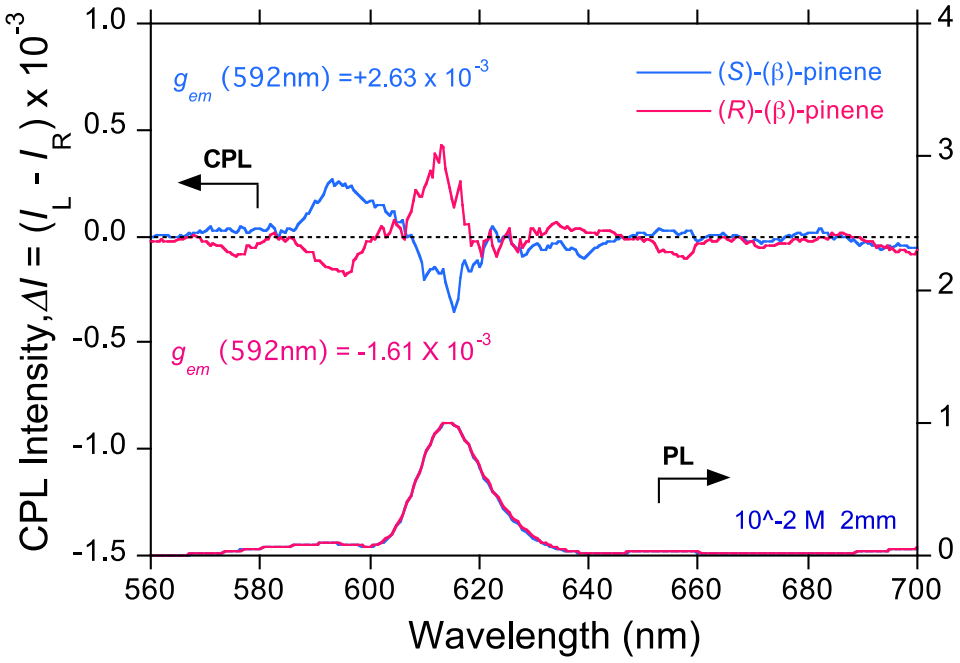

Fig. 2.4 CPL/PL spectra of ***Eu_S/R*-β-pinene** $^5D_0 \rightarrow {}^7F_1$ and $^5D \rightarrow {}^7F_2$ transitions (Ex 335 nm)

***Eu_S/R*-β-pinene** displayed similar profile to ***Eu_S/R*-α-pinene** but the g_{em} values of $+2.63 \times 10^{-3}$ for (*S*)- and -1.61×10^{-3} for (*R*)- at $^5D_0 \rightarrow {}^7F_1$ transition was very much lower as compared to ***Eu_S/R*-α-pinene** (Fig. 2.4). The equilibrium of Eu(III)$(FOD)_3$ is seen perturbed by the chiral β-pinene but the extent of the perturbation is not as significant as

by the chiral α-pinene. It is worth noting that the CPL signals in the two different pinenes (***Eu_S*/*R*-α-pinene** and ***Eu_S*/*R*-β-pinene**) showed the same signs for (*S*)- and (*R*)-enantiomers.

2.4.1.3. Dependency on α-pinene concentration and the binding strength of Eu-S/R-α-pinene

We plot g_{em} values measured at $^5D_0 \rightarrow {}^7F_1$ transition for Eu(III)(FOD)$_3$ dissolved in a mixture of α-pinene and $CHCl_3$ from the absence of α-pinene to pure concentration of α-pinene in order to predict the extent of the association of α-pinene to

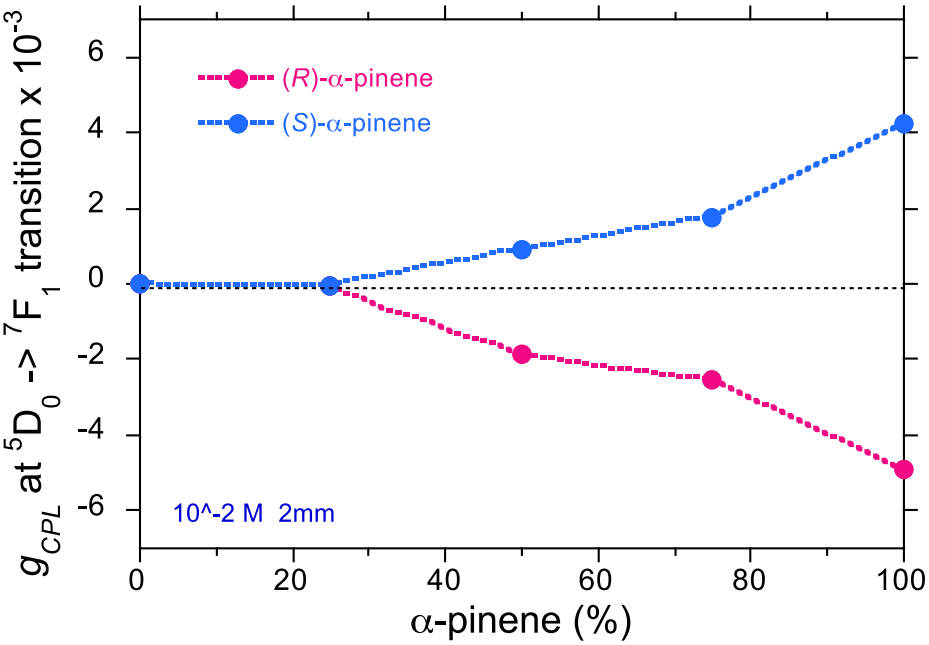

Fig. 2.5. Plot of emission dissymmetry ratio, g_{em} at the peak wavelength of 592 nm for Eu(III)(FOD)$_3$ in a mixture of α-pinene and $CHCl_3$ as a function of α-pinene concentration (%)

Eu(III)(FOD)$_3$. From the plot given by Fig. 2.5, the g_{em} values increased as the concentration of α-pinene increased. This shows that association with the α-pinene induces the chirality.

The binding constant, K can be obtained from the solution equilibria illustrated below:

$$EuFOD + P^* \overset{K}{\leftrightarrow} EuFOD \cdot P^* \quad (2)$$

$$K = \frac{[EuFOD \cdot P^*]}{[EuFOD][P^*]} \quad (3)$$

where

$$[P^*] = [P^*]_0 - [EuFOD \cdot P^*]$$

$$[EuFOD] = [EuFOD]_0 - [EuFOD \cdot P^*] \quad (4)$$

considering that

$$[P^*]_0 \gg [EuFOD]_0 \quad (5)$$

thus,

$$[P^*] = [P^*]_0 \quad (6)$$

and *K* can be arranged as equation (7),

$$K = \frac{[EuFOD \cdot P^*]}{([EuFOD]_0 - [EuFOD \cdot P^*])[P^*]} \quad (7)$$

The relationship with g_{em} is given in equation (8),

$$g_{em}\,(apparent) = \frac{[EuFOD \cdot P^*]}{[EuFOD] + [EuFOD \cdot P^*]} \times g_{em}\,(EuFOD100\%)[EuFOD \cdot P^*] \quad (8)$$

since

$$[EuFOD]_0 = [EuFOD] + [EuFOD \cdot P^*] \quad (9)$$

the equation can be rearranged to equations (10) and (11),

$$\frac{g_{em\,(apparent)}}{g_{em}\,(EuFOD100\%)}\;[EuFOD\cdot P^*]^{-1} = \frac{[EuFOD\cdot P^*]}{[EuFOD]_0} \quad (10)$$

$$\frac{g_{em\,(apparent)}}{g_{em}\,(EuFOD100\%)}\;[EuFOD\cdot P^*]^{-1} = \frac{1}{K[P^*]} + 1 \quad (11)$$

The fitting of equation (11) to the plots in Fig. 2.6 gives the *K* values. The calculated binding constant, *K* given by the fitted plots of both ***Eu_(S)-*** and ***Eu_(R)*-α-pinene** are as low as 10^{-3}.

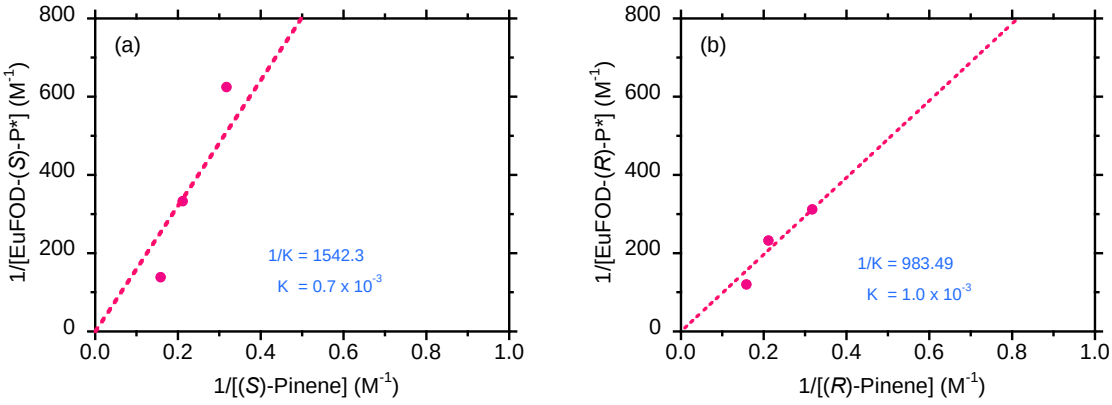

Fig. 2.6 Plot of emission dissymmetry ratio, g_{em} at the peak wavelength of 592 nm for ***Eu_S/R*-α-pinene** as a function of α-pinene concentration (%)

The ultralow *K* values indicate that the coordination between the chelate and the solvent is very weak but strong enough to cause perturbation to the equilibrium (to induce an equilibrium shift) when the solvent quantity is employed. Hence, pure α-pinene is necessary in this system.

2.4.2. CPL Excitation (CPLE) of Eu_S/R-α-pinene

CPLE measures the origin of CPL spectra. Fig. 2.7.(a) presents a nearly

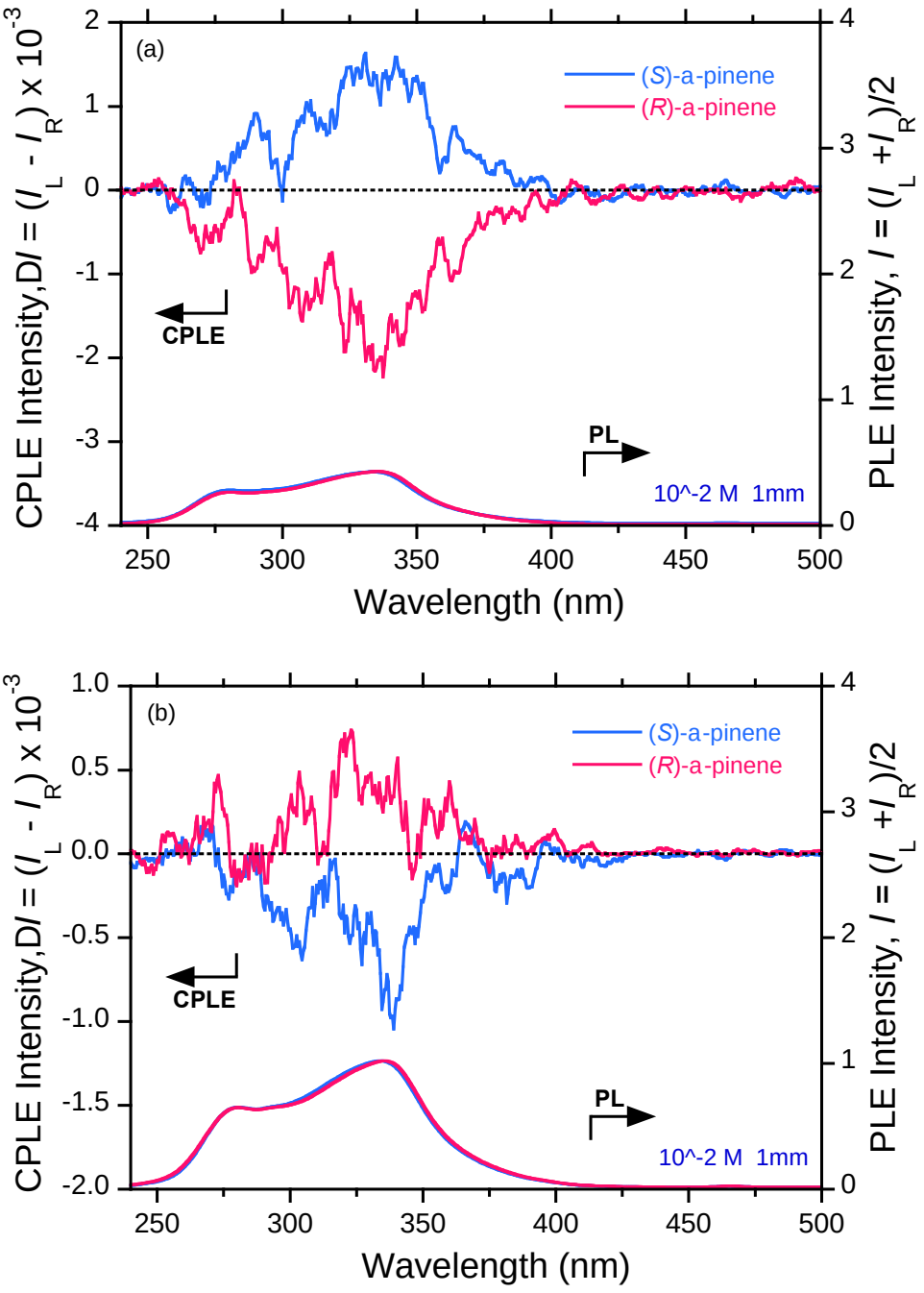

Fig. 2.7. CPLE/PLE spectra of ***Eu_S/R-α-pinene*** monitored at (a) $^5D_0 \rightarrow {}^7F_1$ (λ_{mon} 593 nm) and (b) $^5D_0 \rightarrow {}^7F_2$ (λ_{mon} 613 nm)

mirror-image CPLE spectra of ***Eu_S/R*-α-pinene** monitored at 593 nm which corresponds to the $^5D_0 \rightarrow {}^7F_1$ transition. ***Eu_S*-α-pinene** showed a (+)-sign of CPLE spectra whereas ***Eu_R*-α-pinene** showed a (-)-sign. Both are identical to the (+)- and (-)-signs of the CPL spectra (*see* Fig. 2.3). The same trend was also observed when monitored at 613nm ($^5D_0 \rightarrow {}^7F_2$ transition) as shown in Fig. 2.7. (b) where ***Eu_S*-α-pinene** shows a (-)-sign of CPLE spectra whereas ***Eu_R*-α-pinene** shows a (+)-sign. Similarly, both are identical to the (-)- and (+)-signs of the CPL spectra at second transition which is vice versa to the first transition (Fig. 2.2). These two sets of distinguishable ***Eu_S/R*-α-pinene** CPLE spectra in the region of photoluminescence excitation (PLE) bands corroborate the coexistence of *Δ*- and *Λ*-species of Eu(III)$(FOD)_3$ at the ground state upon association with α-pinene.

2.4.3. Circular dichroism (CD) of Eu_S/R-α-pinene

The CD measures the differential absorption of *left*- and *right*-circularly polarized light within an absorption band. The degree of CD is reported in terms of the absorbance dissymmetry factor, g_{abs} defined by equation (12)

$$g_{abs} = \frac{e_L - e_R}{1/2(e_L + e_R)} \qquad (12)$$

In eqn. (12), ε_L and ε_R represent the extinction coefficients for absorption of *left*- and *right*-circularly polarized light, respectively. From the CD/UV-Vis spectra of

***Eu_S/R*-α-pinene** (Fig. 2.8), the broad shoulder UV signals in the range of 270-350 nm are ascribed to π-π^* and n-π^*/π-π^* bands originating from the double bond of pinenes and diketonates of the $(FOD)_3$ ligands. ***Eu_R*-α-pinene** clearly exhibited CD signals at

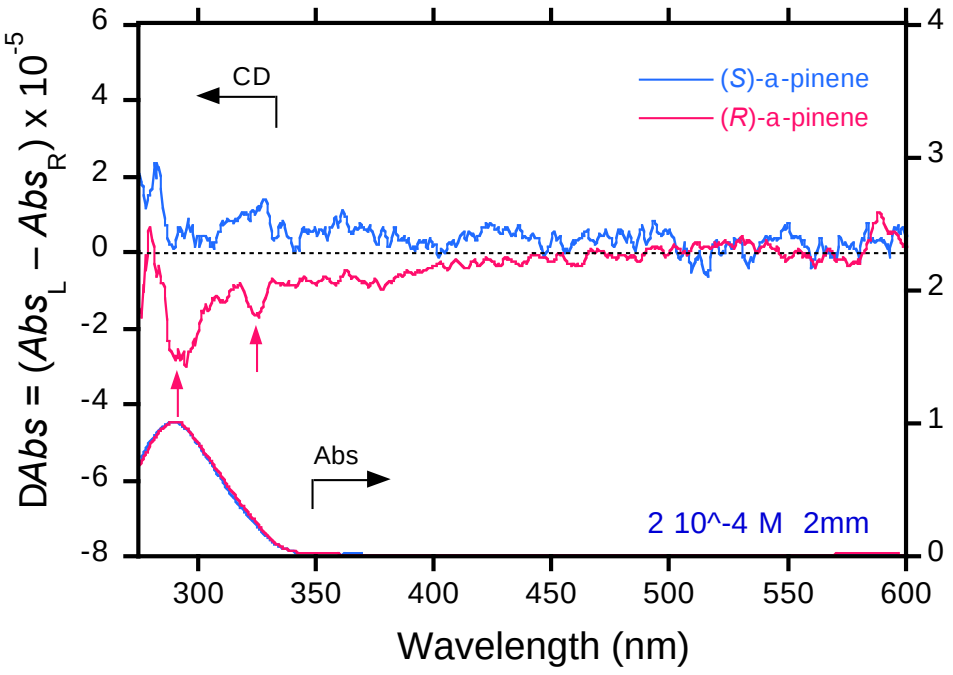

Fig. 2.8 CD/UV-visible spectra of ***Eu_S/R*-α-pinene** at Eu(III)$(FOD)_3$ absorption range

292 nm and 324 nm (given by the arrows) but ***Eu_S*-α-pinene** did not show distinguished signal within the europium absorption range. The absorption dissymmetry factors, g_{abs} of ***Eu_R*-α-pinene** were -3.0×10^{-5} at 292 nm and -5.5×10^{-5} at 324 nm, respectively. The extremely small values could be due to low concentration of the samples for detection.

2.5. Optical properties of *Eu_S/R*-α-pinene

2.5.1. Highly Resolved Photoluminescence (PL) spectra

A photoluminescence spectrum is recorded by fixing the excitation wavelength, while the detection wavelength of the spectrofluorimeter is scanned. Fig. 2.9 shows an intense photoluminescence at $^5D_0 \rightarrow {}^7F_J$ transitions (J=0-6) from the $^5D_0$ excited state to

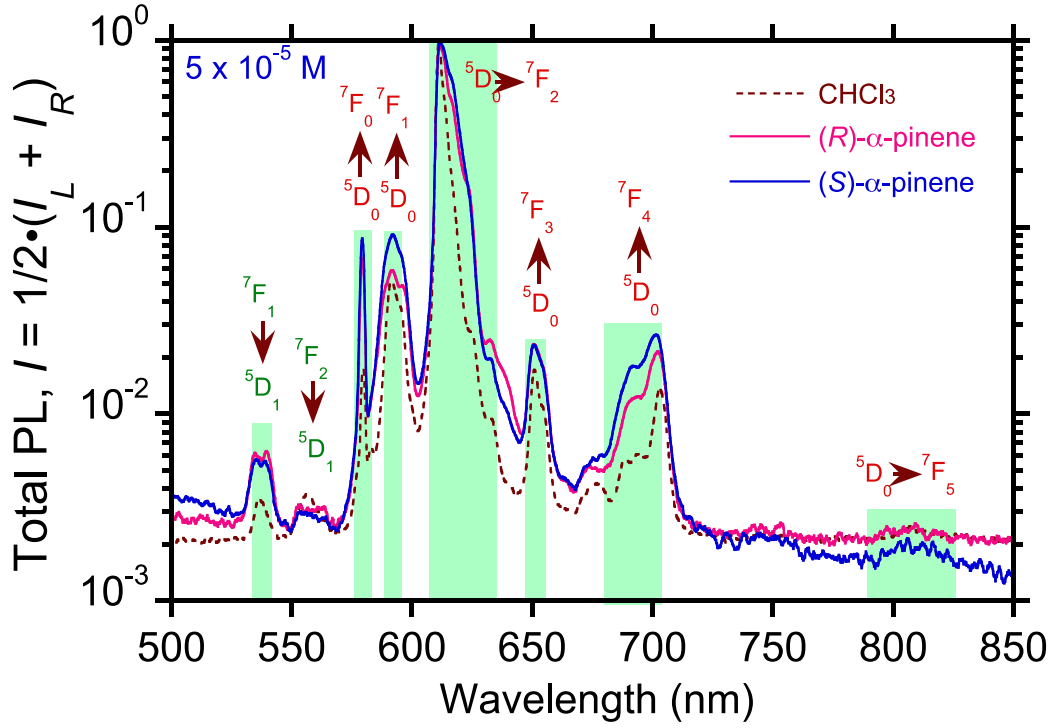

Fig. 2.9. PL spectra of Eu(III)(FOD)$_3$ in $CHCl_3$ (λ_{ex} 278 nm) and ***Eu_S/R*-α-pinene** (λ_{ex} 317 nm)

the J levels of the ground term ^7F at 579, 592, 611, 651, 702, 752, 807 nm for Eu(III)(FOD)$_3$ in EtOH-free, dehydrated chloroform containing amylene as stabiliser. Although much less common, we could also observe the transition from higher excited state of $^5D_1 \rightarrow {}^7F_J$ (J=1,2) at 536 and 556 nm, respectively. The production of bright-red luminescence is indicative of efficient ligand-to-metal charge transfer (LMCT)[2a-d]. The

spectra at $^5D_0 \rightarrow {}^7F_J$ transitions (J=0 -5) for ***Eu_S*-α-pinene** and ***Eu_R*-α-pinene** were so close to that Eu(III)$(FOD)_3$ in $CHCl_3$ but the profiles are slightly broaden giving a hint that weak intermolecular interactions probably occur between Eu(III)$(FOD)_3$ and the chiral α-pinene.

The associated photoluminescence quantum yields, ϕ_{PL} at the europium first and second transitions are summarized in Table 2.1.

Table 2.1 PL quantum yield, ϕ_{PL} of Eu(III)$(FOD)_3$ in $CHCl_3$ and ***Eu_S/R*-α-pinene**

Chelate-ligand	Solvents	Quantum Yield, ϕ_{PL}	
		F_1 transition ($^5D_0 \rightarrow {}^7F_1$)	F_2 transition ($^5D_0 \rightarrow {}^7F_2$)
Eu(III)$(FOD)_3$	$CHCl_3$	0.003	0.039
	(*S*)-α-pinene	0.003	0.034
	(*R*)-α-pinene	0.002	0.028

Quantum yields of ***Eu_S*-α-pinene** and ***Eu_R*-α-pinene** at $^5D_0 \rightarrow {}^7F_1$ and $^5D_0 \rightarrow {}^7F_2$ transitions are estimated to be 0.2–0.3 % and 2.8–3.4 %, respectively in relative to 5,5'-bis[4-(*N*,*N*-diphenylamino)phenyl]-3-dimesitylboryl-2,2'-bithiophene[3] with quantum yield (QY) of 67%. The values are comparable with Eu(III)$(FOD)_3$ in $CHCl_3$ corroborating weak intermolecular interactions and suggesting no indication of new product formation.

2.6. Conclusion

CPL of Eu(III)$(FOD)_3$ was induced when dissolved in neat chiral α-pinene and β-pinene although not satisfactorily induced in neat chiral limonene and *trans*-pinane. Bicyclic α-pinene is the rigid framework as compared to the floppy monocyclic limonene and *trans*-pinane with a bicyclic without C-C double-bond. The C-C double-bond inside the bicyclic ring of α-pinene may contribute to effective intermolecular interaction with the Eu(III)$(FOD)_3$ complex. The effect of the double-bond position could be seen from the comparison with β-pinene, in which the C-C double-bond is outside the ring. As expected, CPL signals were not detected for Eu(III)$(FOD)_3$ without addition of chiral agent affirming the assumption that Eu(III)$(FOD)_3$ exists in equal mixture of *Δ*- and *Λ*-species. Mirror-image spectra shown by CPLE also confirm that the two nearly mirror-image CPL signals arise from two different enantiomeric pairs of *Δ*-(*R)* and *Λ*-(*S*) or *Δ*-(*S)* and *Λ*-(*R*). The shape of Eu(III)$(FOD)_3$ PL spectrum was altered slightly by dissolving in neat α-pinene, indicating the formation of complex-solvent adducts by some weak intermolecular non-bonding interactions. The association by α-pinene does not affect the PL quantum yield, ϕ_{PL} since it only reflects the emission at $^5D_0 \rightarrow {}^7F_2$ where the dissymmetry ratio, g_{em} is the lowest.

2.7. References

[1] (a) N. Berova, P. L. Polavarapu, K. Nakanishi, R. W. Woody (eds), *Comprehensive Chiroptical Spectroscopy: Instrumentation, Methodologies, and Theoretical Simulations,* Vol 1, Wiley (2012). (b) N. Berova, P. L. Polavarapu, K. Nakanishi, R. W. Woody (eds), *Comprehensive Chiroptical Spectroscopy: Appplications in Stereochemical Analysis of Synthetic Compounds, Natural Products, and Biomolecules,* Vol 2, Wiley (2012).

[2] (a) M. D. Ward, *Coord. Chem. Rev*., 2007, **251**, 1663. (b) M. D. Ward, *Coord. Chem. Rev*., 2010, **254**, 2634. (c) F. F. Chen, Z. –Q. Bian and C.-H. Huang, *Coord. Chem. Rev*., 2010, **254**, 991. (d) Z. Chen, H. Xu, in *Rare Earth Coordination Chemistry: Fundamentals and Applications* (ed.: C. Huang), Wiley-VCH, Singapore, 2010, p.473.

[3] A. Wakamiya, K. Mori and S. Yamaguchi, *Angew. Chem., Int. Ed., 2007,* **46**, 4273-4276.

Chapter 3

Comparison of the chiroptical properties with the solvents with P=O, P and N elements and non-fluorinated Eu(III) complex in α-pinene

3.1. Introduction

In a recent previous work, Imai, Fujiki, and coworkers[1] reported on induced-CD and -CPL spectra by solely mixing Eu(III)$(hfa)_3$ (hfa = hexafluoroacetylacetonate) in the presence of C_2-symmetrical BINAP[2a,b] in an equimolar ratio. The D_3-symmetry Eu(III)$(hfa)_3$ could be a racemic mixture of chiral metal complexes, and exists as CD-silent and CPL-silent states. The work inferred a certain perturbation affecting the left-right equilibrium at the inner-sphere by an ultraweak chiral interaction between the soft-base P(III) to the hard-acid Eu(III). This scenario may contradict the conventional hard-soft-acid-base (HSAB) theory, which predicts that lanthanide(III) ions prefer to bind to hard bases such as oxygen and nitrogen elements[3]. Therefore, in this work, we also investigated the interaction of this soft-base, BINAP with the C_3-symmetrical Eu(III)$(FOD)_3$ as well as the hard-base BINAPO[1,2a] and α-phenylethylamine (α-PEA)[4] for comparison with pure hydrocarbon α-pinene. In the case of α-PEA, neat and diluted solutions were sampled. In this chapter, the emergence of CD and CPL signals from Eu(III)$(FOD)_3$ complexed with these solvents is presented. In addition, we also measured CPL for Eu(III)$(DPM)_3$ dissolved in α-pinene for comparison of fluorinated Eu(III)$(FOD)_3$ with non-fluorinated Eu(III) ligands.

3.2. Preparation of CD and CPL samples of *Eu_S/R*-X (X = BINAP, BINAPO, α-PEA) and *EuDPM_ R*-α-pinene

Eu(III) tris(6,6,7,7,8,8,8-heptafluoro-2,2-dimethyl-3,5-octanedionate) (Eu(III)$(FOD)_3$), Eu(III) tris(2,2,6,6-tetramethyl- heptane-3,5-dione) (Eu(III)$(DPM)_3$) and (*S)/(R)*-2,2-bis(diphenylphosphino)-1,1-binaphthalene (BINAP) was purchased from Sigma-Aldrich (Japan). (*S*)/(*R*)-2,2-bis(diphenylphosphinyl)-1,1-binaphthalene (BINAPO) was purchased from Daicel Corporation (Osaka, Japan). (*1S*)-(-)/*(1R*)-(+)-1-phenylethylamine (α-PEA) was purchased from TCI (Tokyo, Japan). Chloroform was purchased from (Wako). The chloroform used was *EtOH*-free and contains amylene as a stabilizer. ***Eu_S/R*-X (1:1)** (**X**= BINAP, BINAPO and α-PEA) were prepared by dissolving Eu(III)$(FOD)_3$ and X compounds in chloroform separately. The Eu(III)$(FOD)_3$ and X solution were mixed into an equimolar mixture. ***Eu_S/R*-α-PEA (neat)** was prepared by dissolving Eu(III)$(FOD)_3$ in neat α-PEA. ***EuDPM*_α-pinene** was prepared by dissolving Eu(III)$(DPM)_3$ in neat α-pinene. All the samples were heated at mild temperature of 50-60°C for about 5 min, then, left to cool to room temperature prior spectroscopic measurements.

3.3. Chiroptical properties of *Eu_S/R*-X (1:1) *(*X = BINAP, BINAPO, and α-PEA)

3.3.1. Circular Dichroism (CD)

The CD/UV-vis spectra of ***Eu-S/R*-BINAP (1:1)** in $CHCl_3$ and (*S*)/(*R*)-BINAP dissolved in $CHCl_3$ is shown in Fig. 3.1. The π-π^* characteristic UV bands of the (*S*)/(*R*)-BINAP naphthyl groups were observed in between 230 and 270 nm and it tailed out to 350 nm. Meanwhile, the UV bands of ***Eu_S/R*-BINAP (1:1)** appeared in between 260 and 350 nm. The absorption of Eu(III)$(FOD)_3$ could be seen from 270 to 350 nm. (*S*)- and *(R)*-BINAP showed a clear mirror-image CD spectra indicating an enantiomeric pair relationship at ground state level. However, the CD signals of ***Eu_S/R*-BINAP (1:1)** were undetectable due to extremely low degree of g_{abs}. Contrarily,

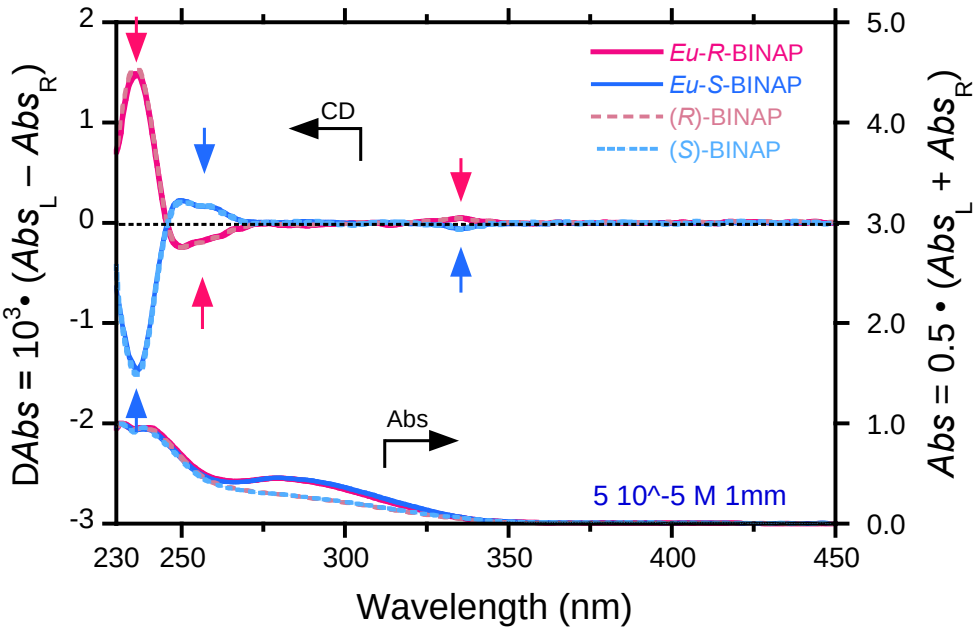

Fig. 3.1. CD/UV-Vis spectra of ***Eu_S/R*-BINAP (1:1)** as compared to (*R*)/(*S*)-BINAP in $CHCl_3$

***Eu_S/R*-BINAPO (1:1)** displayed a clear mirror image CD spectra in the range of Eu(III)$(FOD)_3$ and BINAPO absorption bands as shown in Fig. 3.2. The π-π^* characteristic UV bands of the (*S*)/(*R*)-BINAPO naphthyl groups were observed from 230 to 270 nm and it tailed out to 340 nm. A clear mirror-image CD spectra of (*S*)- and *(R)*-BINAPO were also observed within the absorption bands.

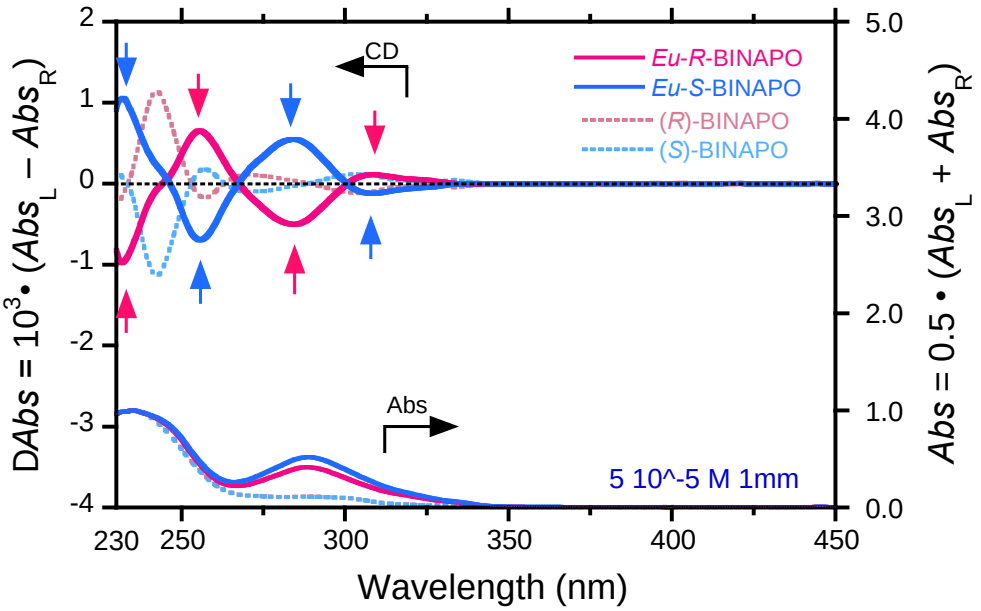

Fig. 3.2. CD/UV-Vis spectra of ***Eu_S/R*-BINAPO (1:1)** as compared to (*R*)/(*S*)-BINAPO in $CHCl_3$

Clearer CD spectra of ***Eu_S/R*-α-PEA (1:1)** were not obtained due to high absorption of α-PEA caused by an overlapping between π-π^* bands of PEA and n-π^* bands of $(FOD)_3$-ligands in near-UV region.

3.3.2. Circularly polarized luminescence (CPL)

At the photoexcited state, ***Eu_S/R*-BINAP (1:1)**, ***Eu_S/R*-BINAPO (1:1)**, ***Eu_S/R*-α-PEA (neat)** and ***Eu_S/R*-α-PEA (1:1)** clearly exhibited CPL signals at both $^5D_0 \rightarrow {}^7F_1$ and $^5D_0 \rightarrow {}^7F_2$ Eu^{3+} ion transitions as shown in Fig. 3.3, Fig. 3.4, Fig. 3.5 and Fig. 3.6.

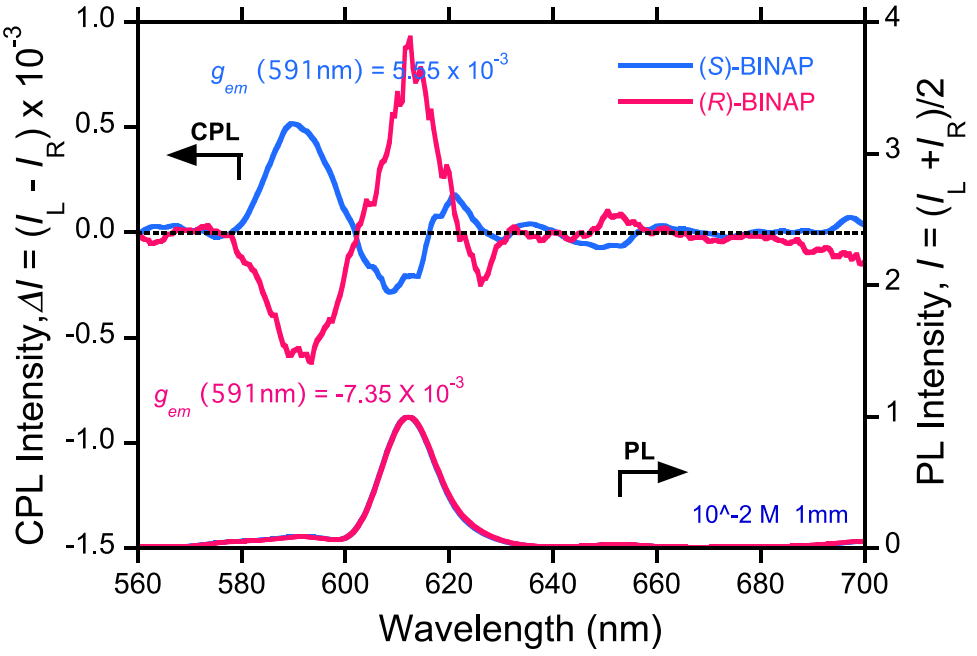

Fig. 3.3 CPL/PL spectra of ***Eu_S/R*-BINAP (1:1)** at $^5D_0 \rightarrow {}^7F_1$ and $^5D_0 \rightarrow {}^7F_2$ transitions (Ex 340nm)

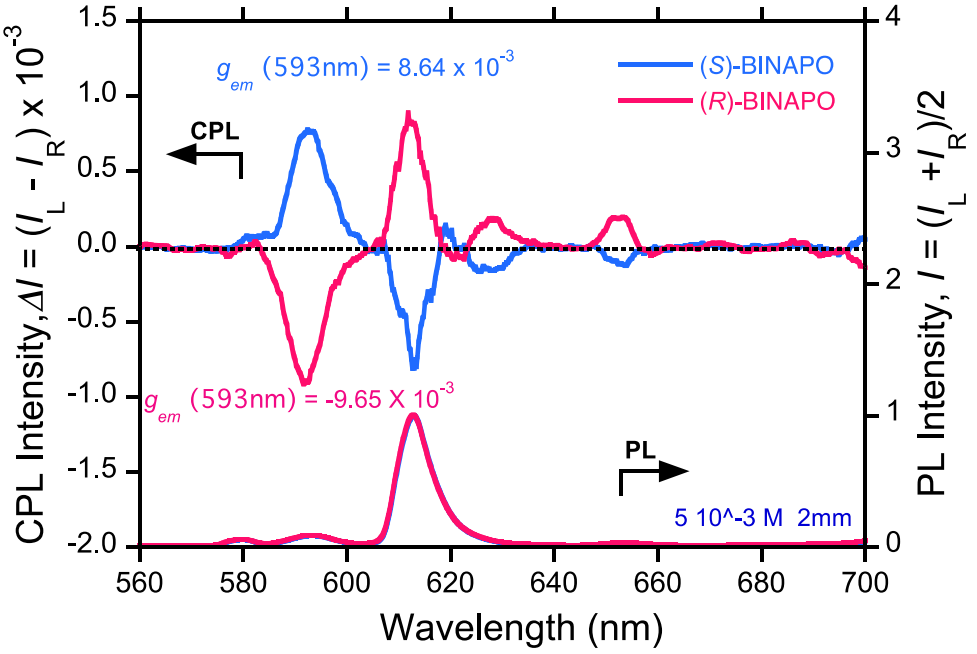

Fig. 3.4 CPL/PL spectra of ***Eu_S/R*-BINAPO (1:1)** at $^5D_0 \rightarrow {}^7F_1$ and $^5D_0 \rightarrow {}^7F_2$ transitions (Ex 345nm)

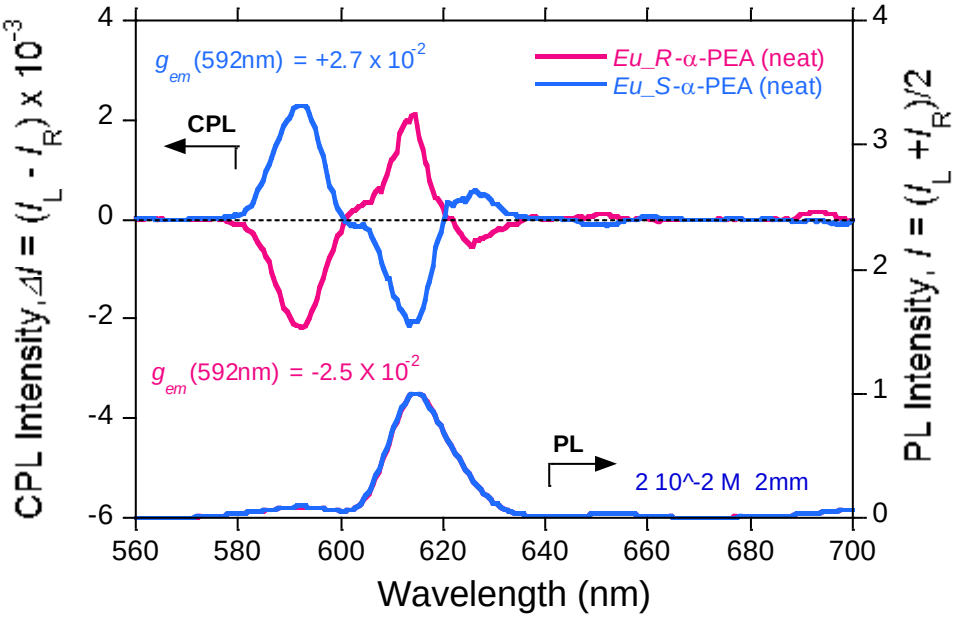

Fig. 3.5 CPL/PL spectra of ***Eu_S/R*-α-PEA (neat)** at $^5D_0 \rightarrow {}^7F_1$ and $^5D_0 \rightarrow {}^7F_2$ transitions (Ex 340nm)

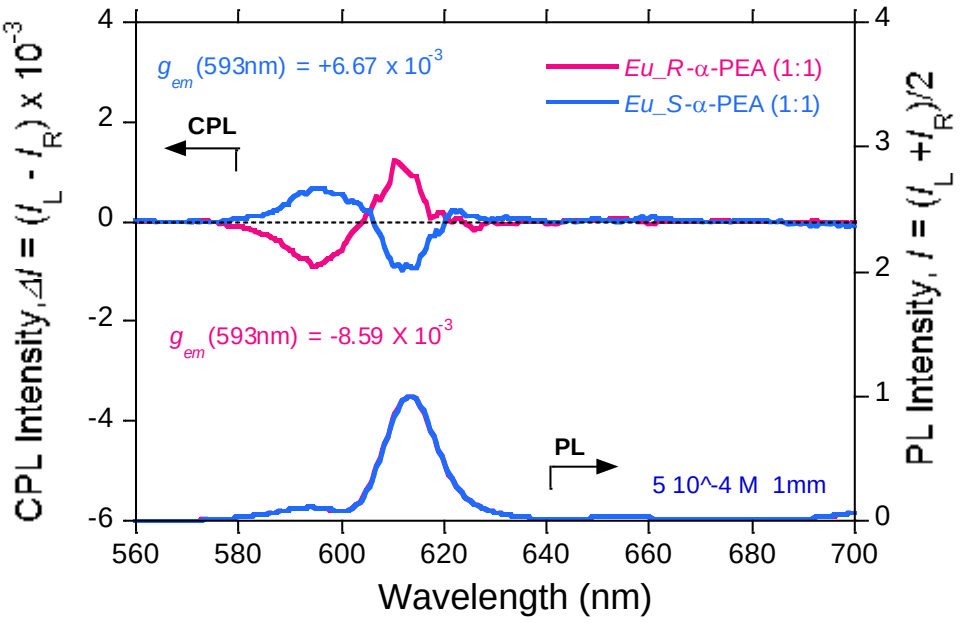

Fig. 3.6 CPL/PL spectra of ***Eu_S/R*-α-PEA (1:1)** at $^5D_0 \rightarrow {}^7F_1$ and $^5D_0 \rightarrow {}^7F_2$ transitions (Ex 320nm)

The g_{em} values of ***Eu_S*- and *Eu_R*-BINAP (1:1)** are $+5.55 \times 10^{-3}$ and -7.35×10^{-3} respectively **(**Fig. 3.3**)**, which is slightly higher as compared to ***Eu_S/R*-α-pinene**. Meanwhile, the spectra displayed by ***Eu_S/R*-BINAPO (1:1)** (Fig. 3.4) and ***Eu_S/R*-α-PEA (neat) (**Fig. 3.5**)** were nearly mirror-image. As for ***Eu_S/R*-BINAPO (1:1)**, the g_{em} values were almost double the values of ***Eu_S/R*-α-pinene** with $+8.64 \times 10^{-3}$ and -9.65×10^{-3} for ***Eu_S*- and *Eu_R*-BINAPO (1:1)**, respectively. The highest g_{em} values could be observed in ***Eu_S/R*-α-PEA (neat)** with $+2.7 \times 10^{-2}$ for ***Eu_S*-α-PEA (neat)** and -2.5×10^{-2} for ***Eu_R*-α-PEA (neat),** which is about one order magnitude higher as compared to ***Eu_S/R*-α-pinene**. In very diluted solution (an equimolar mixture) of ***Eu_S/R*-α-PEA (1:1)**, the g_{em} values were $+6.67 \times 10^{-3}$ and -8.59×10^{-3} for ***Eu_S*-** and ***Eu_R*-α-PEA (1:1)** in which the values were not much decreased.

The g_{em} values of ***Eu_R*-BINAP (1:1)** increase with the increase of mixture concentration from 10^{-4} to 10^{-2} M (Fig. 3.7(a)). This tendency is similar to ***Eu_S/R*-α-pinene** and consistent with the proposed mechanism whereby CPL is induced by the interaction with the solvent. In contrast, the g_{em} values of ***Eu_R*-BINAPO (1:1)** is nearly unchanged at various concentration from 10^{-2} to 10^{-4} M indicating strong coordination between the (Eu(III)$(FOD)_3$) complex and the BINAPO (Fig. 3.7(b)). *Eu_R*-α-PEA (neat) also show the same trend at 10^{-2} to 10^{-3} M but the value abruptly decreased when the concentration reached 10^{-4} M which is the concentration of ***Eu_R/S*-α-PEA (1:1)** (Fig. 3.7(c))**.**

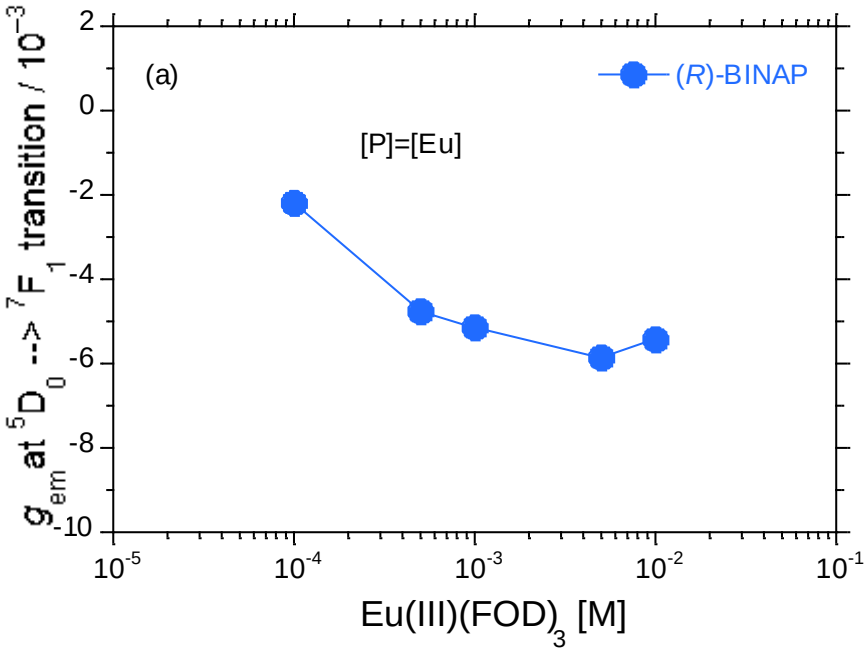

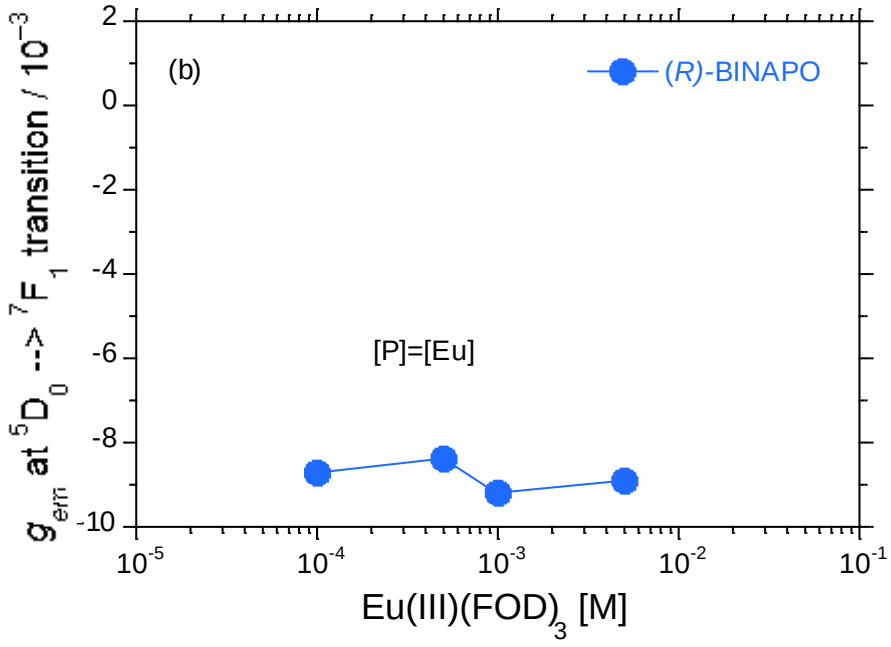

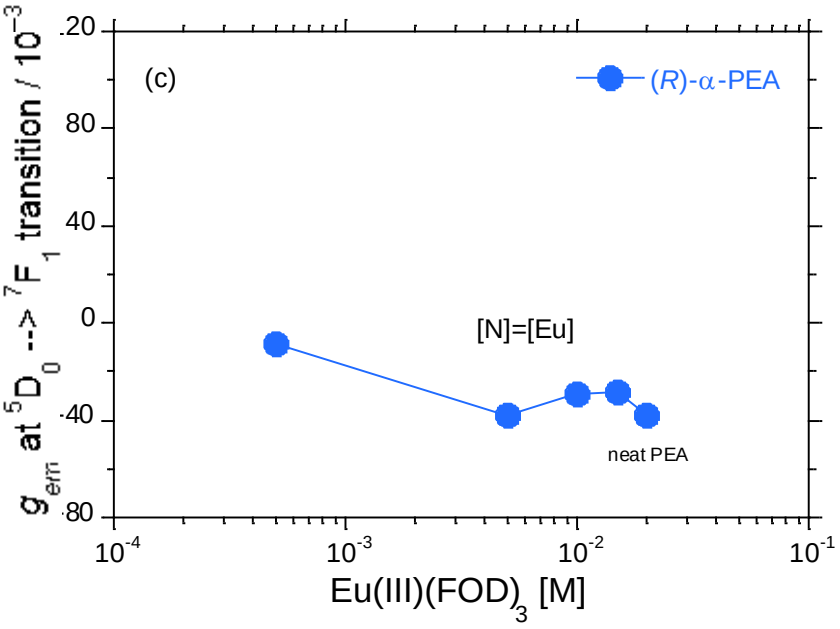

Fig. 3.7 Plots of g_{em} values at F_0-F_1 transition versus 1:1 mixture concentration of (a) ***Eu-S/R*-BINAP**, (b) ***Eu-S/R*-BINAPO** and (c) ***Eu-S/R*-α-PEA**

3.4. CPL of *EuDPM*_α-pinene

Fig. 3.8 shows that CPL signal was undetectable for Eu(III) complex with non-fluorinated ligands in neat α-pinene. This suggests that weak C-*F*/*H*-C interactions could play an important role in the induced-CPL observed in ***Eu_S/R-α-pinene***.

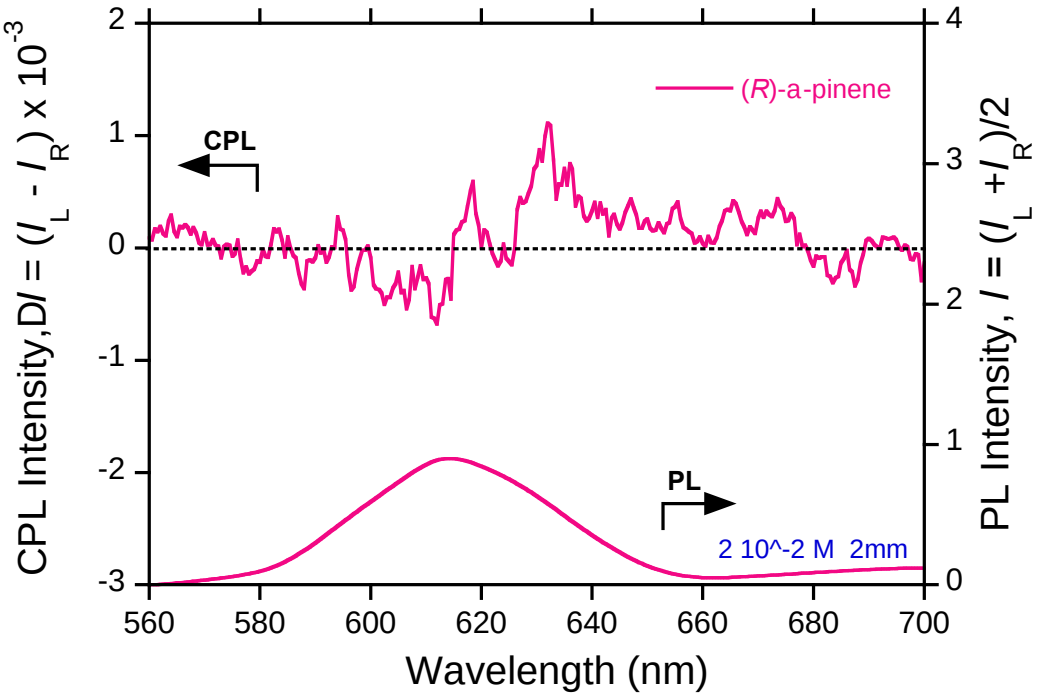

Fig. 3.8. CPL/PL spectra of ***EuDPM_R-α-pinene*** at $^5D_0 \rightarrow {}^7F_1$ and $^5D_0 \rightarrow {}^7F_2$ transitions

3.5. Conclusion

Optical activity at the ground state was induced in ***Eu_S/R*-BINAPO (1:1)**, but not in ***Eu_S/R*-BINAP (1:1)**,. This suggests that perturbation of the equilibrium occurred in ***Eu_S/R*-BINAPO (1:1)** at the ground state due to stronger coordination possibly by the hard base O of BINAPO. However, optical activity at the photoexcited state was induced in ***Eu_S/R*-BINAP (1:1)**, ***Eu_S/R*-BINAPO (1:1)**, ***Eu_S/R-a*-PEA (neat)** and ***Eu_S/R*-α-PEA (1:1)**, implying that not only the hard base O=P(V) of BINAPO and N of α-PEA resulted in CPL-active complex but also the soft base P(III) of BINAP. The degree of g_{em} values at the first transition of these chelate:solvent adducts is slightly higher compared to that of ***Eu_S/R*-α-pinene** and thus, can be arranged in the order of α-pinene < BINAP < diluted **α-PEA** < BINAPO < neat **α-PEA.** The plots of g_{em} values versus concentration suggest that perturbation of the equilibrium by a soft-base occurred through weak interactions and by the hard-base occurred through strong coordination. Nonetheless, the nature of the interactions that caused the induced-CPL in each adduct complex cannot be determined by only the CPL profiles and the extent of the dissymmetry ratio, g_{em}. On the other hand, the undetectable CPL signal from non-fluorinated Eu(III) complex*, EuDPM*_α-pinene has given some hints on the possible interactions that caused the equiblirium shift in ***Eu_S/R-α-pinene***. This will be further confirmed in Chapter 4 and 5.

3.6. References

[1] Md. A. Subhan, Y. Hasegawa, T. Suzuki, S. Kaizaki, S. Yanagida, *Inorg. Chim. Acta,* 2009*,* **362***,* 136.

[2] (a) Y. Kono, K. Nakabayashi, S. Kitamura, M. Shizuma, M. Fujiki and Y. Imai, *RSC Adv.,* 2016, **6**, 40219-40224. (b) Y. Kono, N. Hara, M. Shizuma, M. Fujiki and Y. Imai, *Dalton Trans.,* 2017, **46**, 5170-5174.

[3] R. G. Pearson, *J. Am. Chem. Soc.*, 1963, ***85***, 3533–3539.

[4] H.G. Brittain and F. S. Richardson, *J. Am. Chem. Soc., 1977,* **99**, 65-70.

Chapter 4

Elucidation of the geometrical structures and the chiral origins at the ground state revealed by ^{19}F-NMR and ^{31}P{^{1}H}--NMR analyses

4.1. Introduction

The complex Eu(III)(FOD)$_3$ has two unsymmetrical β-diketonates and because of that it is assumed to have two different stereochemical structures; polar C_3-symmetric *facial* and less-polar C_1-symmetric *meridional* forms in solution. Although single crystal analysis may facilitate the investigation of geometrical structures in the solid, it may not apply to fluidic solution at ambient temperature. Another way to elucidate the geometrical structure of Eu(III)(FOD)$_3$ is by investigating whether the environment for the three ligands are the same for all the three ligands or one is different from the other two or each of it is different. It was long assumed that the structure at ground state might not change much at the photoexcited state. We suggest that this can be solved by ^{19}F-NMR spectroscopy since Eu(III)(FOD)$_3$ is a fluorinated complex. Although NMR spectroscopy reflects only the ground state, the structure might not change much at the photoexcited state. Therefore it is hoped that the investigation would answer the open question on the origin of the chiral induction. In this chapter, we present the ^{19}F-NMR profiles of (FOD)$_3$-ligands, Eu(III)(FOD)$_3$, ***Eu_S/R*-α-pinene (neat)**, ***Eu_S/R*-α-pinene (1:1),** ***Eu_S/R*-BINAP**, ***Eu_S/R*-BINAPO**, ***Eu_S/R*-α-PEA (1:1)** and ***Eu_S/R*-α-PEA (neat)**. We also present the profiles of 2,2-dimethyl-6,6,7,7,8,8,8-heptafluoro-3,5-octanedione (HFOD) as free-ligand

dissolved in $CDCl_3$, neat (*S*)-α-pinene and mixed with (*S*)-BINAPO at equivalent ratio to elucidate the origin of additional small peaks that appeared. The environment of P elements of BINAP and BINAPO before and after complexation with Eu(III)$(FOD)_3$ was also investigated by $^{31}P\{^1H\}$-NMR spectroscopy for supporting evident.

4.2. Preparation of *Eu_S/R*-X (X = α-pinene, BINAP, BINAPO, and α-PEA) in $CDCl_3$

Eu(III) tris(6,6,7,7,8,8,8-heptafluoro-2,2-dimethyl-3,5-octanedionate) (Eu(III)$(FOD)_3$) and (*S)/(R)*-BINAP were purchased from Sigma-Aldrich (Japan). (*S*)/(*R*)-[1,1'-Binaphthalene]-2,2'-diylbis[1,1-diphenyl-1,1'-phosphineoxide] (BINAPO) was purchased from Daicel. (*1S*)-(-)/ *(1R*)-(+)-1-phenylethylamine was purchased from Tokyo Chemical Industry Co. (TCI) (Tokyo, Japan). ***Eu_S/R*-X** (**X**= α-pinene (neat) and α-PEA (neat)) were prepared by dissolving (Eu(III)$(FOD)_3$) in neat X solvent. ***Eu_S/R*-X (1:1)** (**X**= α-pinene, BINAP, BINAPO and α-PEA) were prepared by dissolving Eu(III)$(FOD)_3$ and X compounds in chloroform separately. The Eu(III)$(FOD)_3$ and X solution were mixed into an equimolar amount.

4.2.1. Single-tube measurement

For ^{19}F-NMR measurement, Eu(III)$(FOD)_3$ in $CDCl_3$ and equimolar mixture of Eu(III)$(FOD)_3$ and X solvent *(*X = α-pinene, BINAP, BINAPO, and α-PEA) diluted in $CDCl_3$ were prepared with a drop of diluted hexafluorobenzene in $CDCl_3$ as a reference. For $^{31}P\{^1H\}$-NMR measurement, *(S)/(R)*-BINAP and *(S)/(R)*-BINAPO in $CDCl_3$ were prepared with a drop of diluted trimethyl phosphate (TMP) in $CDCl_3$ as a reference.

4.2.2. Dual-tube measurement

For ^{19}F-NMR measurement, ***Eu_S/R*-α-pinene** and ***Eu_S/R*-α-PEA (neat)** with a drop of diluted C_6F_6 in $CDCl_3$ as reference was inserted into a coaxial tube and the tube was inserted into a NMR tube. For $^{31}P\{^1H\}$-NMR measurement, equimolar mixture of Eu(III)$(FOD)_3$ and X chiral additives *(*X = BINAP, and BINAPO) in $CDCl_3$ is filled in an NMR sample tube. A drop of TMP is diluted in $CDCl_3$ as a reference solution and the solution was filled into a coaxial tube and the tube was inserted into the NMR sample tube.

The C_6F_6 signal appeared was set to -164.9 ppm[1] and the TMP signal was set to 0.0 ppm[2] at the spectra for reference peak.

4.3. . NMR Spectral Analysis

4.3.1. ^{19}F-NMR

4.3.1.1. Profiles of HFOD in $CDCl_3$ and Eu(III)$(FOD)_3$ in $CDCl_3$

HFOD-ligand in $CDCl_3$ displays three significant signals at (*a*) δ 83.78 ppm, (*b*) δ -124.91 ppm and (*c*) δ -130.17 ppm (Fig. 4.1). The three different environments displayed by the spectra match the three different types of fluorine moieties attached to the ligand. From the peak integration, the ratio of (*a*): (*b*): (*c*) is found to be 3:2:2. Thus,

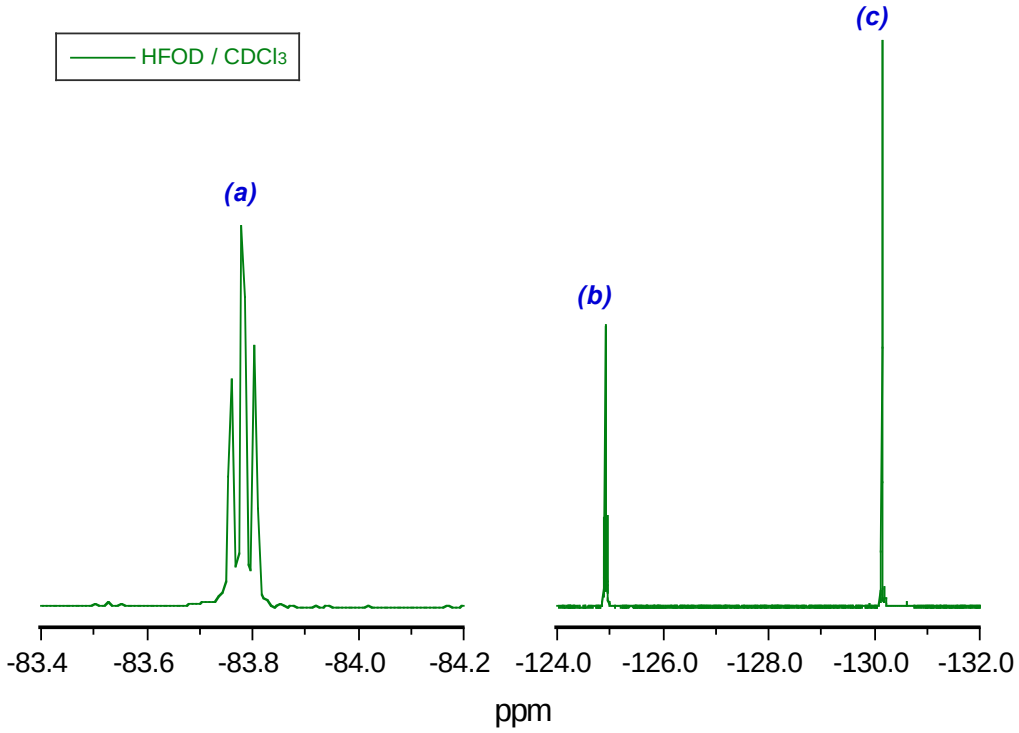

Fig. 4.1 ^{19}F-NMR profile of HFOD-ligand in $CDCl_3$

we could assign (a) for the *outermost* $-CF_3$ (b) for the *middle* $-CF_2$ and (c) for the *inner* $-CF_2$ of the HFOD-ligand (Scheme 4.1).

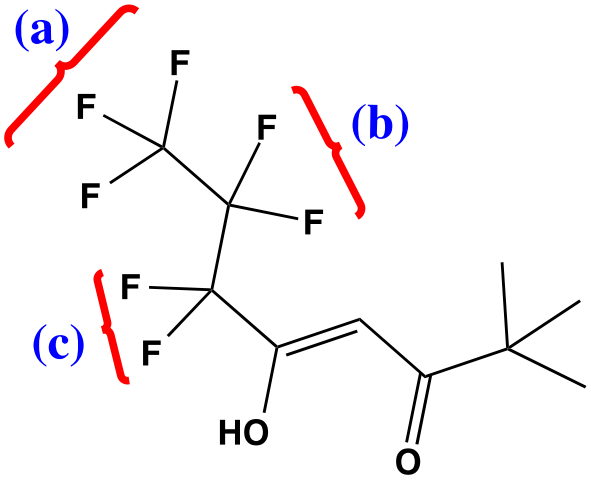

Scheme 4.1 The assignment of ^{19}F-NMR peaks from the profile at Fig. 4.1 to the HFOD-ligand structure

When the peaks are enlarged, we could observe a triplet at (*a*), a quartet at (*b*) and a sharp singlet at (*c*). The enlarged peak (*b*) and (*c*) is shown in Fig. 4.2. The coupling

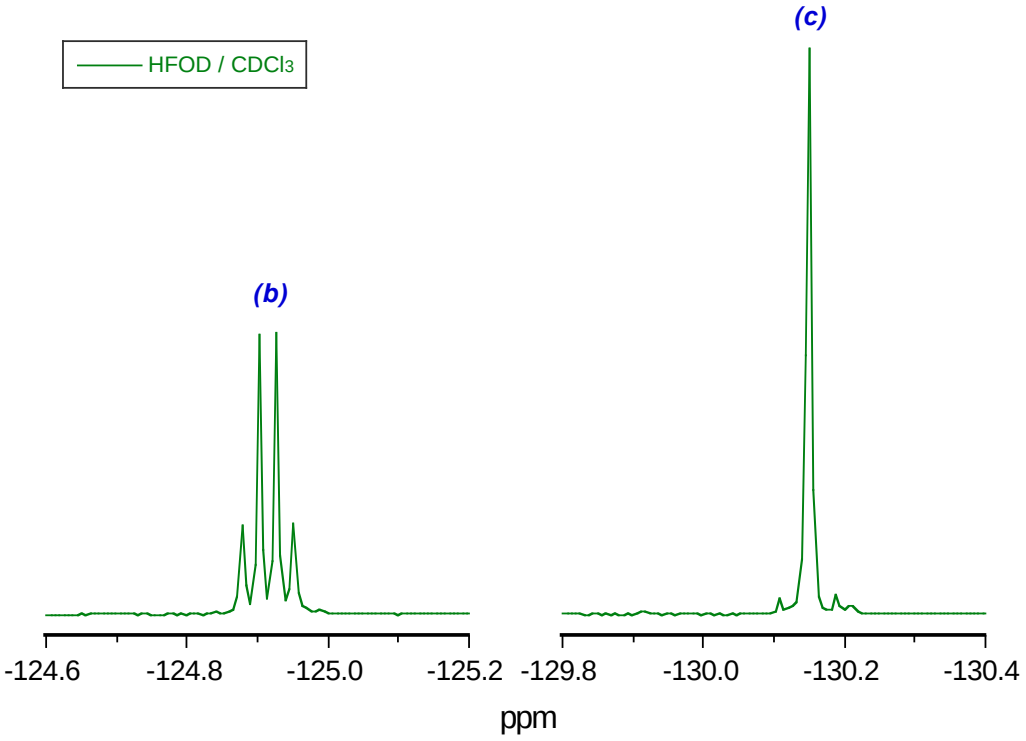

Fig. 4.2 ^{19}F-NMR profile of HFOD-ligand in $CDCl_3$ (enlarged peak (*b*) and (*c*)

constant, ^{3}J between *outermost* $-CF_3$ and *middle* $-CF_2$ was found to be 7.5 Hz but to our surprise, the ^{3}J between *middle* $-CF_2$ and *inner* $-CF_2$ is 0.0 Hz. This explains the appearance of a quartet at (*b*) and a sharp singlet at (*c*) instead of a multiplet at (*b*) and a triplet at (*c*). According to Karplus equation[3a,b], vicinal H-H couplings is maximal with protons with 180° and 0° dihedral angle and that coupling is minimal or near 0 for protons that are 90° from each other. Therefore, in the case of vicinal F-F between peak (*b*) and (*c*), the dihedral angle could be near 90° due to large van der Waals radii of F (1.47Å) resulting in zero coupling constant.

Fig. 4.3 compares the ^{19}F-NMR spectra of the HFOD in $CDCl_3$ (green) as a

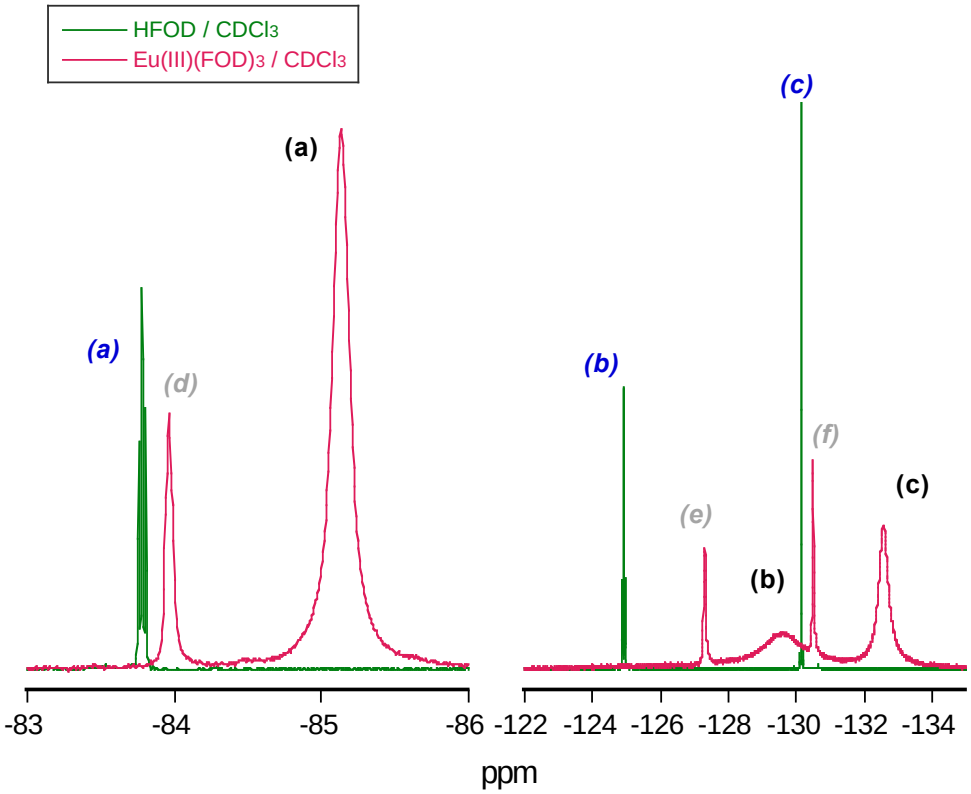

Fig. 4.3 ^{19}F-NMR profiles of Eu(III)$(FOD)_3$ complex in $CDCl_3$ (*red*) and HFOD-ligand in $CDCl_3$ (*green*)

free-ligand with the Eu(III)$(FOD)_3$ complex dissolved in $CDCl_3$ (*red line*). Upon

association with Eu(III) ion (*red line*), we observed three major broaden peaks and three minor sharp peaks and all of the peaks shifted upfield. The three major broaden peaks shifted upfield to (a) δ -85.13 ppm (b) a broad range from δ -127.0 to δ -131.0 ppm and (c) δ -132.55 ppm with peak integrals of 3:2:2 indicating equal environment amongst the three $(FOD)_3$-ligands attached to the Eu(III) ion in the complex. Thus, similar to the HFOD-ligand, we could assign (a) for the *outer* $-CF_3$ group (b) for the *middle* $-CF_2$ group and (c) for the *inner* $-CF_2$ group of the $(FOD)_3$-ligands (Scheme 4.2). The ratio

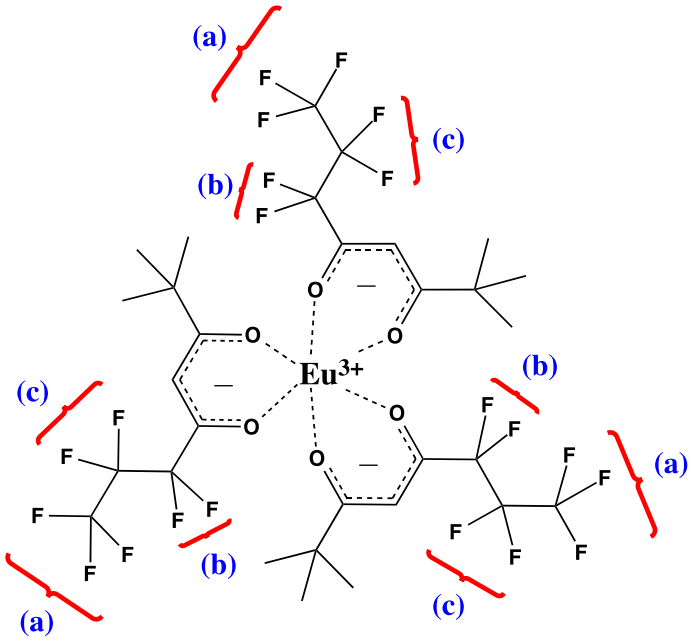

Scheme 4.2 The assignment of ^{19}F-NMR peaks from the profile of Eu(III)$(FOD)_3$ in $CDCl_3$ at Fig. 4.3

of the peak integrals of 3:2:2 gives a polar C_3-symmetric *facial* geometrical structure for Eu(III)$(FOD)_3$ in non-coordinating solvent chloroform and $CDCl_3$. Each *facial* then should contain an enantiomeric pair of Δ- and Λ-species. Referring to scheme 1.2, the ligands in the *facial* geometry are arranged symmetrically around the Eu(III) ion, while the ligands in the *meridional* geometry are arranged in such a way that one ligand is

unsymmetrical. In the case of *meridional*, we would expect two different peaks with 2:1 ratio for each $–CF_3$ and $–CF_2$ moieties but this kind of spectra was not observed. The molecular motion during the interconversion between enantiomeric *Δ*- and *Λ*-species that involves intermediate state could be responsible for the peak broadening.

Since europium can have more than six coordination number[1], the three small sharp peaks, in which we assigned as (*d*), (*e*) and (*f*) could be attributed to the $Eu(III)(FOD)_3 \bullet\ nH_2O$. From the ^{19}F-NMR profile, it is understood that the $Eu(III)(FOD)_3$ in $CDCl_3$ contains two different complexes, where six-coordinated $Eu(III)(FOD)_3$ exists in major and $Eu(III)(FOD)_3 \bullet\ nH_2O$ exists in minor. It can be seen that the minor peaks are not as sharp as the free HFOD-ligand peaks but slightly broaden and shifted upfield.

4.3.1.2. Profiles of Eu-S/R-α-pinene (neat) and Eu-S/R-α-pinene (1:1) in comparison with Eu(III)(FOD)$_3$ in CDCl$_3$

Similar to Eu(III)(FOD)$_3$ in CDCl$_3$, three significant peaks assigned as (a), (b) and (c) appeared for both ***Eu_S-*** and ***Eu_R*-α-pinene** (neat) and those peaks sharpen and shifted upfield to (a) δ -85.55 ppm (b) δ -131.61 ppm and (c) δ -133.20 ppm from that of Eu(III)(FOD)$_3$ in CDCl$_3$ (Fig. 4.3). Upon addition of α-pinene, the interconversion between the enantiomeric Δ- and Λ-species is no longer occurred due to

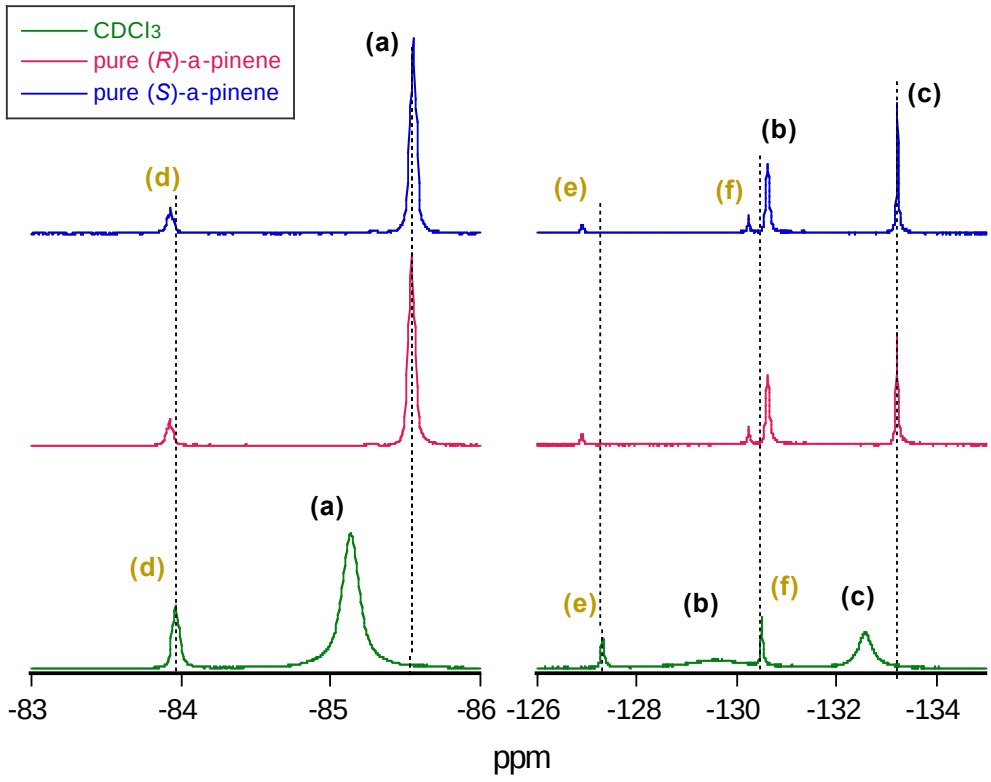

Fig. 4.4 ^{19}F-NMR profiles of Eu(III)(FOD)$_3$ in CDCl$_3$ (green) and ***Eu*_S/*R*-α-pinene (neat)** (blue and red)

interactions with the α-pinene. This explains that the sharpening of the peaks implies the preference towards one-handed chirality of either Δ-*R*/*S* or Λ-*R*/*S* with the ratio of

Δ-R/S : *Λ-R/S* is unequal to one. This creates a diastereomeric pair of *Δ-R* and *Λ-R* and *Δ-S* and *Λ-S*. A mixture of both *Δ*- and *Λ*-species may result in two peaks with different chemical shift for each $-CF_3$ and $-CF_2$ moieties. However, we could not determine the ratio between these two diastereomers because there is also possibility that these two diastereomers have almost the same chemical shift due to weak interactions. This is further confirmed by the profile of ***Eu*_S/*R*-α-pinene** (1:1) given by Fig. 4.5. In diluted α-pinene, the three significant peaks of (a), (b) and (c) shifted

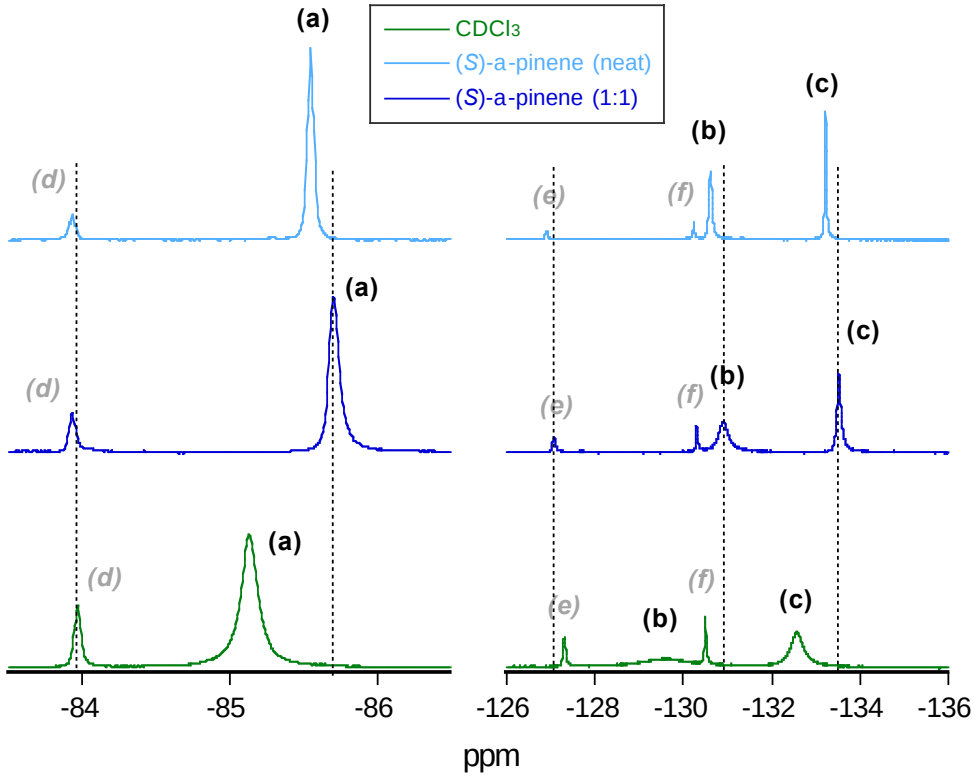

Fig. 4.5 ^{19}F-NMR profiles of Eu(III)(FOD)$_3$ in $CDCl_3$ (green), ***Eu*_S/*R*-α-pinene (neat)** (dark blue) and ***Eu*_S/*R*-α-pinene (1:1)** in **$CDCl_3$** (light blue)

more upfield and slightly broaden as compared to neat α-pinene. This possibly implies the existence of the two species of *Δ*- and *Λ*- in diluted environment. Thus, the preference of one diastereomer in neat α-pinene shown by the sharp peaks is obviously

higher. Furthermore, there obviously exists an interaction between the complex and the solvent, α-pinene because we notice that peak (b) and (c) appeared as singlet whilst peak (a) is vaguely a triplet. This leads to an assumption where the α-pinene interacts with the $(FOD)_3$-ligand of the complex causing a little restriction on the *outermost* $–CF_3$ group as compared to the *inner*- and *middle*-CF_2 groups. The singlet peaks of (b) and (c) imply that the *inner*- and *middle*-CF_2 groups rotate more freely suggesting that the interactions occur very likely between the $–CF_3$ of the $(FOD)_3$-ligand and the α-pinene at the outer-sphere. The overall spectra suggest that ***Eu_S/R*-α-pinene** (neat) also adopts polar C_3-symmetric *facial* structure in solution at the ground state as the peak integrals give 3:2:2 ratio. Both ***Eu_S*-** and ***Eu_R*-α-pinene** (neat) display almost exactly the same profiles.

Traces of Eu(III)$(FOD)_3$• $n H_2O$ were also observed for ***Eu_S/R*-α-pinene** (neat) and ***Eu_S/R*-α-pinene** (1:1) and we assign those as (*d*), (*e*), and (*f*). Fig. 4.6 shows the profile of HFOD dissolved in (*S*)-α-pinene. Those peaks were seen to shift slightly downfield as compared to HFOD in $CDCl_3$ due to interactions with the α-pinene.

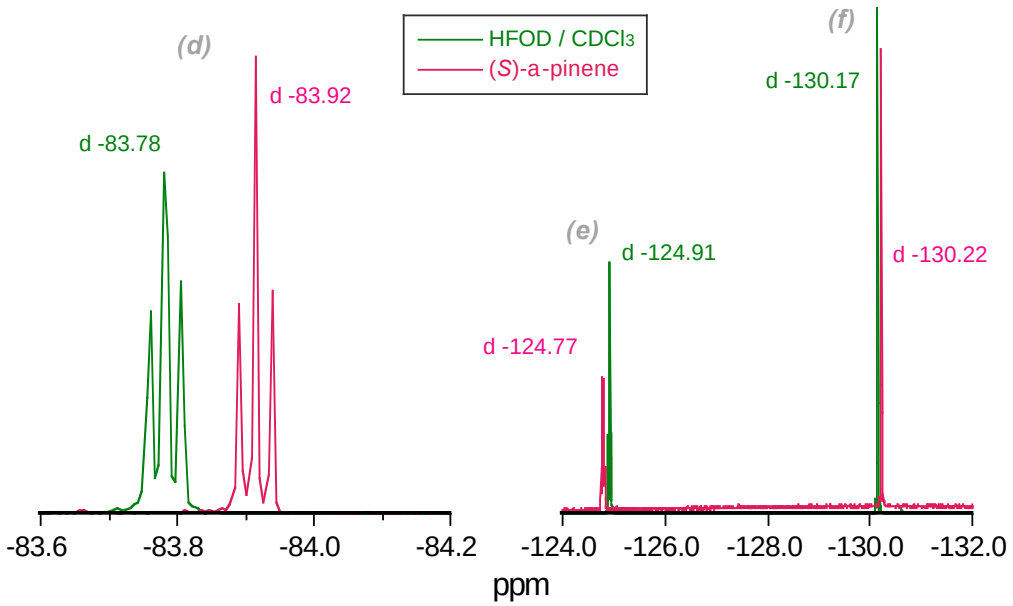

Fig. 4.6 ^{19}F-NMR profile of HFOD-ligand in neat (*S*)-α-pinene in comparison to HFOD-ligand in $CDCl_3$

4.3.1.3. Profiles of Eu_S/R-BINAP in comparison with Eu(III)(FOD)$_3$ in CDCl$_3$

***Eu_S/R*-BINAP** displays exactly the same profile as Eu(III)(FOD)$_3$ in $CDCl_3$ where the three significant peaks (a), (b), and (c) are assigned to (a) the *outer* $-CF_3$ group (b) the *middle* $-CF_2$ group and (c) the *inner* $-CF_2$ group of the three $(FOD)_3-$ ligands (Fig. 4.7). The peak integral also gives 3:2:2 ratios. Those peaks are as broad as

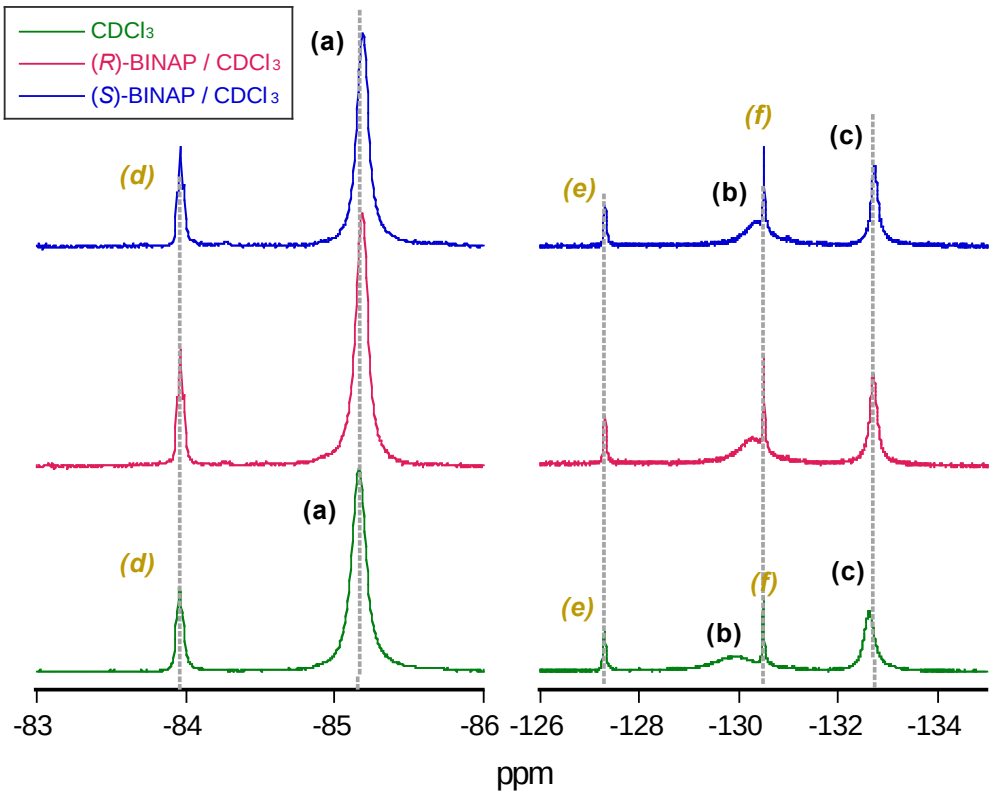

Fig. 4.7 ^{19}F-NMR profiles of Eu(III) $(FOD)_3$ in $CDCl_3$ (green) and ***Eu_S/R*-BINAP in $CDCl_3$** (blue and red)

that of Eu(III)$(FOD)_3$ in $CDCl_3$ indicating that the equilibrium of *Δ*- and *Λ*-species is not perturbed, thus, no preference of one-handed chirality is observed. This implies that ***Eu_S/R*-BINAP** consists of equal fractions of *Δ*- and *Λ*-species, thus, the equilibrium is not perturbed. This is in agreement with the CD profile shown by ***Eu_S/R*-BINAP**

(*refer* Fig. 3.1) in which the spectra of ***Eu_S/R*-BINAP** overlaps with the spectra of chiral *(S)/(R)*-BINAP in chloroform at equimolar mixture. We could also notice that for ***Eu_S/R*-BINAP**, there is no chemical shift at peak (a), whilst peak (b) and (c) shifted upfield very slightly as shown by the enlarged figure of peak (b) and (c) (Fig. 4.8). This

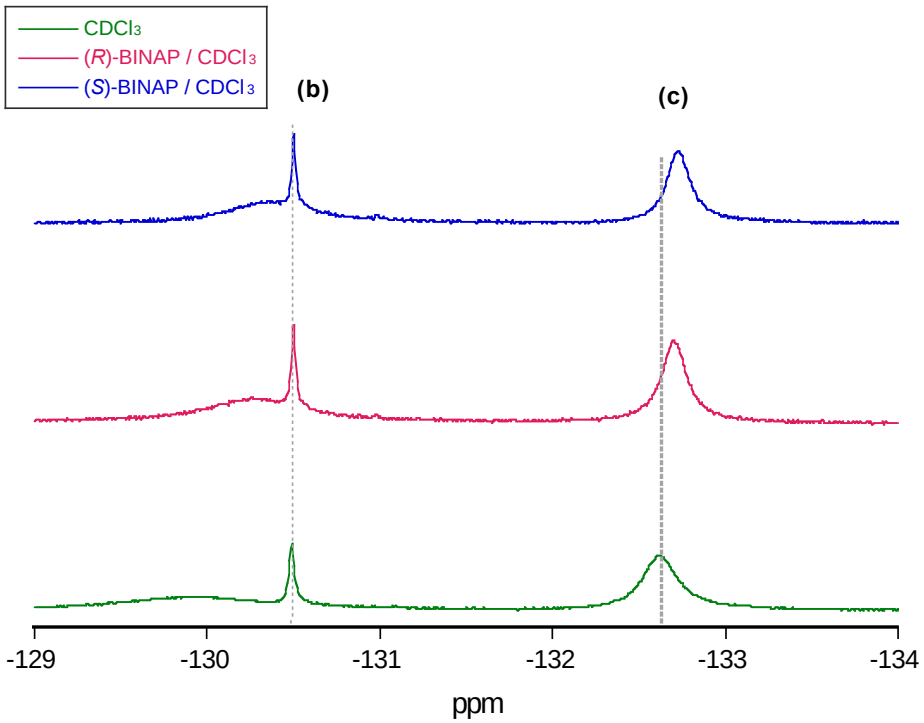

Fig. 4.8 ^{19}F-NMR profiles of enlarged peak (b) and (c) of ***Eu_S/R*-BINAP in $CDCl_3$** (blue and red)

indicates that only the $-CF_2$ groups of the three $(FOD)_3$-ligands are slightly affected instead of the *outermost* $-CF_3$ group as observed in ***Eu_S/R*-α-pinene**. Probably, the P(III)-atoms of BINAP have tendency towards the Eu(III) ion but because of the bulkiness of BINAP and the $(FOD)_3$-ligands' structures, hence, interactions do not easily occur particularly at the ground state. Similar to Eu(III)$(FOD)_3$ in $CDCl_3$, peaks (*d*), (*e*) and (*f*) are attributable to the traces of eight-coordinated Eu(III)$(FOD)_3 \bullet H_2O$ and it can be seen that these peaks do not shift at all in ***Eu_S/R*-BINAP**. Thus, we can

conclude that there is almost no noticeable intermolecular interactions occur between Eu(III)$(FOD)_3$ and the chiral additive *(S)/(R)*-BINAP at the ground state. The profile explains the absence of CD signals at europium absorption range as shown in Fig. 3.1.

4.3.1.4. Profiles of Eu_S/R-BINAPO (1:1) in comparison with Eu(III)(FOD)$_3$ in CDCl$_3$

***Eu_S/R*-BINAPO (1:1)** also displayed three major peaks corresponding to (a), (b) and (c) but in contrast to ***Eu_S/R*-α-pinene**, those peaks much sharpen and greatly shifted downfield especially peak (b) and (c) (Fig. 4.9). Peak (a) clearly shows a triplet and peak (c) shows a singlet while peak (b) is a broad multiplet perhaps due to

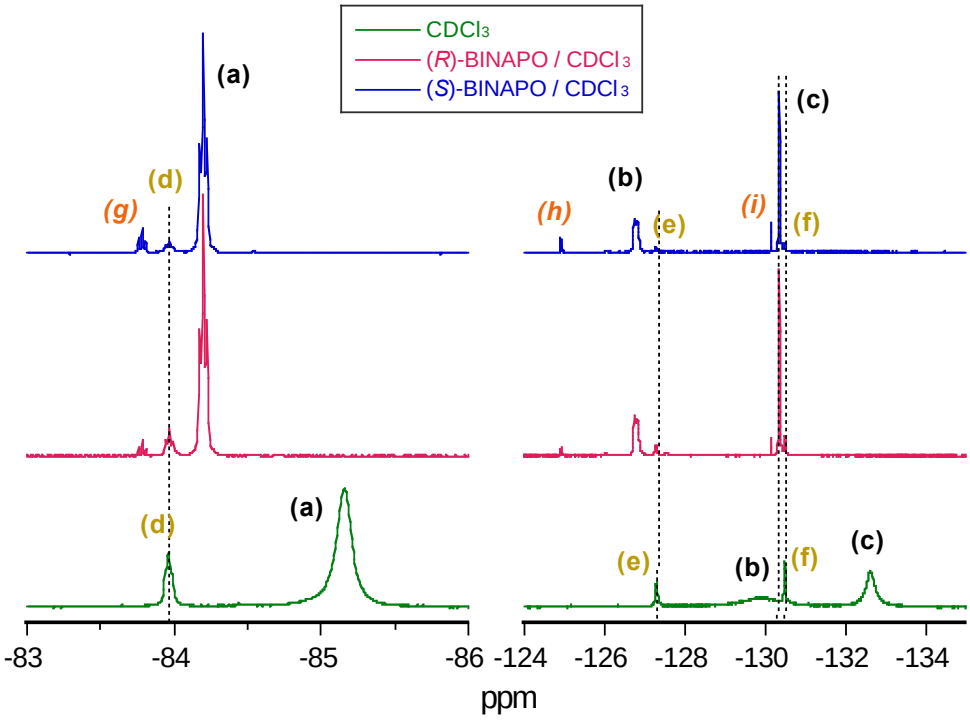

Fig. 4.9 ^{19}F-NMR profiles of Eu(III) (FOD)$_3$ in CDCl$_3$ (green) and ***Eu_S/R*-α-BINAPO in CDCl$_3$** (blue and red)

combination of quartets at different energies.

In contrast to ***Eu_S/R*-α-pinene**, interactions that occur affect the *middle* and *inner* –CF$_2$ groups more than the *outermost* –CF$_3$ and thus, the *outermost* –CF$_3$ could rotate more freely as reflected by the triplet peak (a). This reveals that the interactions occur towards the inner-sphere. From the peak integration, the ratio for the three main

peaks (a), (b) and (c) is unequal 3:2:2 unlike observed in Eu(III)$(FOD)_3$ in $CDCl_3$, ***Eu_S/R*-BINAP** and ***Eu_S/R*-α-pinene**. The peak integrals for (b) and (c) are slightly different where (c) is slightly higher as compared to (b) unlike. This suggests pseudo C_3-symmetric *facial* geometrical structure in solution. The sharpening implies a preference to one-handed chirality and the remarkable downfield shift is interpreted by the strong coordination between the Eu(III)$(FOD)_3$ complex and BINAPO. This is further confirmed by the ^{31}P-NMR measurement (*refer* Fig. 4.14) where P(V) of BINAPO in the presence of Eu(III)$(FOD)_3$ greatly shifted upfield. Most likely, the interaction takes place at the inner-sphere in which Eu(III) ion is directly coordinated to two oxygen (O) lone pairs of the BINAPO additive. Therefore, it is assumed that ***Eu_S/R*-BINAPO (1:1)** is an eight-coordinated Eu(III)$(FOD)_3$ complex. In this case, it seems that what occurs is not perturbation of the equilibrium but new formation of chiral compound through complexation. The opposite direction of the spectral shift observed for ***Eu_S/R*-BINAPO** as compared to ***Eu_S/R*-α-pinene** implies that the induced chirality originated from two different mechanisms.

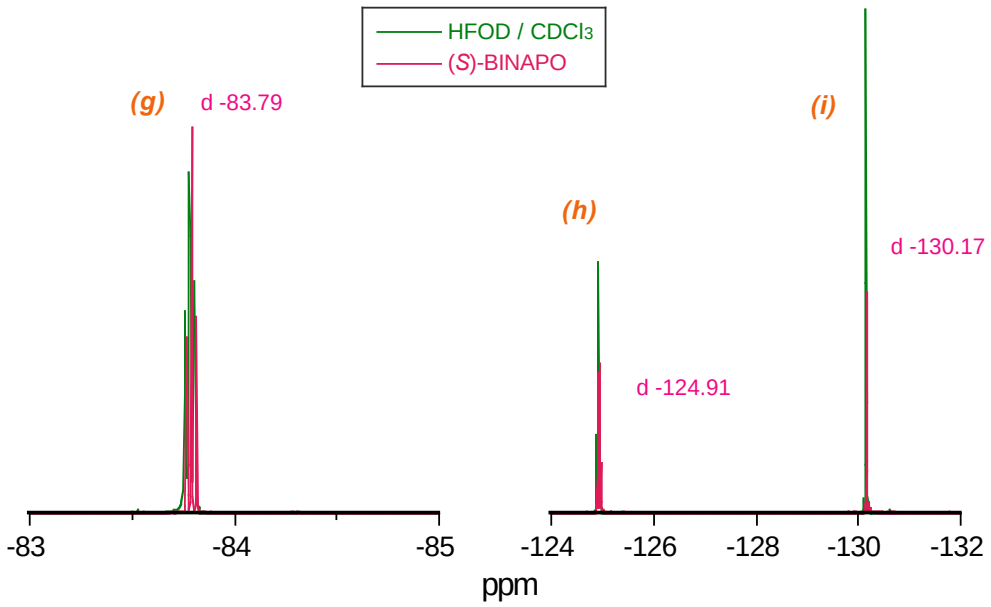

Fig. 4.10 ^{19}F-NMR profile of an equimolar mixture of HFOD and (*S)*-BINAPO in $CDCl_3$ in comparison to HFOD-ligand in $CDCl_3$

For the six small signals appeared with two triplets near peak (a), two singlets near (b) and two singlets also near (c). We could assign one signal from each (a), (b) and (c) as (*d*), (*e*), and (*f*) to the traces of Eu(III)$(FOD)_3$• nH_2O as observed in Eu(III)$(FOD)_3$ in $CDCl_3$ (*see* Fig. 4.3) and another to the traces of completely dissociated free-ligands as (*g*), (*h*), and (*i*). Peaks (*g*), (*h*), and (*i*) have the same chemical shifts with the peaks observed for the equivalent mixture of HFOD and (S)-BINAPO in $CDCl_3$ (Fig. 4.10) suggesting that ***Eu_S/R*-BINAPO (1:1)** also contains a small fraction of free FOD-ligands that do not interact with the BINAPO. This strengthens the assumption that the interactions occur at the inner-sphere which is rather strongly and causes some fractions of the FOD-ligands to completely dissociate from the Eu(III)$(FOD)_3$.

In conclusion, the whole spectra suggest that ***Eu_S/R*-BINAPO (1:1)** possibly

contains eight-coordinated Eu(III)$(FOD)_3$• BINAPO with three $(FOD)_3$-ligands and one BINAPO attached to the Eu(III) ion as major composition and a small fraction of Eu(III)$(FOD)_3$• *n*H2O as well as free FOD-ligands dissociated from Eu(III)$(FOD)_3$• BINAPO as minor compositions. The charge balance in Eu(III)$(FOD)_2$• BINAPO then is balanced by the hydroxyl ion that exists to keep eight-coordination number.

4.3.1.5. Profiles of Eu_S-α-PEA (neat) and Eu_S-α-PEA (1:1) in comparison with Eu(III)(FOD)$_3$ in CDCl$_3$

Fig. 4.11 displays the profiles for an equimolar mixture of Eu(III)(FOD)$_3$ and α-phenylethylamine in CDCl$_3$ (***Eu_S*-α-PEA (1:1)**, red), Eu(III)(FOD)$_3$ dissolved in neat α-phenylethylamine (***Eu_S*-α-PEA (neat)**) and Eu(III)(FOD)$_3$ in CDCl$_3$ as reference. Both ***Eu_R*-α-PEA (neat)** and **(1:1)** show the same profiles with ***Eu_S*-α-PEA.** ***Eu_S/R*-α-PEA (neat)** clearly exhibited three major peaks corresponding to (a), (b) and (c), and the ratio obtained from the peak integration is unequal to 3:2:2 for (a):(b):(c). This is similar to ***Eu-S/R*-BINAPO (1:1)** where the

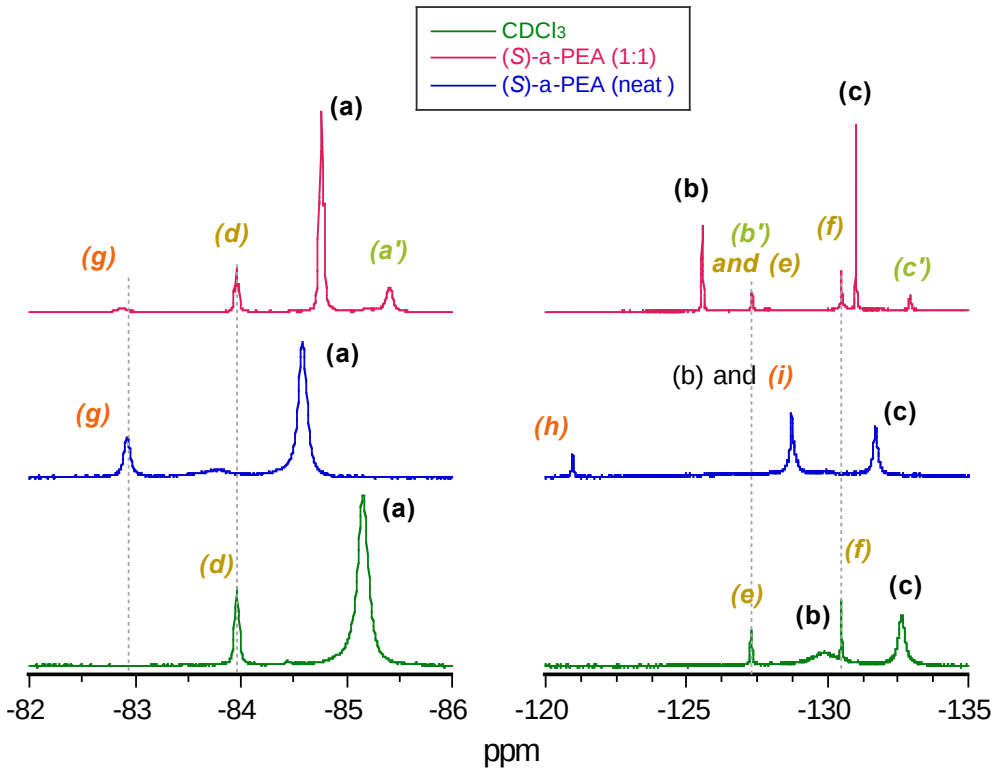

Fig. 4.11 ^{19}F-NMR profiles of Eu(III) (FOD)$_3$ in CDCl$_3$ (green) and ***Eu_S*-α-PEA (neat)** (blue) and ***Eu_S*-α-PEA (1:1)** (red)

integral for the inner part of the ligand is slightly different. For ***Eu_S/R*-α-PEA (neat)** (*blue line*), the integral for peak (b) is slightly higher as compared to (c) also indicating pseudo C_3-*facial* structure. The same trend is also observed in the ^{19}F-NMR profile of HFOD in neat α-PEA (Fig. 4.12). Obviously, the equilibrium has been much perturbed and preference to one enantiomer is also obvious. Those three peaks also sharpen but not as sharp as seen in that of ***Eu_S/R*-BINAPO (1:1)**. The similarity found with ***Eu_S/R*-BINAPO (1:1)** is the downfield shifting of the three significant peaks although the shift is not as same extent as ***Eu_S/R*-BINAPO (1:1)**. This suggests direct coordinative interaction at the inner-sphere. Since according to HSAB principle, the hard acids favour the hard bases, therefore, it is possible to suppose that coordination occurs between the Eu(III) ion and the nitrogen atom of the α-PEA.

In ***Eu_S/R*-α-PEA (neat)**, the trace of Eu(III)$(FOD)_3$• *n*H2O is almost not seen at (*d*). Meanwhile, minor peaks assigned as (*g*), (*h*) and (*i*) where (*i*) is thought to overlap with peak (b) could be attributed to associated Eu(III)$(FOD)_3$• *n*H2O with neat α-PEA. These peaks greatly shifted downfield especially (*g*) and (*h*) and therefore we assume that these ligands interact rather strongly with neat α-PEA. This is in consistent with the profile given by HFOD dissolved in neat α- PEA (Fig. 4.12) where the peaks shifted very much towards downfield as compared to ***Eu_S/R*-α-PEA (1:1)**.

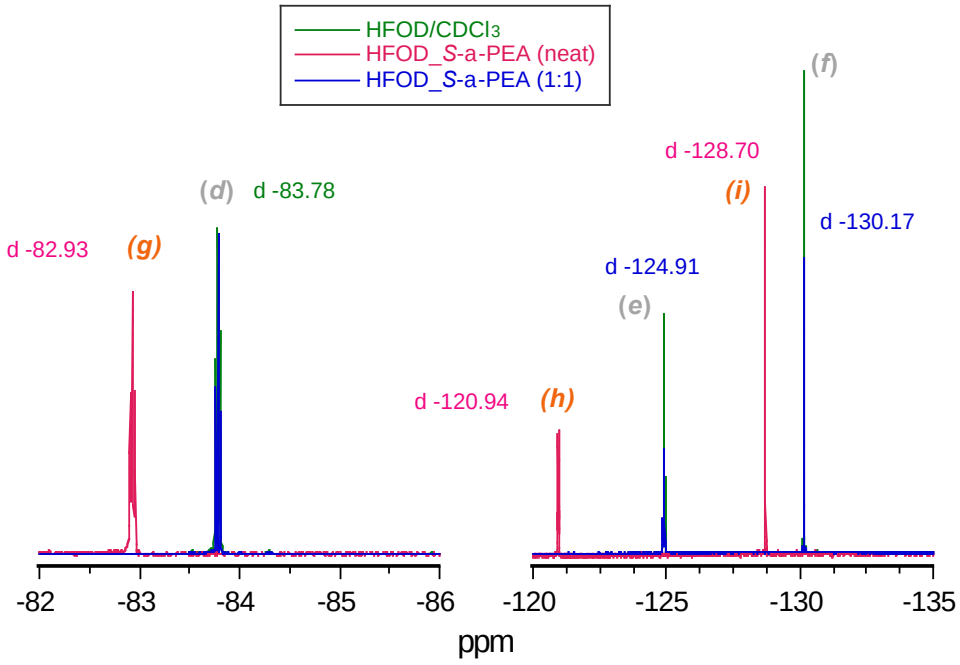

Fig. 4.12 ^{19}F-NMR profiles of *Eu_S/R*-α-PEA (neat) (green) and *Eu_S/R* α-PEA (1:1) in $CDCl_3$ (red) in comparison to HFOD-ligand in $CDCl_3$

On the other hand, ***Eu_S/R*-α-PEA (1:1)** (*red line*) displays 3:2:2 peak integration ratio for the three significant peaks appeared indicating that the polar C_3-symmetric *facial* structure of the Eu(III)$(FOD)_3$ is kept . Those peaks are assigned as (a), (b) and (c). The traces of Eu(III)$(FOD)_3$• *n*H2O are clearly shown by peaks (*d*), (e) and (*f*) where (e) is thought to overlap with (b') (*refer* Fig. 4.11). The trace of associated Eu(III)$(FOD)_3$• *n*H2O with α-PEA appears only for the *outermost* $-CF_3$ assigned as (*g*). In contrast to ***Eu_S/R*-α-PEA (neat)**, peak (*g*) is extremely small. In diluted environment, the association between the Eu(III)$(FOD)_3$• *n*H2O and the solvent is less pronounced as compared to neat environment. Another set of peaks was also observed next to every (a), (b) and(c) for ***Eu_S/R*-α-PEA (1:1)** and we assume that these peaks are the diastereomers of each (a), (b) and (c). We assign those peaks as (a'), (b') and (c').

These peaks give 20% peak integrals from the major peaks of (a), (b) and (c) with 3:2:2 ratios. If this is true, we can claim that the major component, either *Δ*- and *Λ*- composed of 80% and the minor fraction is 20%. Although NMR results reflect the ground state, this somehow explains why the emission dissymmetry ratio, g_{em} remarkably reduced for ***Eu_S/R*-α-PEA (1:1)** as compared to the ***Eu_S/R*-α-PEA (neat)**. It is a regret that neither CD spectrum of ***Eu_S/R*-α-PEA (neat) n**or ***Eu_S/R*-PEA (1:1)** are recorded due to high absorption of the α-PEA even with 1.0 mm pathlength cuvette. Therefore, it is difficult to discuss about the relationship of the downfield shift seen in ***Eu_(S)/(R)*-BINAPO**, ***Eu_S/R*-α-PEA (neat)** and ***Eu_S/R*-α-PEA (1:1)** with the absorption dissymmetry ratio, g_{CD}.

4.3.1. $^{31}P\{^{1}H\}$-NMR

4.3.1.1. $^{31}P\{^{1}H\}$-NMR profiles of (S)-BINAP and Eu_S-BINAP

(*S*)-BINAP in $CDCl_3$ displayed a singlet at δ = -17.955 ppm but the peak shifted slightly upfield to δ-18.061 upon complexation with Eu(III)$(FOD)_3$ (Fig. 4.13).

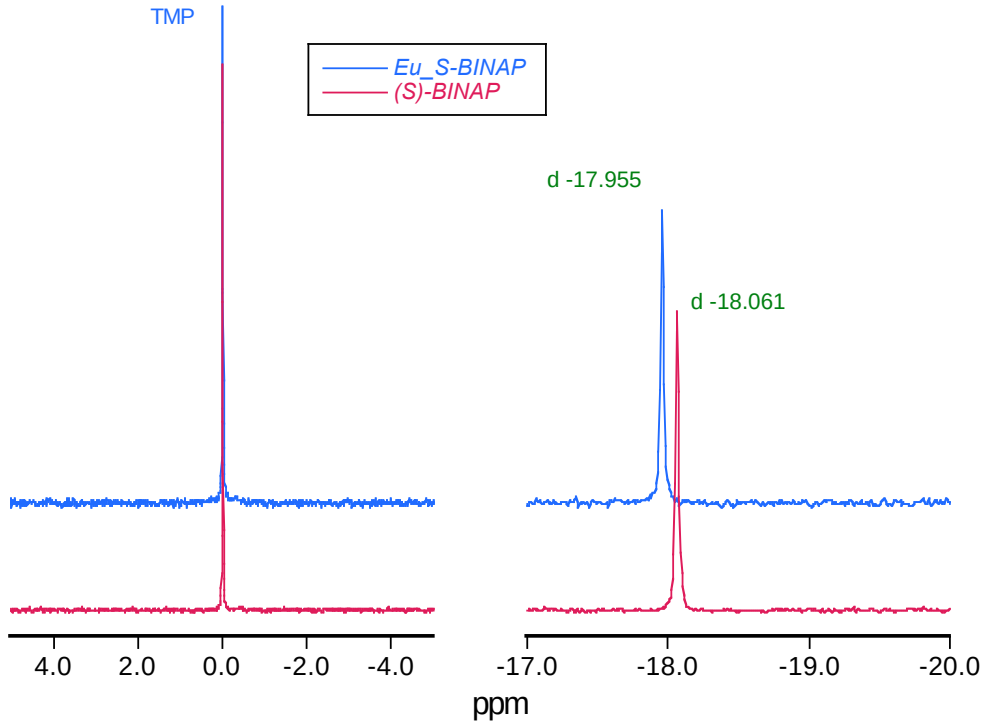

Fig. 4.13 $^{31}P\{^{1}H\}$-NMR profiles of (*S*)-BINAP in $CDCl_3$ (red) and ***Eu_S*-BINAP** in $CDCl_3$ (blue)

The small shift possibly arises from extremely weak interaction or dynamic coordination of Eu(III)$(FOD)_3$ and two P(III) lone pairs at the outer-sphere in non-coordinating solvent which caused undetectable CD signal although perturbation occurs at the ground state. This further supports the assumption that (*R*)/(*S*)-BINAP interacts weakly with Eu(III)$(FOD)_3$ at the outer- sphere. At the photoexcited state, a combination of weak interactions by *C-H/P*, C-*F*/*P*, and/or C-*F*/*H*-C between the

$(FOD)_3$-ligands and BINAP could be much promoted and cause an imbalance in Eu(III)$(FOD)_3$. Hence, we could observe CPL at the photoexcited state.

4.3.1.2. $^{31}P\{^{1}H\}$-NMR profiles of (S)-BINAPO and Eu_S-BINAPO

Contrarily, (*S*)-BINAPO in $CDCl_3$ displays a singlet at δ 28.289 ppm but the peak greatly shifted upfield to δ = -72.029 ppm and broaden upon complexation with $Eu(III)(FOD)_3$ (Fig. 4.14). The shift is typical for P(V) due to strong coordinating ability of O in BINAPO as shown by Hasegawa *et al.*[2] This further supports the remarkable downfield shift displayed by the ^{19}F-NMR profile in which the shift is attributed to direct coordination. This also strengthens the assumption that the interactions of O=P (BINAPO) and the Eu(III) ion may occur at the inner-sphere particularly in ***Eu_S/R*-BINAPO**.

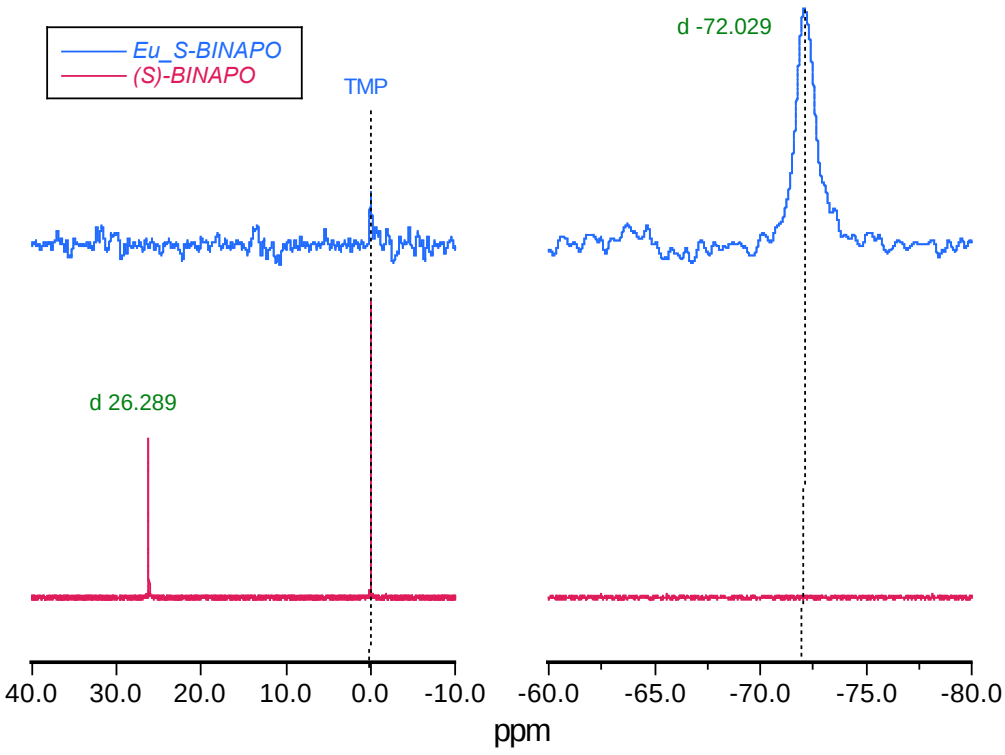

Fig. 4.14 $^{31}P\{^{1}H\}$-NMR profiles of (*S*)-BINAPO in $CDCl_3$ (red) and ***Eu_S*-BINAPO in $CDCl_3$** (blue)

4.4. Conclusion

Although NMR only reveals the behavior at the ground state, the behavior at the photoexcited state is reflected from the nature of the ground state. ^{19}F-NMR analysis reveals that Eu(III)(FOD)$_3$ complex favours polar C_3-symmetric *facial* structure in non-coordinating solvent. Addition of chiral solvent (α-pinene and α-PEA) and chiral additives (**BINAP** and **BINAPO)** has shifted the equilibrium of *Δ*- *facial* and *Λ*- *facial* toward one of the diastereomers. The peaks of ***Eu_S/R*-α-pinene (neat),** ***Eu_S/R*-α-pinene (1:1)** and ***Eu_S/R*-BINAP** shifted upfield but contrarily, the peaks of ***Eu_S/R*-BINAPO, *Eu_S/R*-α-PEA (neat)** and ***Eu_S/R*-α-PEA (1:1)** shifted downfield. ^{31}P-NMR profile has proven that the environment of P(V) is much different in ***Eu_S/R*-BINAPO**, implying the direct coordination of P=*O* to the Eu(III) ion. These results led us to conclude that the downfield shift in ^{19}F-NMR reflects stronger coordination occurring at the inner-sphere. Therefore, the upfield shift in ^{19}F-NMR as observed in ***Eu_S/R*-α-pinene (neat), *Eu_S/R*-α-pinene (1:1)** and ***Eu_S/R*-BINAP** could indicate perturbation of the equilibrium by weak coordination at the outer-sphere.

This is supported by the ^{31}P-NMR profile of ***Eu_S/R*-BINAP** where the P(III) environment of BINAP does not change much. From the peak integral based on the ratio of *outermost* –CF_3 : *middle* –CF_2 : *inner* –CF_2, it can be concluded that ***Eu_S/R*-α-pinene (neat), *Eu_S/R*-α-pinene (1:1)** and ***Eu_S/R*-BINAP** adopt the same configurational structure with Eu(III)(FOD)$_3$ in non-coordinating solvent, the polar C_3-symmetric *facial* structure. Strong direct coordination exemplified by ***Eu_S/R*-BINAPO** and ***Eu_S/R*-α-PEA (neat)** influenced the conversion of geometrical

structure from polar C_3-symmetric *facial* to *pseudo* polar C_3-symmetry or perhaps C_1-symmetry. The coordination that penetrates the inner-sphere could cause a remarkable change to the environments of each $(FOD)_3$-ligand. The peak integral that is unequal to 3:2:2 implies that each of the three ligands has slightly different environment after the complexation with the BINAPO and α-PEA.

In conclusion, perturbation of the equilibrium, the so-called 'Pfeiffer effect' occurs in ***Eu_S/R*-α-pinene** and ***Eu_S/R*-BINAP** through weak C-*H*/*F*-C interactions as multiple attractive Coulombic forces between $(FOD)_3$-ligands and α-pinene at the outer-sphere for the former case; and weak multiple outer-sphere interactions of C-*H*/P, C-*F*/*P*, and/or C-*F*/*H*-C between $(FOD)_3$-ligands and BINAP for the latter. However, the weak perturbation is undetectable by the CD spectroscopy due to limitation of the solution concentration for detection. Meanwhile, this weak perturbation could be detected by the CPL spectroscopy. These interactions seem to be much promoted at the photoexcited state where the molecules are dynamic upon receiving energy and become more delocalized with lengthen bond and altered bond angle.

On the other hand, the origin of induced-CPL in ***Eu_S/R*-BINAPO, *Eu_S/R*-α-PEA (neat)** and ***Eu_S/R*-α-PEA (1:1)** is originated from the direct coordination of P=*O* to Eu(III) for ***Eu_S/R*-BINAPO** and *N* to Eu(III) for ***Eu_S/R*-α-PEA (neat)** and ***Eu_S/R*-α-PEA (1:1)**. In diluted environment as exemplified by ***Eu_S/R*-α-PEA (1:1),** the coordination capability of *N* is sufficiently strong and it can be seen from the CPL spectra that the degree of perturbation is smaller than in neat solvent resulting less preference towards one enantiomer. Although

sufficiently strong, the ratio of *Δ*- and *Λ*-species could be determined by the ^{19}F-NMR profile due to stronger coordination as compared to the Pfeiffer-perturbed system. The ratio may slightly reduce when the energy barrier at the photoexcited state reduces resulting much weaker CPL as shown in chapter 3. The peak integrals in ***Eu_S/R*-α-PEA (1:1)** profile remain as 3:2:2 indicating that polar C_3-symmetric *facial* structure are kept in diluted environment.

4.5. References

[1] V. L. Budarin, J. H. Clark, S. E. Hale, S. J, Tavener, K. T. Mueller and N. M. Washton, *Langmuir*, 2007, **23**, 5412-5418.

[2] R. Streck and A. J. Barnes, *Spectrochim. Acta Part A*, 1999, **55**, 1049-1057.

[3] (a) M. Karplus, *J. Am. Chem. Soc.,* 1963, **85**, 2870-2871. (b) M. J. Minch, *Concepts Magn. Res.,* 1994, **6**, 41-56.

Chapter 5

Supporting analysis on the chiral origin by theoretical Møller-Plesset second-order perturbation (MP2) calculations

5.1. Introduction

In the previous chapter, we have elucidated that Eu(III)$(FOD)_3$ in $CHCl_3$, ***Eu_S*/*R*-α-pinene**, ***Eu_S*/*R*-BINAP** and ***Eu_S/R*-α-PEA (1:1)** adopt C_3-symmetry *facial* geometrical structure but ***Eu_S*/*R*-BINAPO** and ***Eu_S/R*-α-PEA (neat)** adopt C_1-*symmetry* . We also concluded that the origin of induced-CPL by ***Eu_S*/*R*-α-pinene** and ***Eu_S*/*R*-BINAP** is due to Pfeiffer-perturbed system at the outer sphere and the origins of induced-CPL by ***Eu_S*/*R*-BINAPO**, ***Eu_S/R*-α-PEA (neat)** and ***Eu_S/R*-α-PEA (1:1)** are due to direct coordination at the inner sphere. In the Pfeiffer-perturbed system, we assumed that the intermolecular interactions include (i) C-*F*/*H*-C between the F-atoms of the $(FOD)_3$-ligands attached to the complex and the protons of α-pinene or protons at binaphthyl and phenyl rings of BINAP, (ii) C-*F*/*P* between the F-atoms of the $(FOD)_3$-ligands or the P(III) of BINAP, (iii) C-*H*/π between the protons of the *tert*-butyl-ligands and the π-bond of α-pinene and (iv) C-*H*/*P* between the protons of the *tert*-butyl-ligands which contribute to the chiral resolution. In the case of ***Eu_S/R*-α-PEA (1:1)** the direct coordination could be loosen due to low concentration of the solvent α-phenylethylamine and it depicts the 'Pfeiffer effect'. In order to confirm our assumption, we employed the density functional theory (DFT) to investigate the dipole moment of the possible geometries, the *facial*- and *meridional*-

and Mulliken atomic charge[1] distribution in each molecular structure. The Mulliken population is a practical quantity to evaluate the electronegativity of each atom and it enables us to predict weak coordinations between the molecules.

5.2. Computational methods

We carried out the calculations using Gaussian 09 package[2]. Geometries of the models are optimized by molecular mechanics with universal force field followed by PM6, a DFT employing B3LYP (Becke three parameter Lee-Yang-Par) method supplemented with 6-31G(d,p) basis set[3a-c] and also MP2 (Møller Plesset second-order perturbation theory)[4a,b] with 6-311G basis set[5a,b] to yield optimized Mulliken charges and dipole moments. The optimized molecular structures with the numbering of atoms of $Sc(FOD)_3$ including C_3-*facial* and C_1-*meridional*, α-pinene, BINAP and BINAPO are illustrated in Fig.5.1 to Fig. 5.5. Scandium (Sc) is used as replacement for Eu(III) ion in the model of the $Eu(III)(FOD)_3$ structure and the simulation was carried out in vacuum for all structures.

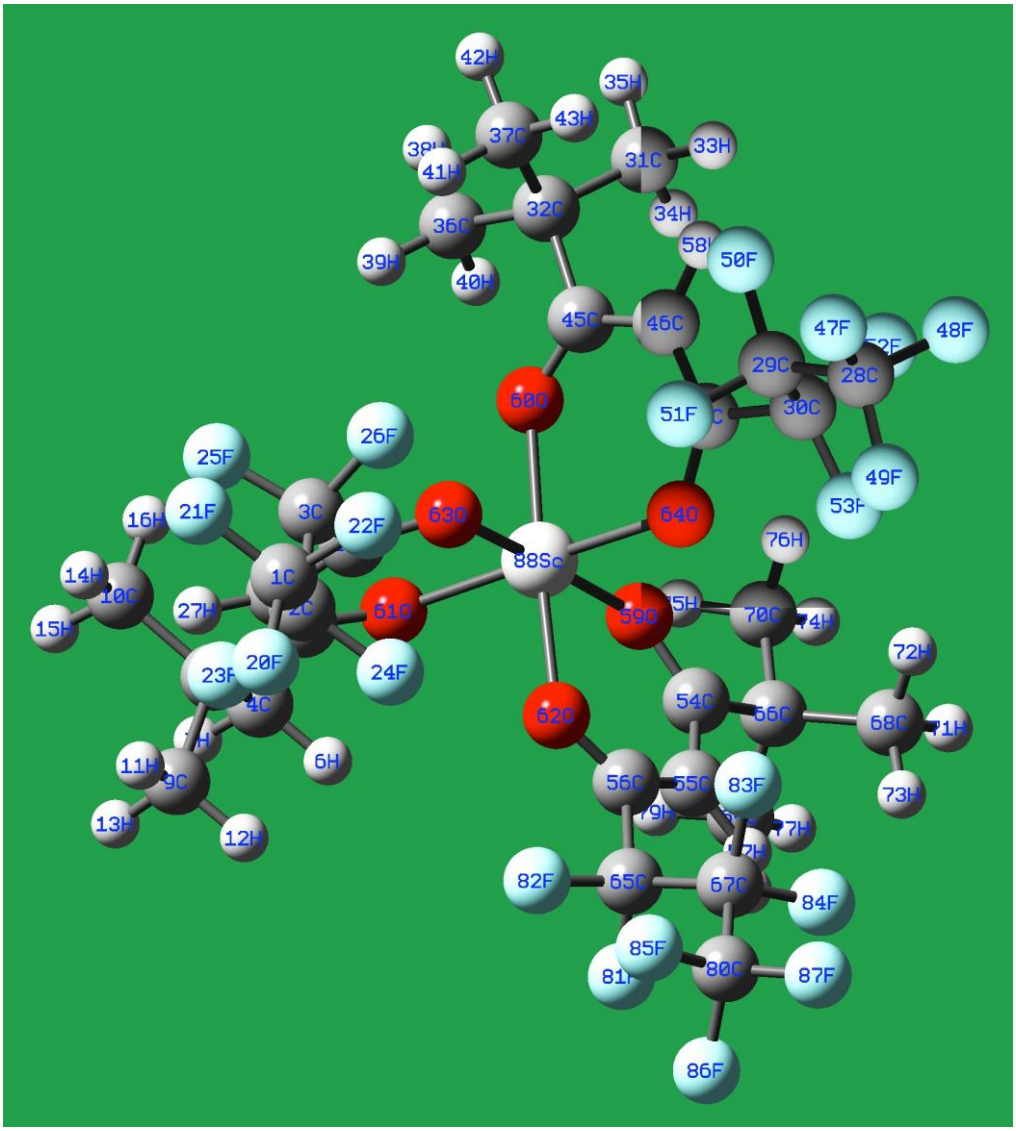

Fig. 5.1 Optimized structure of polar C_3-symmetry *facial* $Sc(FOD)_3$

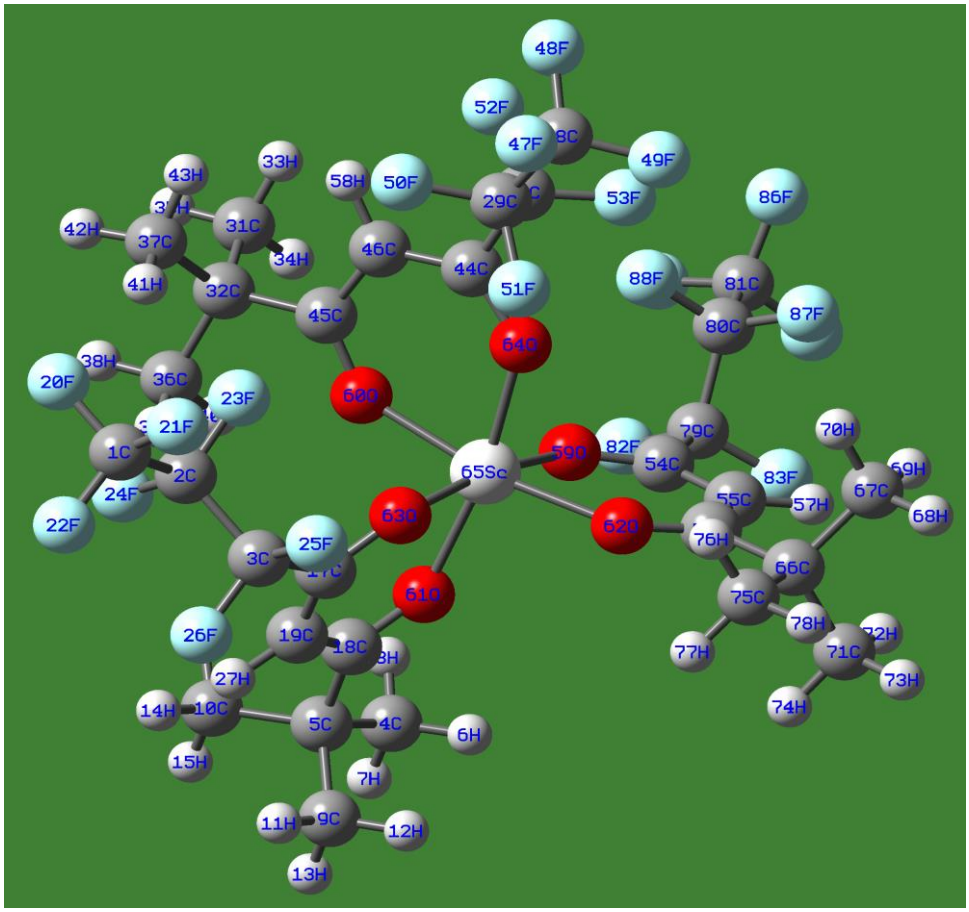

Fig. 5.2. Optimized structure of less-polar C_1-symmetry *meridional* $Sc(FOD)_3$

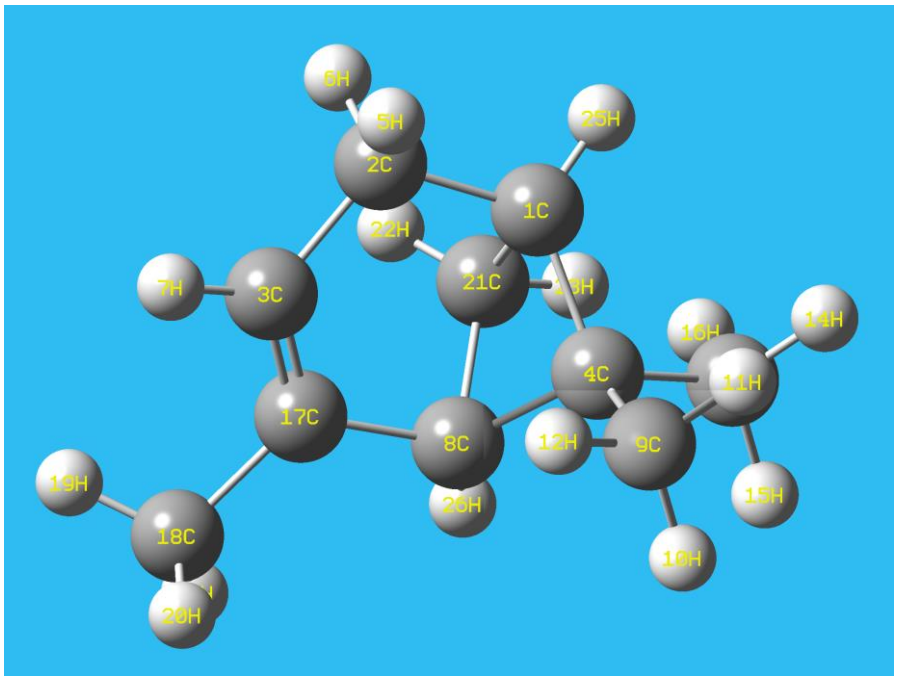

Fig. 5.3. Optimized structure of α-pinene

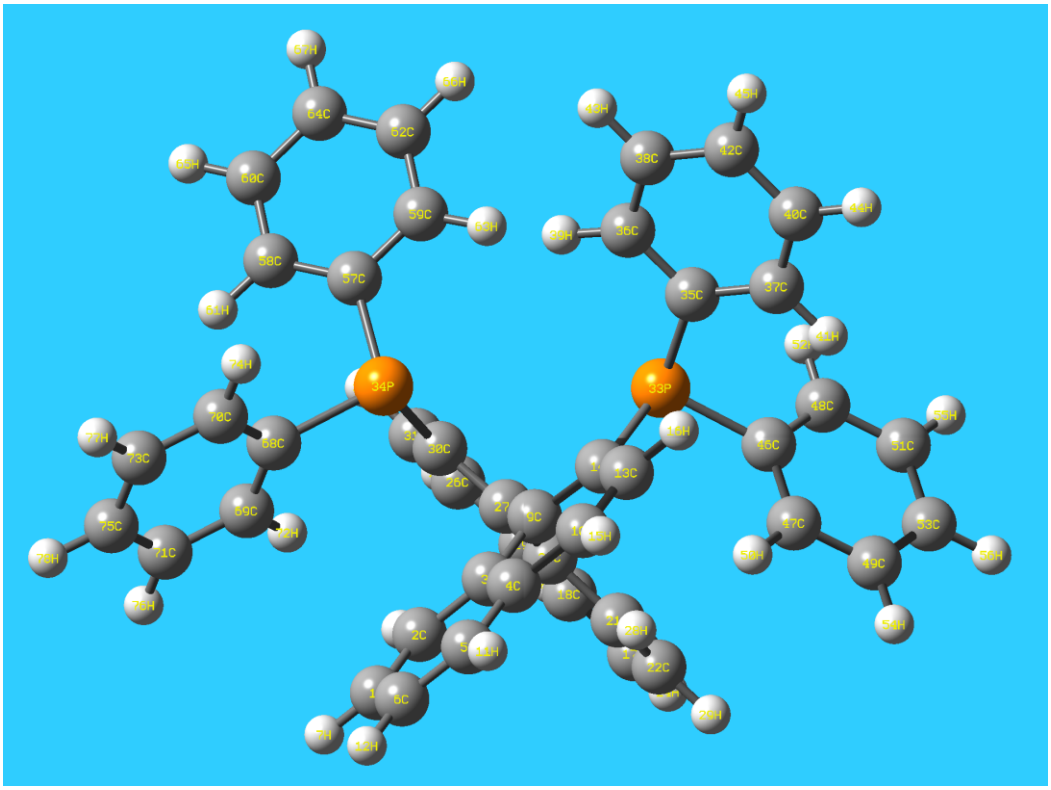

Fig. 5.4 Optimized structure of BINAP

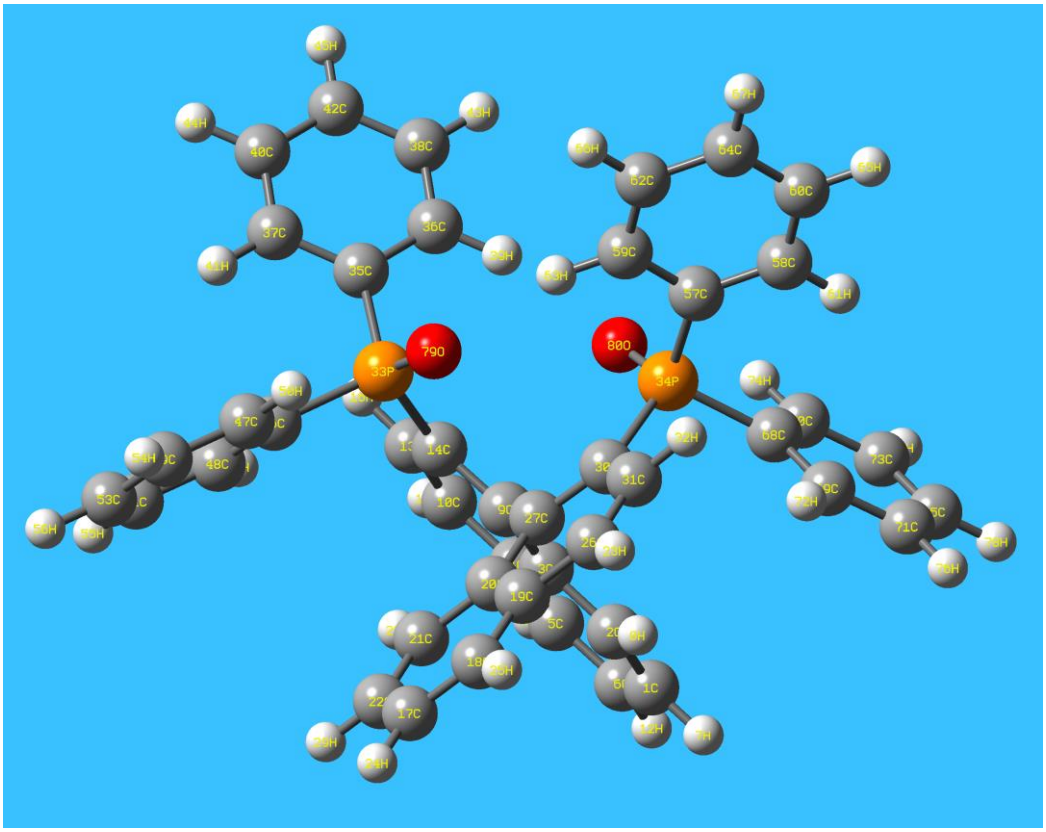

Fig. 5.5 Optimized structure of BINAPO

5.3. Dipole moment (μ) of two possible $Sc(FOD)_3$ geometrical structures

The calculated dipole moment value for *C_3-facial* geometry of $Sc(FOD)_3$ is 11.76 Debye whilst *C_1-meridional* geometry is 6.48 Debye. This indicates that *C_3-facial* is highly polar as compared to *C_1-meridional*. The energy difference, *ΔE* for these two structures is -1.78 $kcalmol^{-1}$. The *C_1-meridional* geometry is more stable than the *C_3-facial one*.

5.4. Mulliken population analysis

The Mulliken atomic charges of $Sc(FOD)_3$ and α-pinene are presented in Fig.5.6 and Fig.5.7, respectively. From the distribution of $Sc(FOD)_3$, it is noted that the charge for all of the F (20-26, 47-53, 81-87) atoms of the ligands are negative, ranging from -0.340 and -0.377, while the distribution of α-pinene gives positive charges, ranging from +0.157 and +0.192, at all protons attached to the carbons of the bicyclic ring. The presence of electron donating, negatively charged F-atoms and electron accepting, positively charged H-atoms supports the assumption that the induced-CPL is influenced by collective effects of intermolecular C-*F*(δ–)/*H*(δ+)-C interactions that take place between the $(FOD)_3$-ligands and the α-pinene. β-pinene and *trans*-pinane display almost the same charge mapping with the α-pinene (Fig. 5.8 and 5.9), however, only the α-pinene shows clear CPL signals particularly at the first transition ($^5D_0 \rightarrow {}^7F_1$). This implies that it is the presence of C-C double bond and the position of the double bond that contribute to the rigidity of the bicyclic ring which enhances the efficiency of the induced chirality. It can be seen that the protons of limonene also exhibit positive

charges ranging from +0.139 to +0.202 (Fig. 5.10), but despite having two C-C double bonds, the monocyclic limonene also did not show CPL signals. This clearly explains that the structure of limonene does not interact efficiently with the Eu(III) complex. Meanwhile, the charges for all of the H (6-8,11-16, 33-35, 38-43, 71-79) atoms of the *tert*-butyl ligands are positive ranging from +0.169 and +0.189 (*see* Fig. 5.6). Although these atoms may have tendency towards the negatively charged C-atoms of the α-pinene bicyclic ring (*see* Fig. 5.7), the attraction seems not effective as the CPL signal of $Eu(DPM)_3$ in (*R*)-α-pinene was undetectable (*see* Fig. 3.8). The Mulliken charge distribution of $Sc(DPM)_3$ is shown in Fig. 5. 11.

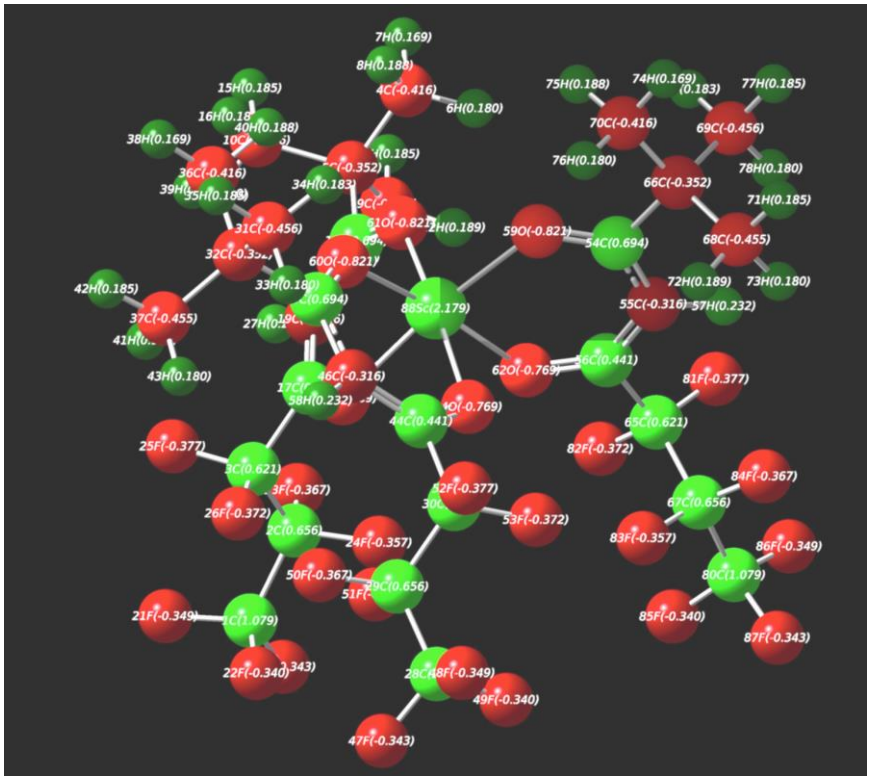

Fig. 5.6 Mulliken charge distribution of C_3-*facial* $Sc(FOD)_3$

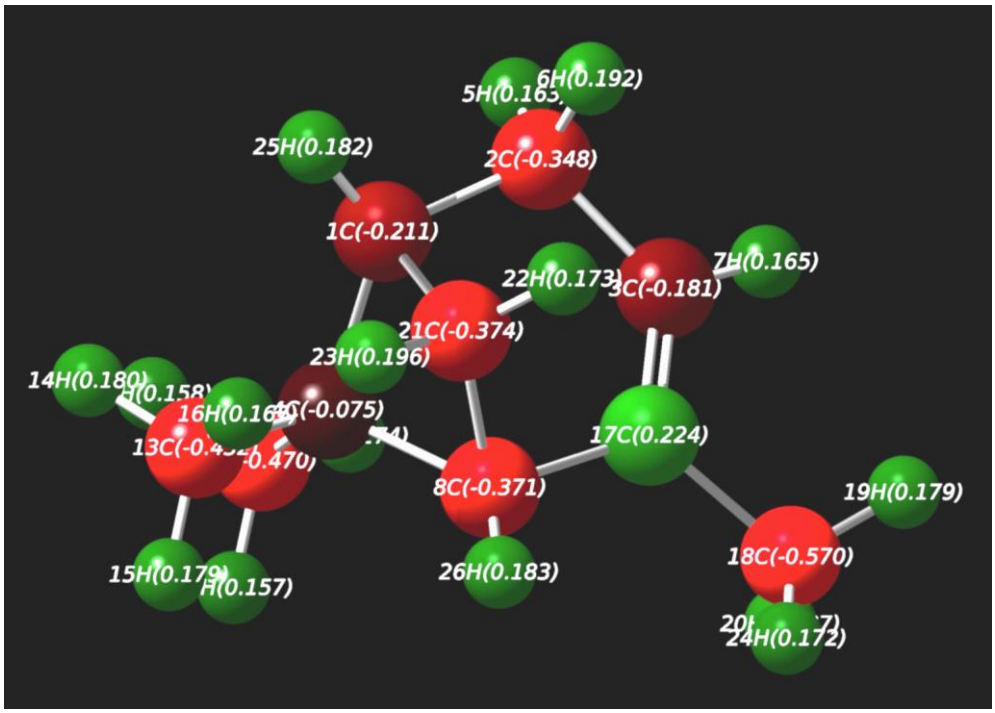

Fig. 5.7 Mulliken charge distribution of α-pinene

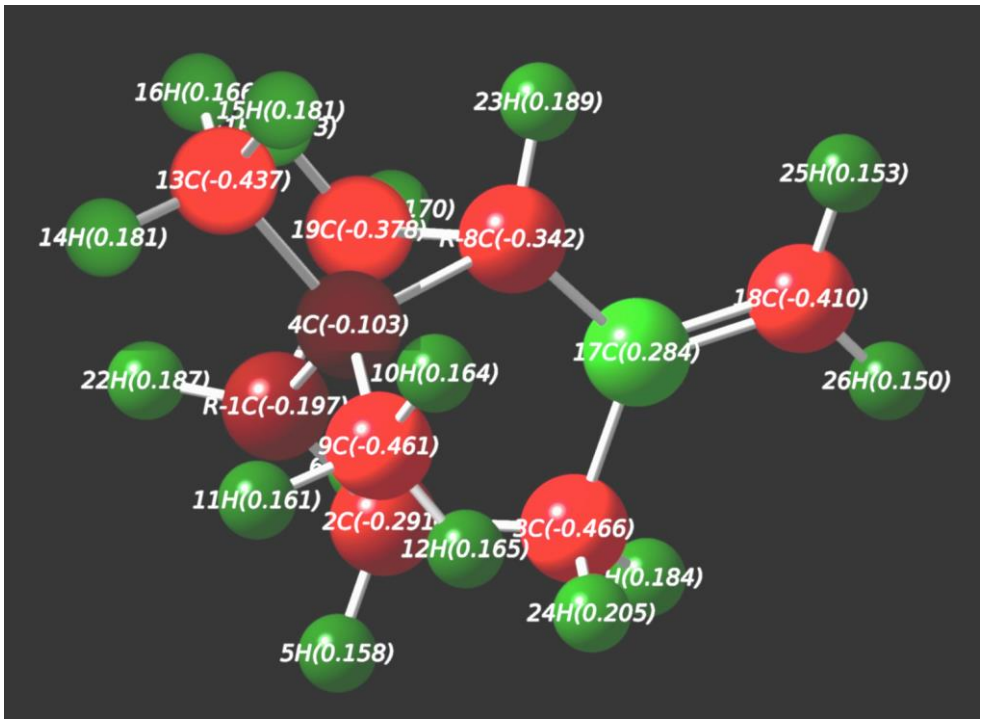

Fig. 5.8 Mulliken charge distribution of β-pinene

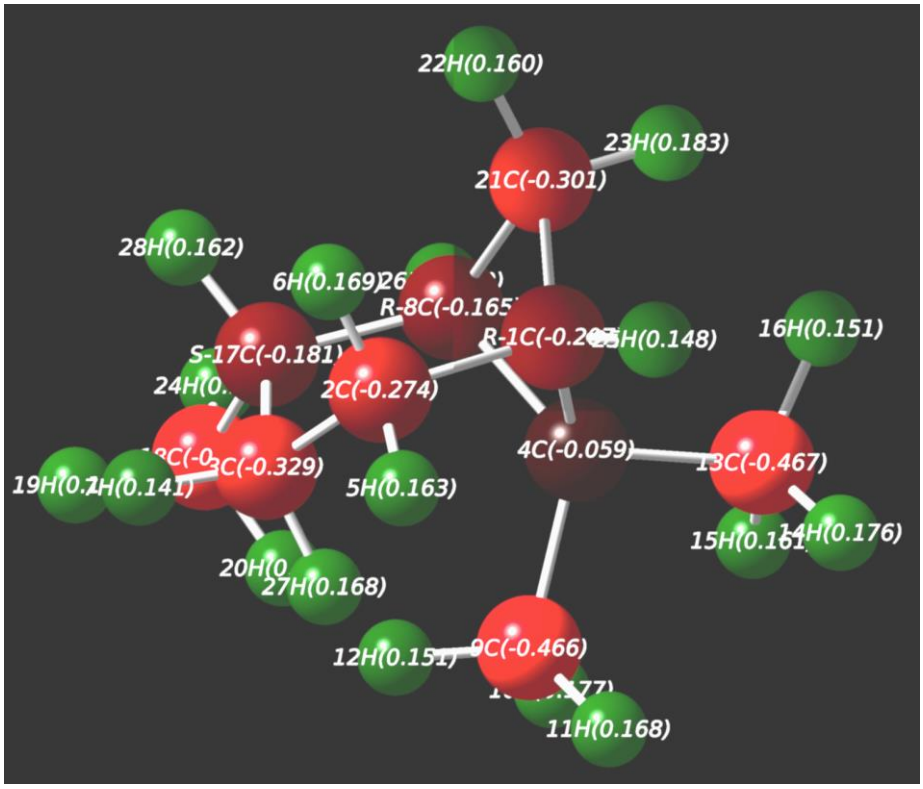

Fig. 5.9 Mulliken charge distribution of *trans*-pinane

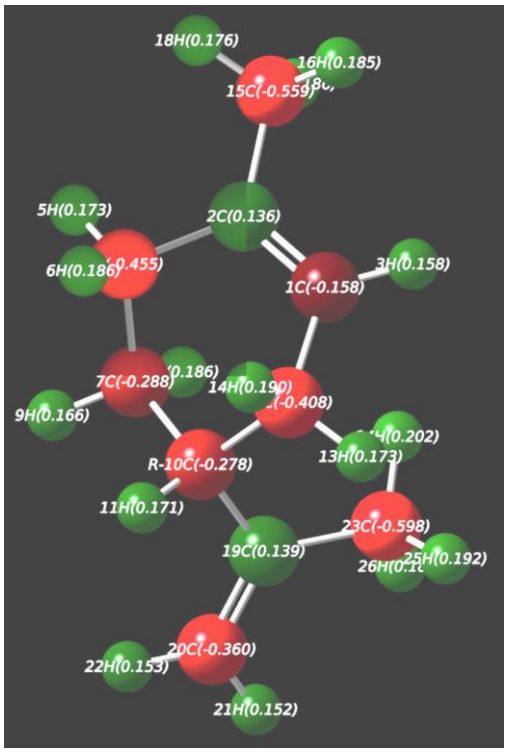

Fig. 5.10 Mulliken charge distribution of limonene

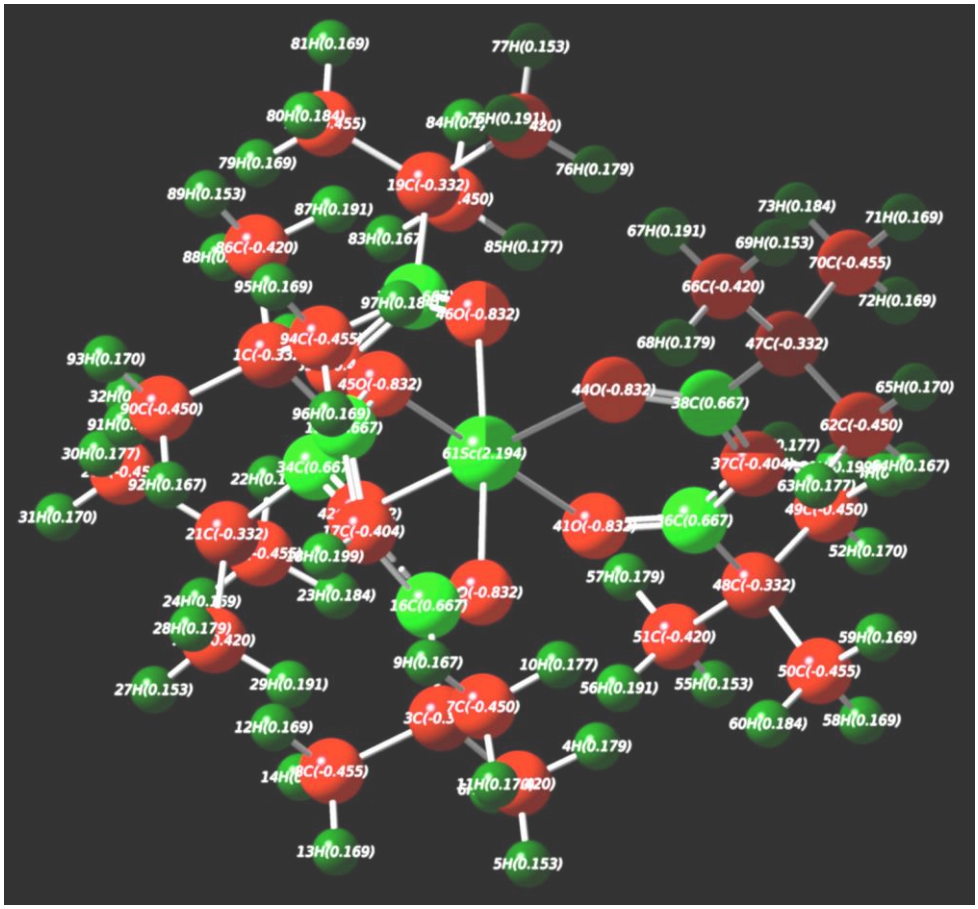

Fig. 5.11 Mulliken charge distribution of D_3-*symmetry* Sc(DPM)$_3$

Fig. 5.12 shows the charge mapping for BINAP and it is seen that the two P(III)-atoms (33P and 34P) of BINAP exhibit substantial positive charges of +1.034. The protons attached to the binaphtyl and the phenyl rings also exhibit positive and negative charges, respectively, suggesting that H-*C*(δ–)/P(δ+), C-*F*(δ–)/*P*(δ+), and/or C-*F*(δ–)/*H*(δ+)-C between (FOD)$_3$-ligands and BINAP are possible.

In the charge mapping of BINAPO, the two O-atoms (79O and 80O) exhibit substantial negative charges of –0.953 (Fig. 5.13), indicating attraction of *P*=*O* to the lanthanide (III) ion atom, *i.e.* Sc(III) is +2.179 (*see* Fig. 5.7) is much favoured. This

further supports the indication of direct coordination at the inner sphere by ^{19}F-NMR and ^{31}P{^{1}H}-NMR analyses.

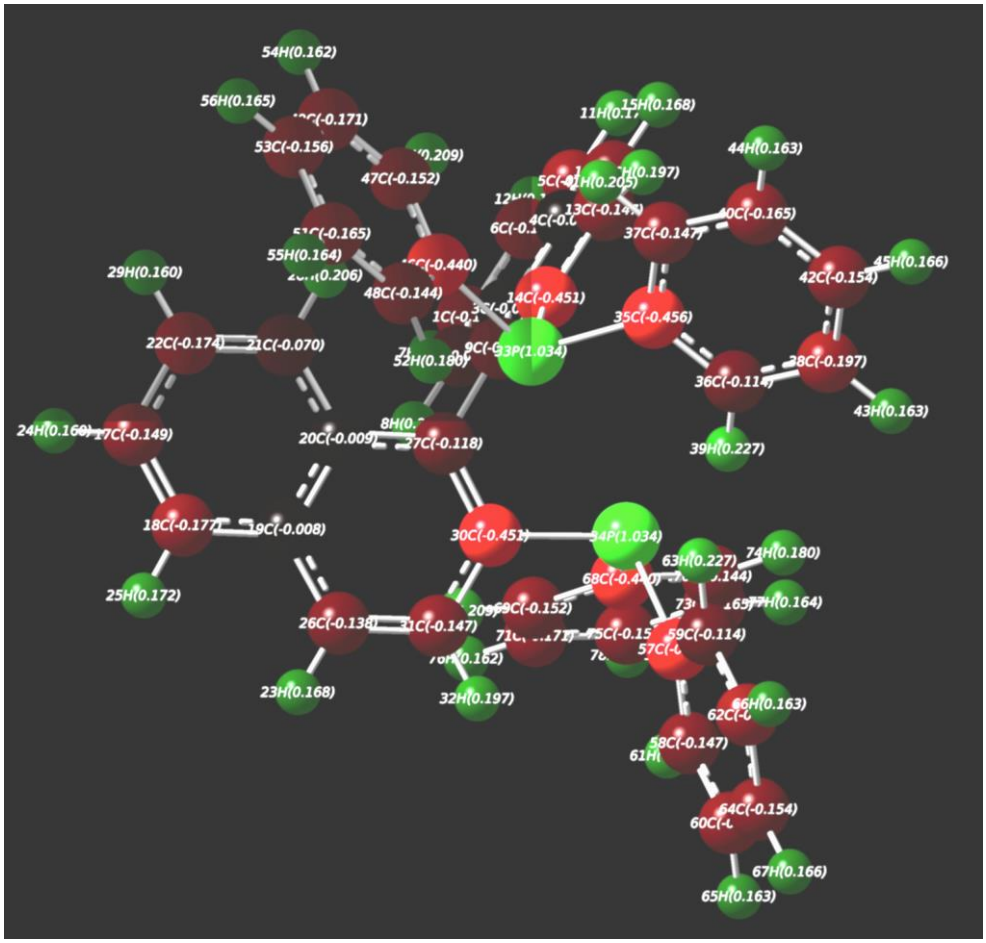

Fig. 5.12 Mulliken charge distribution of (*R*)-BINAP

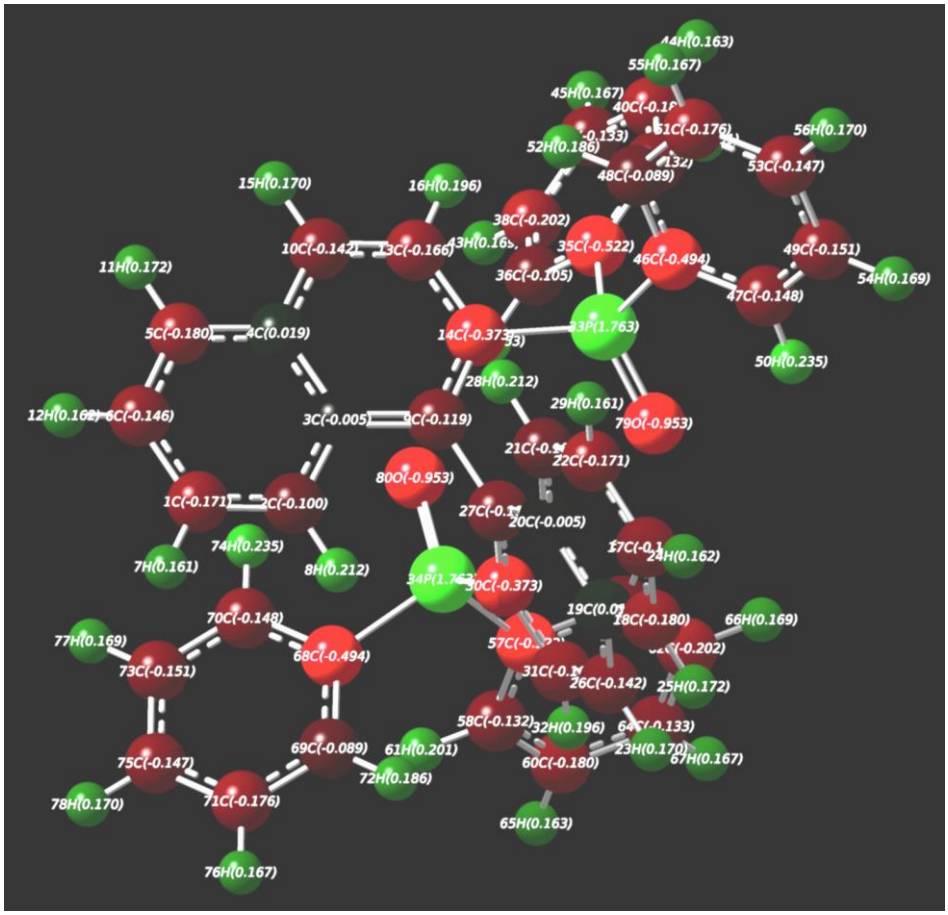

Fig. 5.13 Mulliken charge distribution of (*R*)-BINAPO

For α-phenylethylamine, the Mulliken charge distribution gives substantial negative charge of –0.547 for 18N-atom (Fig. 5.14). This also indicates that an attractive interaction could be favoured between the N-atom and the positively charged lanthanide (III) ion, in this case, the Sc(III) atom (*see* Fig. 5.7).

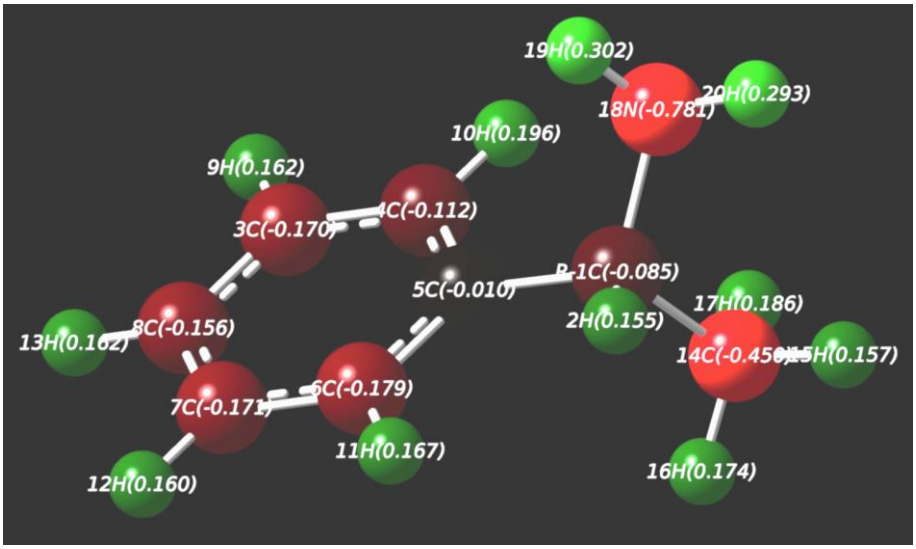

Fig. 5.14 Mulliken charge distribution of α-phenylethylamine

5.5. Conclusion

The simulation of Mulliken charge distribution obtained from the MP2 with 6-311G basis set further supported the assumption of a collective effect of intermolecular weak interactions occur between the $(FOD)_3$-ligands and the α-pinene or BINAP for the Pfeiffer-perturbed systems and also the direct coordination between P=O and N to the Eu(III) ion. Although it is found that *C_1-meridional* is a much more stable structure in a vacuum, the energy difference is very small as compared to *C_3-facial* implying that any of those two structures could be favoured. Nevertheless, $Eu(FOD)_3$ is likely to dominantly adopt *C_3-facial* geometry in chloroform and other non-polar and polar solvents, as demonstrated in previous chapters.

5.6. References

[1] R. S. Mulliken, *J. Chem. Phys.*, 1955, **23**, 1833-1840.

[2] Gaussian 09, Rev. D.01, M. J. Frisch, G.W. Trucks, H. B. Schlegel, G.E. Scuseria, M. A. Robb, et al., Gaussian, Inc., C.T. Wallingford (2013)

[3] (a) P. Hohenberg and W. Kohn, *Phys. Rev.* 1964, **136**, B864-B871 (b) M. A. L. Marques, C. A. Ullrich, F. Nogueira, A. Rubio, K. Burke and E. K. U. Gross. Eds. *Time-Dependent Density Functional Theory,* Springer, Berlin, Germany, 2006. (c) C. A. Ullrich, *Time-Dependent Density Functional Theory*: *Concepts and Applications.* Oxford Univ. Press, Oxford, UK, 2012.

[4] (a) C. Møller and M. S. Plesset, *Phys.Rev.* 1934, **46**, 618-622. (b) M. Head-Gordon, J. A. Pople and M. J. Frisch, *Chem., Phys. Lett.* 1988, **153**, 503-506.

[5] (a) G. Montaudo and P. Finocceiaro, *J. Org. Chem.*, 1972, **37**, 3434-3439. (b) R. E. Sievers, Ed. *Nuclear Magnetic Resonance Shift Reagents*, Elsevier, 1973.

Chapter 6

Summary and Future Perspective

6.1. Summary

Generation of CPL-active luminophores by solvent chirality transfer from a purely hydrocarbon terpene, the α-pinene to a racemic mixture Eu(III)$(FOD)_3$ complex was successful. Induced-CPL from the dissolution of Eu(III)$(FOD)_3$ in neat α-pinene was clearly observed at the magnetic allowed $^5D_0 \rightarrow {}^7F_1$ transition of Eu^{3+} ion. It is assumed that dissolution of a kinetically labile racemic mixture of Eu(III)$(FOD)_3$ resulted in an equilibrium shift where the concentrations of the two enantiomeric *Δ*- and *Λ*-Eu(III)$(FOD)_3$ are no longer equal. The bicyclic structure and the C-C double bond of α-pinene are crucial in the selection of a chiral terpene as a chiral environment and highly soluble fluorinated Eu(III) complex is preferred for this system. The low degree of association and the less altered well-resolved PL spectra suggests that non-covalent chiral discriminatory interactions could be responsible for the equilibrium displacement.

Induced-CPL was also observed in a solution mixture of Eu(III)$(FOD)_3$ and chiral additives/solvent with P, P=O and N elements. Basically, according to the HSAB theory, these elements are classified as hard bases which prefer to bind to a hard acid such as the Eu(III) complex. From the CPL spectra, ***Eu_S/R*-BINAP (1:1)**, ***Eu_S/R*-BINAPO (1:1)**, ***Eu_S/R*–α-PEA (neat)** and ***Eu_S/R*-α-PEA (1:1)** exhibited comparable degree of g_{em} values. Although comparable, it is precisely can be arranged in the order of α-pinene < BINAP < diluted α–phenylethylamine < BINAPO < neat

α–phenylethylamine. The solvent concentration dependency shows that BINAP has the same trend with the α-pinene but BINAPO and α–phenylethylamine shows higher association strength. From this, we can deduce that the induced-CPL in ***Eu_S/R*-α-pinene** and ***Eu_S/R*-BINAP (1:1)** could be from different origin with ***Eu_S/R*-BINAPO (1:1)**, ***Eu_S/R*–α-PEA (neat)** and ***Eu_S/R*-α-PEA (1:1)**.

^{19}F-NMR analysis reveals that perturbation of the equilibrium occurred in ***Eu_S/R*-α-pinene**, ***Eu_S/R*-BINAPO (1:1)**, ***Eu_S/R*–α-PEA (neat)** and ***Eu_S/R*-α-PEA (1:1)** affecting the $(FOD)_3$-ligands. It can be seen that the $(FOD)_3$-ligands were much affected in ***Eu_S/R*-BINAPO (1:1)**, ***Eu_S/R*–α-PEA (neat)** and ***Eu_S/R*-α-PEA (1:1)** particularly the *inner* –CF2 group of the ligands. This observation also leads to the assumption that the chiral origin in ***Eu_S/R*-α-pinene** is different from ***Eu_S/R*-BINAPO (1:1)**, ***Eu_S/R*–α-PEA (neat)** and ***Eu_S/R*-α-PEA (1:1)** where the interactions take place at the outer sphere for the former and the inner sphere for the latter. It is worth noted that perturbation seems did not occur in ***Eu_S/R*-BINAP (1:1)** in which these results are found to be in accordance with the CD. ***Eu_S/R*-α-pinene**, ***Eu_S/R*-BINAPO (1:1)**, ***Eu_S/R*–α-PEA (neat)** and ***Eu_S/R*-α-PEA (1:1)** also show a highly preference towards one enantiomer deciphered from narrowed ^{19}F-NMR peak for each F-moieties. In fact, the fractions of *Δ*- and *Λ*-species were recognized in ***Eu_S/R*-α-PEA (1:1)** due to dilute environment of strong association.

From the ^{19}F-NMR profiles, we also understood that ***Eu_S/R*-α-pinene** favors polar C_3-symmetry *facial* structure, which is the same structure favored by

Eu(III)$(FOD)_3$ in $CDCl_3$. However, ***Eu_S/R*-BINAPO (1:1)**, ***Eu_S/R*–α-PEA (neat)** and ***Eu_S/R*-α-PEA (1:1)** displayed *pseudo* C_3-symmetry or perhaps C_1-symmetry due to distortion by direct coordination to Eu3+ ion. Further evidence on direct coordination was obtained from the ^{31}P-NMR analysis of ***Eu_S/R*-BINAP (1:1)** and ***Eu_S/R*-BINAPO (1:1)**. This implies that the interactions occurred in ***Eu_S/R*-α-pinene** rules out direct coordination. As such, the possible interactions in ***Eu_S/R*-α-pinene** could be weak C-H/F-C interactions as multiple attractive Coulombic forces between FOD-ligands and α-pinene.

Mulliken charge distributions obtained by theoretical DFT calculations further support the assumption that weak C-*F*/*H*-C and also C-*H*/*C*-H interactions are the possible interactions occurred in ***Eu_S/R*-α-pinene** that caused the imbalance in the equilibrium and induced-CPL. The results also clearly show that direct coordination of P=O of BINAPO and the metal ion is much favored in ***Eu_S/R*-BINAPO (1:1)**, which is in agreement with the ^{19}F-NMR and ^{31}P-NMR analyses. Meanwhile, the possible interactions that occurred in ***Eu_S/R*-BINAP (1:1)** at the photoexcited state could be the weak interactions of H-*C*/P, C-*F*/*P*, and/or C-*F*/*H*-C between $(FOD)_3$-ligands and BINAP.

In conclusion, 'Pfeiffer effect' was observed in dissolution of a racemic mixture C_3-symmetry Eu(III)$(FOD)_3$ complex in purely hydrocarbon α-pinene. δ– Mulliken charges of F-C bonds (FOD) and δ+ Mulliken charges of H-C bonds (α-pinene) and also δ+ Mulliken charges of H-C bonds (*tert*-butyl of FOD) and δ- Mulliken charges of C-H bonds (α-pinene) that occurred at the outer-sphere have

brought an imbalance between *Δ*- and *Λ*-species and the equilibrium shift is responsible for the induced optical activity observed by CPL spectroscopy. This study also demonstrated that ^{19}F-NMR is a powerful tool in obtaining information on the absolute configuration of the dissymmetric Eu(III)$(FOD)_3$ complex in solution, the enantiomeric ratio as well as recognizing the 'Pfeiffer effect' .

6.2. Future perspective

'Pfeiffer effect' by a combination of highly soluble Eu(III) complex with non-toxic α-pinene offers an environmental friendly, simple and convenient approach in designing CPL materials. Although the effect does not result in high emission dissymmetry ratio, one could anticipate the applications in chiral sensing and the development of solution-processable coordination polymers by embedding into a polymer system.

LIST OF PUBLICATIONS AND CONFERENCES

PUBLICATION

1. Abd Jalil Jalilah, Fumio Asanoma and Michiya Fujiki
   Unveiling controlled breaking of the mirror symmetry of Eu(fod)3 with α-/β-pinene and BINAP by circularly polarized luminescence (CPL), CPL excitation, and ^{19}F-/^{31}P{1H}-NMR spectra and Mulliken charges.
   Inorganic Chemistry Frontiers (RSC), 2018, DOI:10.1039/C8QI00509E.

CONFERENCES

1. Abd Jalil Jalilah and Michiya Fujiki
   Circularly polarized luminescence (CPL) from achiral $Eu(FOD)_3$ in pure α-pinene.
   Chirality 2017, ISCD-29, Waseda University, 9-12 July 2017.

2. Abd Jalil Jalilah and Michiya Fujiki
   The origin of circularly polarized luminescence (CPL) from C3-facial and C1-meridional $Eu(FOD)_3$ endowed with α-pinene, BINAP and BINAPO.
   The 98th Chemical Society of Japan (CSJ) Annual Meeting, Nihon University, 20-23 March 2018.

3. Nanami Ogata, Michiya Fujiki, Wang Lai Bing and Abd Jalil Jalilah
   光学活性１-フェネチルアミンから光学不活性希土類錯体 (Tb,Eu)への不斉転写法による緑色/赤色円偏光発光(CPL) 特性の発現とCPL符合反転現象
   The 98th Chemical Society of Japan (CSJ) Annual Meeting, Nihon University, 20-23 March 2018.